(19)

(14) AFWL-TR-77-69

(2) **LEVEL** II

DDC

AFWL-TR-
77-69

ADE200 091

AD A061864

(6)

DYADIC GREEN'S FUNCTION FOR A TWO-LAYERED EARTH.

University of Colorado
Boulder, CO 80309

(10) Hussain A. /Haddad   David C. /Chang

(11)
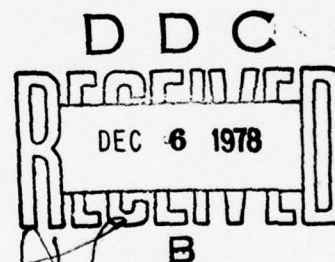
November 1977

(9)

(12) 108p.

D D C

Final Report.

RECEIVED
DEC 6 1978
B

(16) 1209   (17) 05

(18) SBIE   (19) AD-E200 091

AIR FORCE WEAPONS LABORATORY
Air Force Systems Command
Kirtland Air Force Base, NM 87117
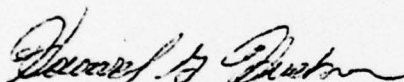
DDC FILE COPY

013 150

This final report was prepared by the University of Colorado, Boulder, Colorado under Project Orders 75-382 and 76-041, Job Order 12090516 with the Air Force Weapons Laboratory, Kirtland Air Force Base, New Mexico. Captain Howard G. Hudson (ELP) was the Laboratory Project Officer-in-Charge.

When US Government drawings, specifications, or other data are used for any purpose other than a definitely related Government procurement operation, the Government thereby incurs no responsibility nor any obligation whatsoever, and the fact that the Government may have formulated, furnished, or in any way supplied the said drawings, specifications, or other data, is not to be regarded by implication or otherwise, as in any manner licensing the holder or any other person or corporation, or conveying any rights or permission to manufacture, use, or sell any patented invention that may in any way be related thereto.
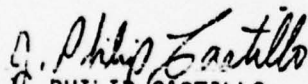
This report has been reviewed by the Information Office (OI) and is releasable to the National Technical Information Service (NTIS). At NTIS, it will be available to the general public, including foreign nations.

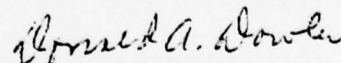This technical report has been reviewed and is approved for publication.

HOWARD G. HUDSON
Captain, USAF
Project Officer

FOR THE COMMANDER

J. PHILIP CASTILLO
Acting Chief
Technology Branch

DONALD A. DOWLER
Colonel, USAF
Chief, Electronics Division

SECURITY CLASSIFICATION OF THIS PAGE *(When Data Entered)*

REPORT DOCUMENTATION PAGE		READ INSTRUCTIONS BEFORE COMPLETING FORM
1. REPORT NUMBER AFWL-TR-77-69	2. GOVT ACCESSION NO.	3. RECIPIENT'S CATALOG NUMBER
4. TITLE *(and Subtitle)* DYADIC GREEN'S FUNCTION FOR A TWO-LAYERED EARTH		5. TYPE OF REPORT & PERIOD COVERED Final Report
		6. PERFORMING ORG. REPORT NUMBER Scientific Rpt. No. 22
7. AUTHOR(*s*) Hussain A. Haddad David C. Chang		8. CONTRACT OR GRANT NUMBER(*s*) Project Orders 75-382 and 76-041
9. PERFORMING ORGANIZATION NAME AND ADDRESS University of Colorado Dept of Electrical Engr, Electromagnetics Lab Boulder, CO 80309		10. PROGRAM ELEMENT, PROJECT, TASK AREA & WORK UNIT NUMBERS 64747F 12090516
11. CONTROLLING OFFICE NAME AND ADDRESS Air Force Weapons Laboratory (ELP) Kirtland Air Force Base, NM 87117		12. REPORT DATE November 1977
		13. NUMBER OF PAGES 106
14. MONITORING AGENCY NAME & ADDRESS*(if different from Controlling Office)*		15. SECURITY CLASS. *(of this report)* UNCLASSIFIED
		15a. DECLASSIFICATION/DOWNGRADING SCHEDULE

16. DISTRIBUTION STATEMENT *(of this Report)*

Approved for public release; distribution unlimited.

17. DISTRIBUTION STATEMENT *(of the abstract entered in Block 20, if different from Report)*

18. SUPPLEMENTARY NOTES

19. KEY WORDS *(Continue on reverse side if necessary and identify by block number)*

Dipole   Sommerfeld integral
Green's function   Dielectric slab
Dyadics   Lossy media
Stratified half space
Layered earth

20. ABSTRACT *(Continue on reverse side if necessary and identify by block number)*

Both the near-zone and far-zone electromagnetic field of an arbitrarily oriented dipole above a two-layer earth surface is obtained to a high degree of accuracy using a combination of numerical and analytical computational schemes. It is shown that marked differences exist between the field structures of a vertical dipole and a horizontal dipole in the case when the observation is made on the earth surface in the plane of the dipole. The magnitude of the power flux in the near field zone is shown to have maxima and minima depending upon the thickness and the electric constants of the first layer.

DD ₁ FORM JAN 73 1473   EDITION OF 1 NOV 65 IS OBSOLETE

SECURITY CLASSIFICATION OF THIS PAGE *(When Data Entered)*

PREFACE

We wish to acknowledge the assistance we received during
the course of this project from Professors J.R. Wait, E.F. Kuester
of the University of Colorado; Dr. David Hill of the Institute of
Telecommunication Sciences, U.S. Department of Commerce, and
Dr. C.E. Baum and Mr. M. Harrison of Air Force Weapons Laboratory,
Kirtland AFB, New Mexico.

TABLE OF CONTENTS

LIST OF FIGURES

LIST OF TABLES

SECTION I

INTRODUCTION

Investigation of VHF and UHF performance of thin wire structures in the presence of a realistic ground environment is important in electromagnetic pulse simulation as well as other antenna applications (ref.1). Since the earth is not very conductive in these frequency ranges, effect of the ground reflection can no longer be accounted for by the structure's mirror image. In some cases, wire structures large compared with the free-space wavelength are actually placed on the top of a prepared ground surface such as a nonreinforced concrete slab of finite thickness. The problem of finding the scattered field is then further complicated by the fact that the slab can now provide a physical mechanism for energy to spread out in the lateral direction in the form of a lossy surface wave.

As a first step leading to the better understanding of this problem, we shall discuss in this report the development of a numerically efficient scheme for computing electromagnetic fields produced by an arbitrarily oriented electric dipole source located in air over a multilayered, dissipative half-space. Typically, the medium consists of only two layers with a top layer being a concrete slab of finite thickness and the bottom layer, a homogeneous earth of infinite extent. To be able to obtain all the electric and magnetic field components accurately and efficiently in both the near-field and the far-field regions is important, due to the fact that an integral equation formulation of a thin-wire structure can usually be constructed once the field components produced by individual dipole sources are known.

In what follows, we shall discuss first the spectral representation of the scattered field due to a horizontally stratified half-space using an

7

approach similar to that of Wait's (ref. 2-3). We then proceed to discuss a

numerical scheme for the computation of the so-called Sommerfeld integrals.

Since all six field components are needed, a method is developed for

simultaneous integration of these components. Also investigated is the

choice of possible paths of integration, with specific reference made to the

work of Lytle and Lager (ref. 4-5) which finds the field components of

a homogenous half-space. In addition to the numerical integration, we

shall also discuss the appropriate asymptotic and near-zone expansions of

each field component. They are then incorporated into the computer program

in order to improve the computational efficiency. A related work in this

case is that of Tsang and Kong (ref.6) where various asymptotic evaluations

of the longitudinal magnetic field were found for a horizontal dipole

placed on a lossy dielectric slab, having a thickness in the order of a

few wavelengths. However, their computation was restricted to observation

on the slab surface. Also included in the report is a comparison of the

numerical results with various known special cases.

SECTION II

FORMULATION OF THE PROBLEM

Following Baum's notation (ref. 7), the electromagnetic field generated by a source in air above a stratified half-space can be written as

$$\tilde{\vec{E}}(\bar{r},s) = - s\mu_o \langle \tilde{\vec{G}}(\bar{r},\bar{r}';s); \tilde{\vec{J}}(\bar{r}',s) \rangle$$

$$\tilde{\vec{H}}(\bar{r},s) = \langle \nabla \times \tilde{\vec{g}}(\bar{r},\bar{r}';s); \tilde{\vec{J}}(\bar{r}',s) \rangle \tag{1}$$

the $\tilde{\vec{G}}$ and $\tilde{\vec{g}}$ are the dyadic Green's function in the air region of a current source above a multi-layered lossy media; $\tilde{\vec{J}}$ is the source electric current density; $s \equiv \Omega - i\omega$ is the Laplace transform variable; μ_o is the permeability of free space. The operation $\langle , \rangle$ is a symmetric product defined as;

$$\langle \vec{A}(\bar{r},\bar{r}'); \bar{b}(\bar{r}') \rangle \equiv \int_{S \text{ or } V} \vec{A}(\bar{r},\bar{r}') \cdot \bar{b}(\bar{r}') \begin{pmatrix} dS' \\ or \\ dV' \end{pmatrix}$$

where the integration is over some surface S or a volume V. The arrow $\rightarrow$ and the bar $-$ over the quantities indicates a dyadic and a vector form respectively. The comma separates quantities with a common variable of integrations. The dot $\cdot$ or the cross $\times$ directly above the separating comma, i.e. $;$ or $\overset{\times}{,}$ indicates respectively the multiplication sense as a dot product or a cross product.

The dyadic function $\tilde{\vec{G}}$ is defined as

$$\tilde{\vec{G}}(\bar{r},\bar{r}';s) = [\vec{I} + k_o^{-2} \nabla\nabla] \tilde{\vec{g}}(\bar{r},\bar{r}';s) \tag{2}$$

and $\tilde{\vec{g}}$ is then the basic dyadic we need to evaluate. Here, $\vec{I}$ designates the identity dyad

$$\vec{I} = \bar{a}_x \bar{a}_x + \bar{a}_y \bar{a}_y + \bar{a}_z \bar{a}_z$$

and $\bar{a}_x$, $\bar{a}_y$ and $\bar{a}_z$ are unit vectors in the x, y and z direction respectively. k_o = is/c is the free space propagation constant.

Provided that the surface of the stratified half-space is located in the x-y plane, $\overset{\approx}{g}$ is a 3×3 matrix of which only five elements are non-zero for fields of an arbitrarily oriented current source above a stratified half-space;

$$\overset{\approx}{g}(r,r,s) = \begin{bmatrix} \tilde{g}_{xx} & 0 & 0 \\ 0 & \tilde{g}_{yy} & 0 \\ \tilde{g}_{zx} & \tilde{g}_{zy} & \tilde{g}_{zz} \end{bmatrix}$$

In this report only the derivation leading to the expressions for fields produced by a dipole placed in the x-z plane is demonstrated. This implies finding the components g_{xx} and g_{zx} of a horizontal dipole source placed in the x-direction and g_{zz} of a vertical dipole source in the z-direction. It is obvious that, by a simple coordinate rotation of $\phi \to \phi + 90°$ in the x-y plane, the x-directed dipole fields g_{xx} and g_{zx} will yield the fields of the y-directed dipole fields g_{yy} and g_{zy}.

Figure 1 shows a tilted electric Hertzian dipole above a finitely conducting stratified half-space. This dipole is placed at a height h_o from the layered media making an angle of θ' with respect to the vertical z-axis; and ϕ' with respect to the x-axis; the prime refers to the source coordinate system. The dipole can be decomposed into three components; one parallel to the earth surface along the x-axis with a dipole moment Idx', another along the y-axis with a dipole moment $I\,dy'$ and the third one perpendicular to the earth along the z-direction with a dipole moment of $I\,dz'$.

Now we can write the current density of the dipole as follows:
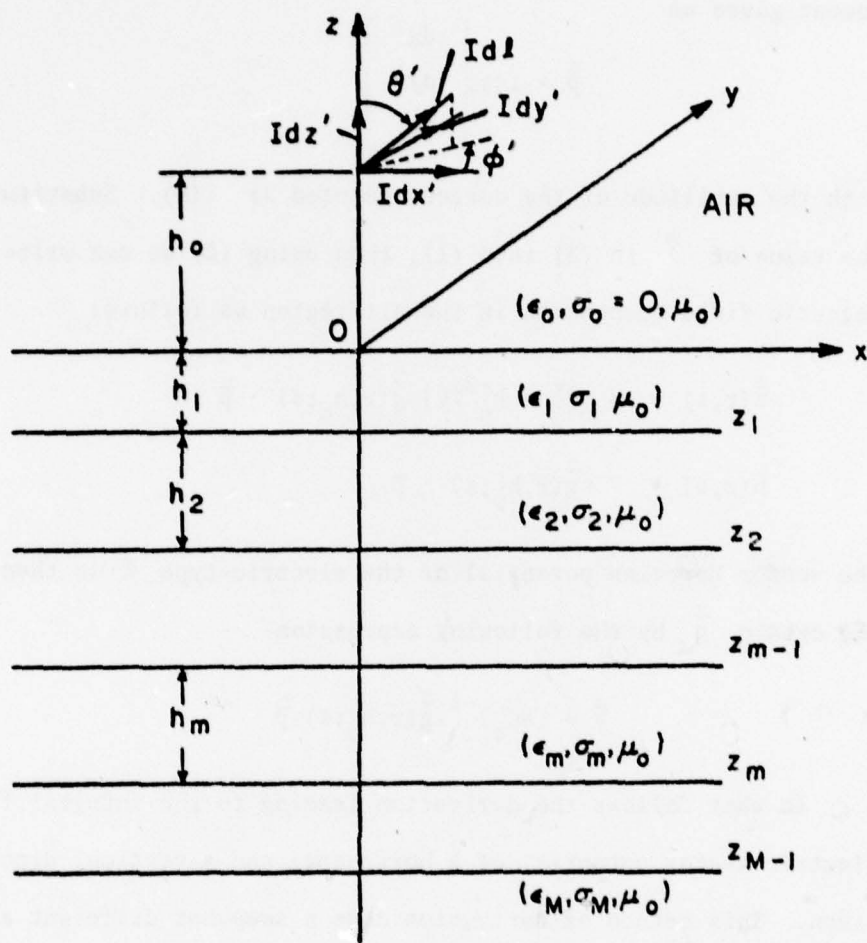
Figure 1. Arbitrary oriented dipole above a finitely
conducting stratified half-space

$$\vec{\tilde{J}}(r') = \vec{\tilde{p}} \, \delta(x')\delta(y')\delta(z'-h_o) \tag{3}$$

where $\delta(u)$ is the Dirac delta function and $\tilde{p}$ is the vector dipole moment given as

$$\vec{\tilde{p}} = \tilde{I}(s)\begin{bmatrix} dx' \\ dy' \\ dz' \end{bmatrix}$$

with the amplitude of the current denoted as $\tilde{I}(s)$. Substituting for the value of $\vec{J}$ in (3) into (1), then using (2) we can write the electromagnetic field components in the air region as follows:

$$\vec{\tilde{E}}(r,s) = -s\mu_o[\vec{I} + k_o^{-2}\nabla\nabla] \, \vec{\tilde{g}}(r,h_o;s) \cdot \vec{\tilde{p}}$$

$$\vec{\tilde{H}}(r,s) = \nabla \times \vec{\tilde{g}}(r,h_o;s) \cdot \vec{\tilde{p}} \tag{4a}$$

The vector Hertzian potential of the electric-type $\vec{\tilde{\pi}}$ is then related to the dyadic $\vec{\tilde{g}}$ by the following expression

$$\vec{\tilde{\pi}} = (s\epsilon_o)^{-1} \, \vec{\tilde{g}}(r,h_o;s)\cdot\vec{\tilde{p}} \tag{4b}$$

In what follows the derivation leading to the integral form of the electric vector potential of a horizontal and a vertical dipole will be given. This method of derivation uses a somewhat different approach than the one derived by Wait (ref. 3) even though the two solutions are formally the same.

For a horizontal Hertzian dipole, the scattered field in the mth-layer can be written in terms of $\tilde{g}^s_{xx,m}$ and $\tilde{g}^s_{xz,m}$, which has the following form:

$$\tilde{g}^s_{xx,m} = (Q_o/n_m^2) \iint\limits_{-\infty}^{\infty} \Phi_{x,m}(\xi,\eta)\exp[-\gamma_o H_o + i(\xi X + \eta Y)]d\xi \, d\eta \tag{5a}$$

$$\tilde{g}^s_{xz,m} = (ik_o Q_o/n_m^2)\int\limits_{-\infty}^{\infty}\!\!\!\int \xi\Phi_{z,m}(\xi,\eta)\exp[-\gamma_o H_o + i(\xi X + \eta Y)]d\xi d\eta$$

$$m = 1,2,\ldots M$$

12

where $\gamma_o = (\xi^2 + \eta^2 - 1)^{\frac{1}{2}} = -i(1 - \xi^2 - \eta^2)^{\frac{1}{2}}$; $n_m^2 = \varepsilon_{rm} + \sigma_m/(s\varepsilon_o)$, n_m, ε_{rm} and σ_m are the refractive index, relative permittivity and conductivity of the layered media; ε_o is the permittivity of free space, $Q_o = k_o/(8\pi^2)$ is the normalized dipole strength; $X = k_o x$, $Y = k_o y$ and $H_o = k_o h_o$ are the normalized distances.

Since both components $\tilde{g}_{xx,m}^s$ and $\tilde{g}_{xz,m}^s$ satisfies a homogeneous wave equation of the kind:

$$(\nabla^2 + k_o^2 n_m^2)\tilde{g}_{xw}^s = 0 ; \quad w = x \text{ or } z$$

expression for $\Phi_{x,m}$ and $\Phi_{z,m}$ are then readily known

$$\Phi_{w,m}(z) = T_{w,m}\{\exp[\gamma_m(Z + H_m)] + R_{w,m}^H \exp[-\gamma_m(Z + H_m)]\} \tag{5b}$$

$$w = x,z ; \quad m = 1,2,\ldots M$$

and $\gamma_m = (\xi^2 + \eta^2 - n_m^2)^{\frac{1}{2}}$; $\text{Re}(\gamma_m) \geq 0$; $z = k_o z$ and $H_m = k_o(h_1 + h_2 + \ldots h_m)$ are both normalized distances.

Thus, the values of $\Phi_{w,m}(z)$ and its derivative with z, $\Phi'_{w,m}$ at the top surface of the mth layer, i.e. $Z = -H_{m-1}$, are related to the values at the bottom, i.e. $Z = -H_m$, by the matrix given as

$$\begin{bmatrix} \Phi_{w,m} \\ \Phi'_{w,m} \end{bmatrix}_{Z = -H_{m-1}} = \begin{bmatrix} c_m & \gamma_m^{-1}s_m \\ \gamma_m s_m & c_m \end{bmatrix} \begin{bmatrix} \Phi_{w,m} \\ \Phi'_{w,m} \end{bmatrix}_{Z = -H_m} \tag{5c}$$

Here, the prime denotes derivative ; $c_m = \cosh(\gamma_m H_m)$ and $s_m = \sinh(\gamma_m H_m)$. We now proceed to find $\Phi_{w,m-1}$ in the $(m-1)^{th}$-layer from a knowledge of $\Phi_{w,m}$ in the mth-layer. The boundary conditions at the interface $z = -h_{m-1}$ are

$$k_m^2 \tilde{g}_{xw,m} = k_{m-1}^2 \tilde{g}_{xw,m-1} \qquad w = x,z$$

$$k_m^2 \frac{\partial}{\partial z}\tilde{g}_{xx,m} = k_{m-1}^2 \frac{\partial}{\partial z}\tilde{g}_{xx,m-1}$$

and

$$\frac{\partial}{\partial x}\tilde{g}_{xx,m} + \frac{\partial}{\partial z}\tilde{g}_{xz,m} = \frac{\partial}{\partial x}\tilde{g}_{xx,m-1} + \frac{\partial}{\partial z}\tilde{g}_{xz,m-1}.$$

By applying the above boundary conditions to (5a), (5b) and (5c) we can establish a matrix expression for $\Phi_{x,m-1}$, $\Phi'_{x,m-1}$, $\Phi_{z,m-1}$ and $\Phi'_{z,m-1}$ at one layer in terms of Φ_{xm}, $\Phi_{x,m}$, $\Phi_{z,m}$ and $\Phi_{z,m}$ at the adjacent layer as follows:

$$\left.\begin{bmatrix} \Phi_{x,m-1} \\ \Phi'_{x,m-1} \\ \Phi_{z,m-1} \\ \Phi'_{z,m-1} \end{bmatrix}\right|_{Z = -H_{m-1}} = \begin{bmatrix} c_m & \gamma_m^{-1}s_m & 0 & 0 \\ \gamma_m s_m & c_m & 0 & 0 \\ 0 & 0 & c_m & \gamma_m^{-1}s_m \\ \Delta_m^{-1}c_m & (\gamma_m\Delta_m)^{-1}s_m & \gamma_m\Delta_m s_m & \Delta_m c_m \end{bmatrix} \left.\begin{bmatrix} \Phi_{x,m} \\ \Phi'_{x,m} \\ \Phi_{z,m} \\ \Phi'_{z,m} \end{bmatrix}\right|_{Z = -H_m}$$

(6)

where

$$\Delta_m = n_{m-1}^2/n_m^2$$

Thus the field at any layer interface can be obtained in terms of the field in the bottom layer, i.e. the Mth layer, by successive interation. Let us now define a transverse coupling matrix as follows:

$$\begin{bmatrix} \Phi'_{x,m} \\ \Phi'_{z,m} \end{bmatrix} = \begin{bmatrix} N_m & \tau_m \\ n_m^2\lambda_m & n_m^2 K_m \end{bmatrix} \begin{bmatrix} \Phi_{x,m} \\ \Phi_{z,m} \end{bmatrix}$$

(7)

14

It is interesting to note that N_m, K_m can be considered as the transverse impedance of the TE and TM mode, respectively, in each layer. λ_m and τ_m are the coupling coefficients of these two modes across the interface between the $(m-1)^{th}$ and the mth layer. After the substitution of (7) into (6) and then equating like coefficients for $\Phi_{x,m}$ and $\Phi_{z,m}$, it is possible to obtain a relationship between the transverse coupled impedances at the $(m-1)^{th}$ in terms of the impedances at the mth layer as,

$$N_{m-1} = \gamma_m[N_m + \gamma_m \tanh(\gamma_m H_m)]/[\gamma_m + N_m \tanh(\gamma_m H_m)] \tag{8}$$

$$K_{m-1} = \beta_m[K_m + \beta_m \tanh(\gamma_m H_m)]/[\beta_m + K_m \tanh(\gamma_m H_m)] \tag{9}$$

where in the above result $\beta_m = \gamma_m/n_m^2$. The cross coupling terms λ_m and τ_m are given by

$$\lambda_{m-1} = \lambda_m/W_m + (1 - \Delta_m^{-1})/n_m^2; \quad \tau_{m-1} = \tau_m/W_m \tag{10}$$

where Δ_m can be found in (6) and W_m can be written as follows:

$$W_m = [\gamma_m + N_m \tanh(\gamma_m H_m)][\beta_m + K_m \tanh(\gamma_m H_m)]\cosh^2(\gamma_m H_m)/(\gamma_m \beta_m)$$

$$m = 1,2,\ldots M \tag{11}$$

Since no reflection can occur at the bottom layer, i.e. the Mth layer, this implies $R_{x,M}^H = R_{z,M}^H = 0$ in (5a) then we conclude that $N_M = \gamma_M$; $K_M = \gamma_M/n_M^2$ and $\tau_M = \lambda_M = 0$. Therefore by using (8)-(11) the following information can be obtained;

$$N_{M-1} = \gamma_M ; \quad K_{M-1} = \gamma_M/n_M^2$$

and

$$\lambda_{M-1} = 1/n_M^2 - 1/n_M^2 ; \quad \tau_{M-1} = 0 \tag{12}$$

15

Up to now, the impedances in each of the M layered earth are explicitly known via an iterative procedure based upon (8) - (12). To find the total field in the air region, we note that the electric vector potential of a horizontal dipole in the air region can be written in terms of a primary field plus a scattered one.

$$\tilde{g}_{xw,o} = \tilde{g}^p_{xw,o} + \tilde{g}^s_{xw,o} \qquad w = x,z \qquad (13)$$

p and s refer to primary and scattered field, respectively, and the subscript o refers to air region. $\tilde{g}^p_{x,o}$ and $\tilde{g}^p_{z,o}$ are given by

$$\tilde{g}^p_{xw,o} = Q_o \iint\limits_{-\infty}^{\infty} \gamma_o^{-1} exp[-\gamma_o|Z-H_o| + i(\xi X + \eta Y)]d\xi d\eta \qquad (14)$$

$$\tilde{g}^p_{xz,o} = 0 \qquad (15)$$

The primary field given in (14) and (15) were obtained using the wave equation in free space with a source excitation. The scattered $\tilde{g}^s_{xw,o}$ field can be written as in (5a) and (5b) with $\Phi_{w,o}$ given by

$$\Phi_{w,o} = R^H_{w,o} \; exp(-\gamma_o Z) \qquad w = x,z \qquad (16)$$

Now by applying the boundary conditions at the interface $z = 0$ to (5a), (14),(15) and (16),the following results for the reflection coefficients in free space can be obtained:

$$R^H_{x,o} = \gamma_o^{-1}(\gamma_o - N_o)/(\gamma_o + N_o) \qquad (17)$$

$$R^H_{z,o} = -2\lambda_o[(\lambda_o + N_o)(\lambda_o + K_o)]^{-1} \qquad (18)$$

16

where N_o, K_o and λ_o can be found from (8)-(12) by successive iterations depending on the number of the earth layers. It can be shown that solutions for $R_{x,o}^H$ and $R_{z,o}^H$ are consistent with an earlier work given by Wait (ref.3), even though the concept associated with the coupling coefficient λ_o is not explicitly used in his work.

The derivation of the Hertz vector potential for a vertical dipole is much simpler because only the z-component of the Hertz potential is needed. Thus, following the same procedure previously described, we have

$$\tilde{g}_{zz,o} = \tilde{g}_{zz,o}^p + \tilde{g}_{zz,o}^s \tag{19}$$

where V refers to field due to a vertical dipole, and the primary field $\tilde{g}_{zz,o}$ is given as

$$\tilde{g}_{zz,o}^p = Q_1 \iint_{-\infty}^{\infty} \gamma_o^{-1} \exp[-\gamma_o|Z-H_o| + i(\xi X + \eta Y)] d\xi d\eta \tag{20}$$

and the scattered field $\pi_{z,o}^s$ is given by

$$\tilde{g}_{zz,o}^s = Q_o \iint_{-\infty}^{\infty} \psi_{z,o}(\xi,\eta) \exp[-\gamma_o H_o + i(\xi X + \eta Y)] d\xi d\eta \tag{21}$$

$$\psi_{z,o} = R_{z,o}^V \exp(-\gamma_o Z)$$

and

$$R_{z,o}^V = \gamma_o^{-1}(\gamma_o - K_o)/(\gamma_o + K_o) \tag{22}$$

where K_o can be obtained from (9) by successive iterations.

Now if we write $dx' = \sin\theta'\cos\phi' d\ell$, $dy' = \sin\theta'\sin\phi' d\ell$ and $dz' = \cos\theta' d\ell$ and using the following identities:

17

$$G_{11} = \exp(iR_{11})/R_{11} = (\tfrac{1}{2}\pi)\iint\limits_{-\infty}^{\infty} \gamma_0^{-1}\exp[-\gamma_0|Z-H_0| + i(\xi X + \eta Y)]d\xi d\eta$$

(23)

$$G_{12} = \exp(iR_{12})/R_{12} = (\tfrac{1}{2}\pi)\iint\limits_{-\infty}^{\infty} \gamma_0^{-1}\exp[-\gamma_0(Z+H_0) + i(\xi X + \eta Y)]d\xi d\eta$$

where $R_{11} = [(Z-H_0)^2 + \rho^2]^{\frac{1}{2}}$; $R_{12} = [(Z+H_0)^2 + \rho^2]^{\frac{1}{2}}$ and $\rho = X^2 + Y^2$, we can write from (4b) the three components of the Hertzian vector potential,

$$\tilde{\pi}_x = C(G_{11} - G_{12} + V_2) \sin\theta' \cos\phi'$$

(24)

$$\tilde{\pi}_y = C(G_{11} - G_{12} + V_2) \sin\theta' \sin\phi'$$

(25)

$$\tilde{\pi}_z = C[(G_{11} - G_{12} + V_1) \cos\theta' + V_3 \sin\theta' \cos\phi'$$
$$+ V_4 \sin\theta' \sin\phi']$$

(26)

where $C = iZ_0 Id\ell/(4\pi)$; $Z_0 = \sqrt{\mu_0/\varepsilon_0}$ represents the free space intrinsic impedance, and V_1, V_2, V_3 and V_4 are given by

$$V_m = \int_0^\infty F_m(\alpha) \exp[-\gamma_0(Z + H_0)] J_0(\alpha\rho)_\alpha d\alpha \qquad m = 1,2$$

(27)

$$\begin{pmatrix} V_3 \\ V_4 \end{pmatrix} = \begin{pmatrix} -\cos\phi \\ \sin\phi \end{pmatrix}\int_0^\infty F_3(\alpha) \exp[-\gamma_0(Z+H_0)] J_1(\alpha\rho)\alpha^2 d\alpha$$

(28)

where J_0 and J_1 are the Bessel functions of zero and first order respectively and

$$F_1(\alpha) = 2(\gamma_0 + K_0)^{-1}$$
$$F_2(\alpha) = 2(\gamma_0 + N_0)^{-1}$$

(29)

18

and

$$F_3(\alpha) = -2\lambda_o[(\gamma_o + N_o)(\gamma_o + K_o)]^{-1}$$

In getting V_1, V_2, V_3 and V_4 given in (27) and (28) we have used the following transformations:

$$x = r \cos \phi \; ; \quad y = r \sin \phi$$
$$\xi = \alpha \cos \phi_\alpha \; ; \quad \eta = \alpha \sin \phi_\alpha$$

which implies $\xi^2 + \eta^2 = \alpha^2$ and $\gamma_m = (\alpha^2 - n_m^2)^{\frac{1}{2}}$; Re $\gamma_m \geq 0$, where $m = 0, 1 \ldots M$.

We have listed the field components (E_w, H_w); $w = x$, y, or z, of a dipole arbitrarily oriented in the x - z plane $(\phi' = 0)$ in Table 1 and 2.

Table I gives the field due to the direct contribution of the dipole, designated as (E_{w1}, H_{w1}) with $w = x$, y or z. In order to obtain the field due to the perfect image, designated as (E_{w2}, H_{w2}), one just replaces R_{11} by R_{12} and $(Z-H_o)$ by $(Z + H_o)$ in Table I. In Table 2, we have written the remainder field as a sum of two parts; one contains a Bessel function of zero order J_o and the other has the Bessel function of order one J_1:

$$(E_{w3}, H_{w3}) = \sum_{m=0}^{1} \int_0^\infty (\mathcal{E}_w^m, \mathcal{H}_w^m) \exp[-\gamma_o(Z+H_o)] J_m(\alpha\rho)\alpha\gamma_o^{-1}d\alpha \qquad (30)$$
$$m = 0, \text{ or } 1$$

Thus the total field for each component (E_w^t, H_w^t) is then given as

$$(E_w^t, H_w^t) = (E,H) \sum_{m=1}^{3} (-1)^{m-1} (E_{wm}, H_{wm}) \qquad w = x,y,z \qquad (31)$$

where
$$E = i\zeta_o k_o^2(Id\ell/4\pi) \quad \text{and} \quad H = k_o^2(Id\ell/4\pi).$$

19

TABLE 1

LIST OF PRIMARY FIELD COMPONENTS

	Horizontal Dipole	Vertical Dipole
E_{x1}	$-(1+3i/R_{11}-3/R_{11}^2)[(Z-H_o)\rho\cos\phi/R_{11}^2]G_{11}\cos\theta'$	$-[(1+3i/R_{11}-3/R_{11}^2)(\rho^2\cos^2\phi/R_{11}^2)-1-i/R_{11}+1/R_{11}^2]G_{11}\sin\theta'$
E_{y1}	$-(3+3i/R_{11}-3/R_{11}^2)[(Z-H_o)\rho\sin\phi/R_{11}^2]G_{11}\cos\theta'$	$-(1+3i/R_{11}-3/R_{11}^2)(\rho^2\sin\phi\cos\phi/R_{11}^2)\,G_{11}\sin\theta'$
E_{z1}	$-[(1+3i/R_{11}-3/R_{11}^2)(Z-H_o)^2/R_{11}^2-1-i/R_{11}+1/R_{11}^2]G_{11}\cos\theta'$	$-(1+3i/R_{11}-3/R_{11}^3)[(Z-H_o)\rho\cos\phi/R_{11}^2]G_{11}\sin\theta'$
H_{x1}	$(i-1/R_{11})(\rho\sin\phi/R_{11})G_{11}\cos\theta'$	0
H_{y1}	$-(i-1/R_{11})(\rho\cos\phi/R_{11})G_{11}\cos\theta'$	$(i-1/R_{11})[(Z-H_o)/R_{11}]G_{11}\sin\theta'$
H_{z1}	0	$-(i-1/R_{11})(\rho\sin\phi/R_{11})G_{11}\sin\theta'$

$$G_{11} = \exp(iR_{11})/R_{11}$$ as given in equation (24)

20

TABLE 2

LIST OF GROUND CORRECTION FIELD COMPONENTS

w	$\mathcal{E}_w^0$	$\mathcal{E}_w^1$
x	$\gamma_o[F_2 - (F_2 - \gamma_o F_3)\alpha^2\cos^2\phi]\sin\theta'$	$\alpha\gamma_o\{[(F_2 - \gamma_o F_3)/\rho]\cos(2\phi)\sin\theta' + \gamma_o F_1\cos\phi\cos\theta'\}$
y	$-(\gamma_o\alpha^2/2)[F_2 - \gamma_o F_3]\sin(2\phi)\sin\theta'$	$\alpha\gamma_o\{[(F_2 - \gamma_o F_3)/\rho]\sin(2\phi)\sin\theta' + \gamma_o F_1\sin\phi\cos\theta'\}$
z	$\gamma_o(\gamma_o^2 + 1)F_1\cos\theta'$	$\alpha\gamma_o[\gamma_o(F_2 - \gamma_o F_3) - F_3]\cos\phi\sin\theta'$

w	$\mathcal{H}_w^0$	$\mathcal{H}_w^1$
x	$-(\alpha^2\gamma_o^2/2)F_3\sin(2\phi)\sin\theta'$	$\alpha\gamma_o[(F_3/\rho)\sin(2\phi)\sin\theta' - F_1\sin\phi\cos\theta']$
y	$\gamma_o[-\gamma_o F_2 + \alpha^2 F_3\cos^2\phi]\sin\theta'$	$\alpha\gamma_o[-(F_3/\rho)\cos(2\phi)\sin\theta' + F_1\cos\phi\cos\theta']$
z	0	$\alpha\gamma_o F_2\sin\phi\sin\theta'$

$$(E_{w3}, H_{w3}) = \frac{1}{2}\sum_{m=0}^{1}\int_0^\infty (\mathcal{E}_w^m, \mathcal{H}_w^m)\exp[-\gamma_o(Z+H_o)]\, J_m(\alpha\rho)\alpha\gamma_o^{-1}\, d\alpha \;;\; F_m, \; m=1,2,3 \text{ are given in (29)}$$

$$w = x, y, z$$

21

SECTION III

NUMERICAL SCHEME

In this section we discuss the numerical method used for the computation of those integrals listed in table 2. Our primary concern is to compute all six field components for a two-layer earth representing a slab of lossy dielectric which has the electric constants of a nonreinforced concrete and is located above a homogeneous earth having electric property of a wet dirt. A typical integral form can be written as follows:

$$Q = \int_0^\infty T(\alpha) \alpha \gamma_0^{-1} \, d\alpha \tag{32}$$

where $T(\alpha)$ is given by

$$T(\alpha) = G(\alpha) \exp[-\gamma_0(Z + H_0)] J_m(\alpha\rho); \quad m = 0,1$$

and $G(\alpha)$ is a typical function listed in table 2, which has poles and other algebraic singularities in the complex α-plane. Typically the integrand in (32) has branch cut singularities due to $\gamma_0 = (\alpha^2 - 1)^{\frac{1}{2}}$ and another due to $\gamma_2 = (\alpha^2 - n_2^2)^{\frac{1}{2}}$; γ_0 and γ_2 are the normalized propagation constants along the z-direction for the two infinite layers $0 \le z < \infty$ and $-\infty < z < -h_1$, respectively, where h_1 is the width of the slab in a two layered earth media. The integration given in (32) can be split up into two parts.

$$Q = \left[\int_0^1 + \int_1^\infty \right] T(\alpha) \alpha \gamma_0^{-1} d\alpha \tag{33}$$

and by using the transformation $\tau = (1 - \alpha^2)^{\frac{1}{2}}$ in the first term of (33) and $\tau = (\alpha^2 - 1)^{\frac{1}{2}}$ in the second term, Q can be reduced to the following form:

$$Q = i \int_0^1 T[1 - \tau^2]^{\frac{1}{2}} d\tau + \int_0^\infty T([1 + \tau^2]^{\frac{1}{2}}) d\tau \tag{34}$$

22

The form of Q given in (34)   is   used in our computation algorithms

discussed in   appendix C. We note that, in a similar work by Lytle and Lager

(ref. 4), a deformed path was used beneath the real axis as shown in figure 2.

While such a deformation avoids the numerical difficulties

arising from possible poles and other discontinuities close to the real axis,

it necessitates the use of a Bessel function with complex argument. Since

the value of the Bessel function grows exponentially for a large but complex

argument, it appears such a deformation would not be a particularly efficient

one when the horizontal distance is substantially greater than the free space

wavelength unless it is very close to the real axis.
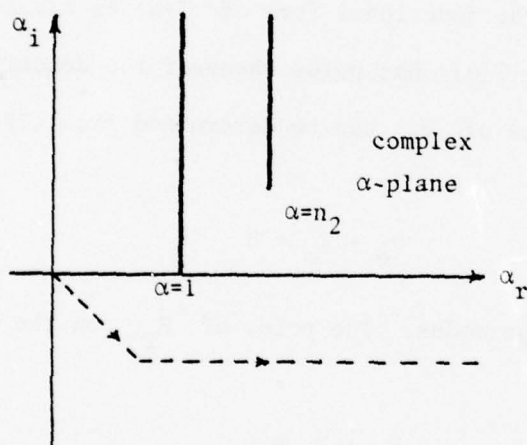
Figure 2: A path beneath the real axis avoiding the branch
            point at $\alpha = 1$ and pole singularities close to
            the real axis.

Lytle and Lager (ref.4) pointed out that one way to avoid such a problem
is to use a deformed path formulation based upon a maximum decay and, or
minimum oscillation criteria. Actually, the use of the steepest-descent
path as a function of observation angle is another appropriate alternative
[Kong (ref. 6), Banõs (ref. 8)]. In any case, the extension of such an approach
to a multilayered earth would involve the inclusion of contribution from
possible singularities as a result of the deformation of the path.

We next consider the pole locations of $T(\alpha)$ in the complex α-plane particularly those, if any, close to the path of integration on the real axis in the range $1 \le \alpha_r < \infty$ (with the choice of branch cuts shown in Figure 3, pole(s) located in the range $0 < \alpha_r < 1$ is less significant since it would have to be on the other side of the cut in the same Riemann sheet and, hence, can influence the integrand value only indirectly through the contribution around the branch point). The strategy that we have adopted is first to determine possible existence of poles, then for each pole which is close to the real axis, we would define a circle of influence within which smaller partition of the integral is adopted to insure the accuracy of the numerical integration.

By investigating the functional form of $T(\alpha)$ as tabulated in table 2, it is easy to see that $T(\alpha)$ has poles whenever the denominator of F_1 or F_2 vanishes. The poles of F_1 can be determined from (29) as the root of the following equation:

$$\gamma_o + K_o = 0 \tag{35}$$

and they are the TM-type modes. The poles of F_2, on the other hand, can be found from

$$\gamma_o + N_o = 0 \tag{36}$$

corresponding to a set of TE-type modes. By using the relationships given in (8) through (12) for a two-layer earth, a more explicit representation of (35) and (36) is

$$[\gamma_o \gamma_2 H_1^2/n_2^2 - Z^2] \tan Z + (Z/n_1^2)[\gamma_o H_1 + \gamma_2 H_1/n_2^2] = 0 \tag{37}$$

24
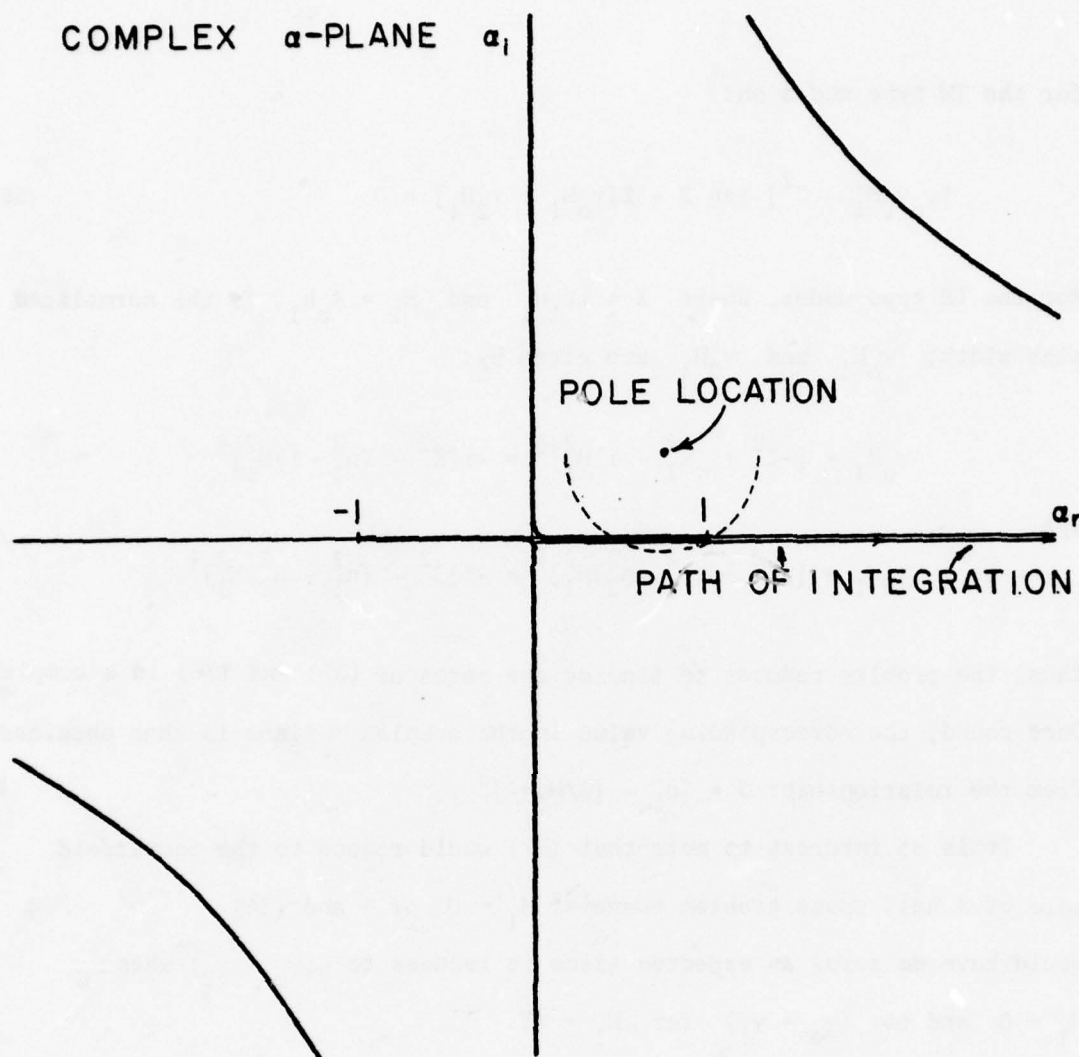
Figure 3 - Path of integration in the complex α-plane

25

for the TM type modes and

$$[\gamma_o \gamma_2 H_1^2 - Z^2] \tan Z + Z[\gamma_o H_1 + \gamma_2 H_1] = 0 \qquad (38)$$

for the TE type modes, where $Z = i\gamma_1 H_1$ and $H_1 = k_o h_1$ is the normalized slab width; $\gamma_o H_1$ and $\gamma_2 H_1$ are given by:

$$\gamma_o H_1 = [-Z^2 + (n_1^2 - 1)H_1^2]^{\frac{1}{2}} = -i[Z^2 - (n_1^2 - 1)H_1^2]^{\frac{1}{2}}$$

and

$$\gamma_2 H_1 = [-Z^2 + (n_1^2 - n_2^2)H_1^2]^{\frac{1}{2}} = -i[Z^2 - (n_1^2 - n_2^2)H_1^2]^{\frac{1}{2}}$$

Thus, the problem reduces to finding the zeros of (37) and (38) in a complex Z-plane. Once found, the corresponding value in the complex α-plane is then obtained from the relationship: $\alpha = [n_1^2 - (Z/H_1)^2]^{\frac{1}{2}}$.

It is of interest to note that (35) would reduce to the Sommerfeld pole of a half space problem whenever $H_1 \rightarrow 0$ or ∞ and (36) would have no zeros as expected since it reduces to $(\gamma_o + \gamma_2)$ when $H_1 \rightarrow 0$ and to $(\gamma_o + \gamma_i)$ for $H_1 \rightarrow \infty$.

In the case of $\sigma_2 \rightarrow \infty$ or where the second earth layer is a perfect conductor, equations (37) and (38) reduce to

$$-[(n_1^2 - 1)H_1^2 - Z^2]^{\frac{1}{2}} + (Z/n_1^2)^{\frac{1}{2}} \tan Z = 0 \qquad (39)$$

for the TM-type modes and

$$Z + [(n_1^2 - 1)H_1^2 - Z^2]^{\frac{1}{2}} \tan Z = 0 \qquad (40)$$

for the TE-type modes. Thus for a lossless slab where n_1 is a real quantity, (39) and (40) represent a set of even TM-type and odd TE-type surface wave modes, respectively. These real roots are then used as a starting value in

26

the search of the complex roots when the conductivities of earth and slab are finite. The computational technique for finding these roots is described in appendix C.

We have plotted in figure 4a location of the pole corresponding to the TM_1-mode over a frequency range from 100 to 370 MHz, for a cement slab ($\varepsilon_{r1} = 3$ and $\sigma_1 = 0.002$ mho/m) of width $h_1 = 10$ cm over a wet earth ($\varepsilon_{r2} = 10$, $\sigma_2 = 0.01$ mho/m). As frequency increases, the pole moves upward and the branch cut moves downward. At about 400 MHz the pole disappears in the next Riemann surface. If we now reduce the slab width gradually, but fix the operating frequency at 400 MHz as shown in figure 4b, the pole reappears in the proper sheet when the slab width is reduced to 9 cm, and continuously moves downward as width decreases. At $h_1 = 0$, it reduces to a Sommerfeld pole for a half space region. (The disappearance, followed by a reappaerance, of a slab mode was also observed earlier in related work by Shevchenko (ref.9)]. It is noteworthy that equation (38) presents no TE-type of solution until the slab width is greater than 10 cm. In table 3, we have tabulated the locations of both TE and TM modes for h_1 ranging from 10 cm to 50 cm. It is obvious that those poles which are far away from the real axis should present no real problem for our numerical computation of the Q-integrals.

Except for the region with the possible appearance of a simple pole, the path of integration in (34) is subdivided basically according to the extent of oscillation associated with the Bessel function and the rate of decay of the exponential function in the integrand. The finite integral is then truncated at a value of τ where either the integral beyond that point is negligible, or an analytical approximation to the remainder is possible. Incorporation of this scheme is detailed in appendix C.

27

TABLE 3

ROOTS AS A FUNCTION OF SLAB WIDTH AND FREQUENCY

Frequency MHz	h_1 = 10 cm	h_1 = 20 cm	h_1 = 30 cm	h_1 = 50 cm
100	TM 0.954452 + i·0378452	TM 0.950803 + i·0770147	TM 0.933858 + i·137896	TM 1.14523 + i·505429
	TM 0.951733 + i·0728692	TM 0.918351 + i·298208		TM 1.52873 + i·25662
200			TE 0.981837 + i·253395	TE 1.37374 + i·150405
	TM 0.942977 + i·13541	TE 0.986075 + i·235745	TE 1.31183 + i·155028	TM 1.0953 + i·212372
300				TE 1.5402 + i·0747219
				TM i·60042 + i·152418

28
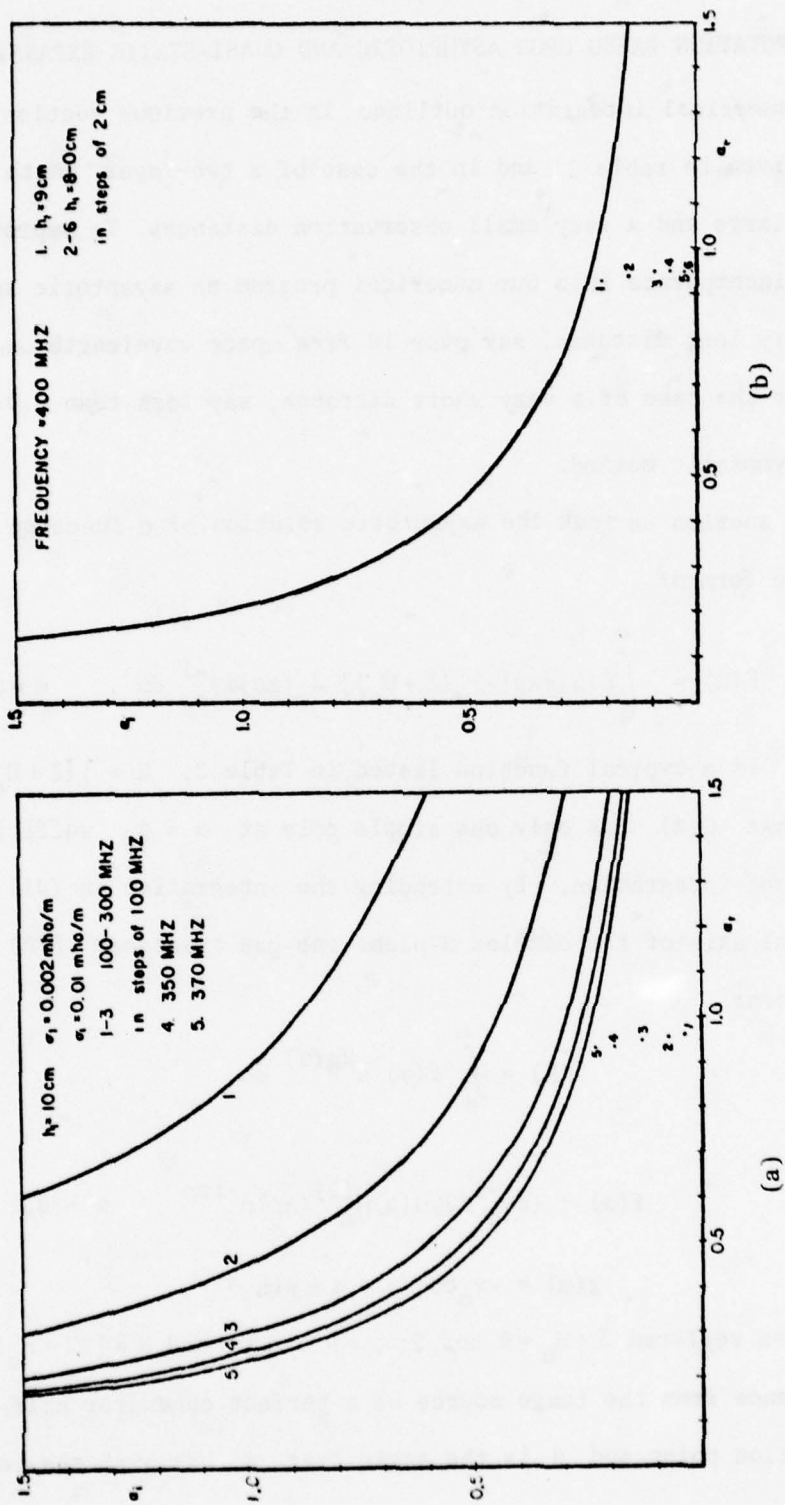
Figure 4: (a) Location of poles and branch cuts as a function of frequency for a fixed slab width.
(b) Location of poles as a function of slab width for a fixed frequency.

COMPUTATION BASED UPON ASYMPTOTIC AND QUASI-STATIC EXPANSIONS

The numerical integration outlined in the previous section for the functions given in table 2 and in the case of a two-layer earth is inefficient for very large and a very small observation distances. To improve the efficiency we need to incorporate into our numerical program an asymptotic solution for the case of a very long distance, say over 10 free space wavelengths, and a quasi-static solution for the case of a very short distance, say less than 0.01 wavelength.

1. Asymptotic method.

In this section we seek the asymptotic solution of a function $\Gamma(R)$ in the form of

$$\Gamma(R) = \int_0^\infty G(\alpha) \exp[-\gamma_0(Z + H_0)] \, J_m(\alpha\rho)\alpha\gamma_0^{-1} \, d\alpha \, , \quad m = 0 \text{ or } 1 \tag{41}$$

where $G(\alpha)$ is a typical function listed in Table 2, $R = [(Z + H_0)^2 + \rho^2]^{\frac{1}{2}}$. *
We assume that $G(\alpha)$ has only one simple pole at $\alpha = \alpha_p$ sufficiently close to the path of integration. By extending the integration in (41) over the negative real axis of the complex α-plane one can transform $\Gamma(R)$ into the following form:

$$\Gamma(R) = \int_{-\infty}^\infty f(\alpha) \, e^{Rg(\alpha)} \, d\alpha \tag{42}$$

where

$$f(\alpha) = (\alpha\gamma_0^{-1}/2)G(\alpha)H_m^{(1)}(\alpha\rho)e^{-i\alpha\rho} \, , \quad m = 0,1 \tag{43}$$

$$g(\alpha) = -\gamma_0\cos\theta + i\,\alpha\sin\theta \tag{44}$$

where we have replaced $Z + H_0 = R\cos\theta$; $\rho = R\sin\theta$; and $R = [(Z + H_0)^2 + \rho^2]^{\frac{1}{2}}$ is the distance from the image source of a perfect conductor half-space to the observation point and θ is the angle that R has with the vertical z-axis.

---

* In what follows, R_{12} will be replaced by R.

$H_m^{(1)}(\alpha\rho)$ given in (43) is the Hankel function of the first kind of m order. It has been assumed that $G(\alpha)$ is an even function of α whenever the order of Bessel function $J_m(\alpha\rho)$ is even and odd function of whenever the Bessel function order is odd.

In order to develop an appropriate asymptotic expansion, we now follow the work of Brekhovskikh (ref.10) by deforming the contour of integration from the real axis to the steepest descent path in the complex α-plane passing through a saddle point α_s where $g'(\alpha_s)=0$. Assuming such a deformation yields no additional residue contribution and defining a real variable s along the steepest descent path so that $s^2 = g(\alpha_s) - g(\alpha)$, we have the following expression

$$\Gamma(R) = e^{Rg(\alpha_s)} \int_{-\infty}^{\infty} \phi(s)\ e^{-Rs^2} ds$$

where $\phi(s) = f(\alpha)\dfrac{d\alpha}{ds}$. From (44), it is not difficult to show that $\alpha_s = \sin\theta$ so that $g(\alpha_s) = i$. Now since we have assumed the existance of a pair of poles at $\alpha = \pm\alpha_p$ in the complex α-plane, the expression $\phi(s)$ also possesses a pair of poles in the complex s-plane located correspondingly at $s = \pm\beta$ where

$$\beta = [g(\alpha_s) - g(\alpha_p)]^{\frac{1}{2}} = e^{i\pi/4}[1 - (1-\alpha_p^2)^{\frac{1}{2}}\cos\theta - \alpha_p\sin\theta]^{\frac{1}{2}}$$

Thus, we can rearrange the expression for $\Gamma(R)$ in the form of

$$\Gamma(R) = e^{iR} \int_{-\infty}^{\infty} \psi(s)\ \frac{e^{-Rs^2}}{s^2-\beta^2}\ ds \tag{45}$$

The term $\psi(s) = (s^2-\beta^2)\phi(s)$ is then a smooth function near the saddle

31

point $s=0$ and therefore can be expanded in Taylor series as

$$\psi(s) = \sum_{n=0}^{\infty} \frac{C_n}{n!} s^n$$

Substitution of this expression into (45) and subsequent evaluation of the individual integrals yield the following asymptotic expression

$$\Gamma(R) = 2\pi^{\frac{1}{2}} e^{iR} e^{-u^2} \sum_{n=0}^{\infty} \frac{C_{2n}}{4^n n! R^{n-\frac{1}{2}}} Q_{2n}(u)$$ (46)

where

$$Q_{2n}(u) = \int_{u}^{i\infty} \frac{e^{x^2}}{x^{2m}} dx$$

and $u = \pm\beta\sqrt{R}$ and, again, $R = R_{12}$. Typically, only two terms are used in our computation. The coefficients C_0 and C_2, in this case, are known explicitly in terms of $f(\alpha)$, $g(\alpha)$ and their derivatives [Brekhovskikh (ref.10) and Felson and Marcuvitz (ref.11)],

$$C_o = \psi(0) = -\beta^2 \phi(0)$$

$$\tfrac{1}{2}C_2 = \psi''(0)/2 = -\beta^2 \frac{\phi(0)}{f(0)} \left\{ \frac{g'''}{(g'')^2} f'(0) - \frac{f''(0)}{g''} \right.$$

$$\left. + \left[\frac{1}{4} \frac{g^{IV}}{(g'')^2} - \frac{5}{12} \frac{(g''')^2}{(g'')^3} - \frac{1}{\beta^2} f(0) \right] \right\}$$

Here, the primes denote derivatives with respect to α. Now, since

$$\left. \frac{d\alpha}{ds} \right|_{s=0} = 2^{\frac{1}{2}} e^{-i\pi/4} \cos\theta$$

along the steepest descent path we have from (44) and the definition that $f(\alpha)(d\alpha/ds) = \Phi(s)$ the following expression

$$C_o = -\beta^2 (2^{\frac{1}{2}} e^{-i\pi/4} \cos\theta) f(0)$$ (47)

32

$$\tfrac{1}{4}C_2 = j \, 2^{\frac{1}{2}} e^{-i\pi/4} \cos\theta\{3\sin\theta \, f'(0) - \cos^2\theta \, f''(0) + (3/4 + j/\beta)f(0)\} \qquad (48)$$

Here we note that, because the function f typically behaves like $(\alpha_o + \Omega)^{-1}$, where Ω is some slowly varying function around $\gamma_o \approx 0$, its derivatives are singular at $\alpha = 1$ even though the value of C_2 is finite. Thus, in order to avoid the difficulty in numerical computation, we can define a new variable $\alpha = \sin w$ so that

$$\tfrac{1}{4}C_2 = - (1+j)\beta^2 \left\{ 2 \sin\theta \left.\frac{df}{dw}\right|_{w=\theta} - \cos\theta \left.\frac{d^2 f}{dw^2}\right|_{w=\theta} \right.$$

$$\left. + (3/4 + j/\beta^2) f(w=\theta) \cos\theta \right\} \qquad (49)$$

and f is given in (43).

2. Quasi-Static approximation

We have mentioned earlier that the typical numerical computation of the field integral becomes very time consuming when an observation distance is much smaller than a wavelength. Due to the slow convergence of the exponential and Bessel function the numerical computation of the integral in (30) needs to be carried out for excessively large values of α.

Obviously, for a two layered earth, N_o and K_o as found in (8) and (9) can be approximated by

$$K_o \approx \gamma_o/n_1^2$$

$$N_o \approx \gamma_o$$

for those values of α where

$$\alpha \geq \max(6/H_1, \, 10|n_1|)$$

Thus, the leading terms of $F_\ell(\alpha)(\ell = 1,2,3)$ as given in (29) will behave as

$$F_{\ell q} = B_\ell \gamma_0^{-1} \qquad \ell = 1,2$$

$$F_{3q} = B_3 \gamma_0^{-2}$$

where $B_1 = 2n_1^2/(n_1^2 + 1)$, $B_2 = 1$ and $B_3 = (n_1^2 - 1)/(n_1^2 + 1)$.

The subscript q refers to quasi-static.

We can now add and subtract these terms to the original integrals given in (27) and (28) and write the Sommerfeld integrals as follows

$$V_\ell = V_\ell^{(1)} + V_\ell^{(2)} + \Delta V_\ell \tag{50}$$

where

$$V_\ell^{(1)} = B_\ell \int_0^\infty e^{-\gamma_0 b} J_0(\alpha\rho) \alpha \gamma_0^{-1} d\alpha$$

$$V_\ell^{(2)} = \int_{\alpha_0}^\infty [F_\ell(\alpha) - F_{\ell q}(\alpha)] e^{-\gamma_0 b} J_0(\alpha\rho) \alpha d\alpha$$

and $\Delta V_\ell = \displaystyle\int_0^{\alpha_0} [F_\ell(\alpha) - F_{\ell q}(\alpha)] e^{-\gamma_0 b} J_0(\alpha\rho) \alpha d\alpha$ \hfill (51)

where $\alpha_0 = \max(6/H_1, 10|n_1|)$, $b = Z + H_0$ and $\ell = 1$ or 2.
The leading integral $V_\ell^{(1)}$ is known explicitly from (24) in terms of G_{12} as

$$V_\ell^{(1)} = B_\ell \frac{e^{iR}}{R} \tag{52}$$

The integral ΔV_ℓ, integrating from 0 to α_0 still needs to be evaluated numerically in the usual manner. However, the remaining integral $V_\ell^{(2)}$ can be obtained analytically since now the integrand converges rapidly as $F_\ell(\alpha)$ approaches $F_{\ell q}(\alpha)$ for large α. This integral is evaluated in Appendix A with the result given as

$$V_\ell^{(2)} = C_\ell \{b \ln(R+b) - R \quad [\gamma + \ln(\alpha_0/2)/]b - e^{-\alpha_0 b}/\alpha_0\} \qquad \ell = 1,2 \tag{53}$$

34

where $C_1 = 2n_1^2/(n_1^2 + 1)$, $C_2 = (n_1^2-1)/4$; and $\gamma \approx 0.57721566$ is Euler's constant.

Similarly, we can split up the expression for V_3 given in (28) in the following form

$$V_3 = V_3^{(1)} + V_3^{(2)} + V_3^{(3)} + \Delta V_3 \tag{54}$$

where

$$V_3^{(1)} = B_3 \cos \theta \frac{\partial}{\partial \rho} \int_b^\infty db \int_0^\infty e^{-\gamma_o b} J_o(\alpha \rho) \alpha \gamma_o^{-1} d\alpha$$

$$V_3^{(2)} = B_3 \cos \theta \frac{\partial}{\partial \rho} \int_{\alpha_o}^\infty [\frac{1}{\gamma_1^2} - \frac{1}{\gamma_o^2}] e^{-\gamma_o b} J_o(\alpha \rho) \alpha d\alpha$$

$$V_3^{(3)} = B_3 \cos \theta \frac{\partial}{\partial \rho} \int_{\alpha_o}^\infty [F_3(\alpha) - B_3 \gamma_1^{-2}] e^{-\gamma_o b} J_o(\alpha) \alpha d\alpha$$

and finally

$$\Delta V_3 = B_3 \cos \theta \frac{\partial}{\partial \rho} \int_0^{\alpha_o} [F_3(\alpha) - B_3 \gamma_1^{-2}] e^{-\gamma_o b} J_o(\alpha \rho) \alpha d\alpha \tag{55}$$

We note that in (54) an additional term $B_3 \gamma_1^{-2}$ has been added and subtracted instead of just adding and subtracting $B_3 \gamma_o^{-2}$. The reason for this kind of arrangement is to avoid the singularity at $\alpha = 1$ when we integrate numerically from 0 to α_o along the real axis in the complex α-plane. On the other hand, in the analytical evaluation of $V_3^{(2)}$, the path of integration is to be understood as being indented into the lower half plane around the branch point at $\alpha = 1$.

A similar technique as applied to $V^{(2)}$ can be applied to the different terms of V_3. Analytical expression for $V_3^{(1)}$ is derived in appendix B as

$$V_3^{(1)} = -B_3 \rho \cos \theta \{ [R(R+b)]^{-1} - 0.5) \ell n (R+b) - \frac{1}{2}(\gamma - \frac{1}{2} - \pi i/2 - \ell n\ 2)\} \tag{56}$$

35

Thus, the leading term of V_3 behaves as $1/R$, which is similar to the leading terms of V_1 and V_2. On the other hand, analytical expressions for $V_3^{(2)}$ and $V_3^{(3)}$ are known as (Appendix B).

$$V_3^{(2)} = \frac{(n_1^2 - 1)}{2} B_3 \rho \cos \theta \left[b(R+b)^{-1} + \left(\gamma - \tfrac{1}{2} - \pi i/2 - \ell n 2 + \frac{n_1^2}{(n_1^2 - 1)} \ell n \, n_1 \right) \right.$$
$$\left. + \ell n (R+b) \right] \tag{57}$$

and

$$V_3^{(3)} = -C_3 \rho \cos \phi [\ell n (b+R) + b(R-B)^{-1} + (\gamma - \tfrac{1}{2} - \ell n \, 2 + \ell n \, \alpha_0)] \tag{58}$$

where $C_3 = (3n_1^2 + 1)(n_1^2 - 1)^2 (n_1^2 + 1)^{-2}/8$ and γ is Euler's constant. The last term ΔV_3 will be evaluated numerically. We note that, once all the V's are found and then substitute in (25) and (26), expressions for the field components are then carried out analytically according to (29a).

36

SECTION V

DISCUSSION OF RESULTS

A computer program was developed for the computation of the
frequency-domain electromagnetic response of an electric dipole located
above a two-layer earth representing a non reinforced concrete slab on the
surface of a dissipative earth. The program computes all three components
of the electric and magnetic fields simultaneously for an arbitrarily oriented
dipole with a known dipole moment. Unless otherwise specified, the dipole
source is assumed to be always located along the vertical axis at a given
height h_o. Geometry indicating relative positions of the source and
observation points is shown in figure 5. Also, relevant parameters for
the computations in this section are chosen as follows.

Frequency of operation = 300 MHz

Relative dielectric constant and conductivity in

1) Air, $(\varepsilon_{ro}, \sigma_o) = (1.0, \quad 0.00)$

2) Cement slab, $(\varepsilon_{r1}, \sigma_1) = (3.0, \quad 0.002)$

3) Earth, $(\varepsilon_{r2}, \sigma_2) = (10.0, \quad 0.01)$

Slab width h_1 0.1 m

In order to check the numerical accuracy of the program, we have first
computed the vertical electric field component due to a vertical dipole
above a homogenous dissipative earth, for which the analytical solution as
well as the numerical solution is available [Chang and Wait(ref.12), Chang and
Fisher (ref.13)]. Accuracy to within 5 digits is achieved for any given distance.

Next, asymptotic expansion of the exact Sommerfeld integrals for high-
angle observations is used to compare with results obtained numerically for
the case when the observation point is located on the slab surface at a fixed
observation angle $\theta = 5°$. We vary the separation between the source and the

37

$$R_{11} = \left[(z-h_0)^2 + r^2\right]^{1/2}$$
$$R_{12} = \left[(z+h_0)^2 + r^2\right]^{1/2}$$
$$d\ell' = \left[(dx')^2 + (dz')^2\right]^{1/2}$$

Observation Point
$P(x, y, z)$

r

R_{11}

θ'

Idz'

$Id\ell'$ R_{12}

Idx'

Air

$(\epsilon_0, \mu_0, \sigma_0 = 0)$

h_0

O

x

Non-reinforced
Concrete Slab

h_0

θ

h_1 $(\epsilon_1, \mu_0, \sigma_1)$

Earth

$(\epsilon_2, \mu_0, \sigma_2)$
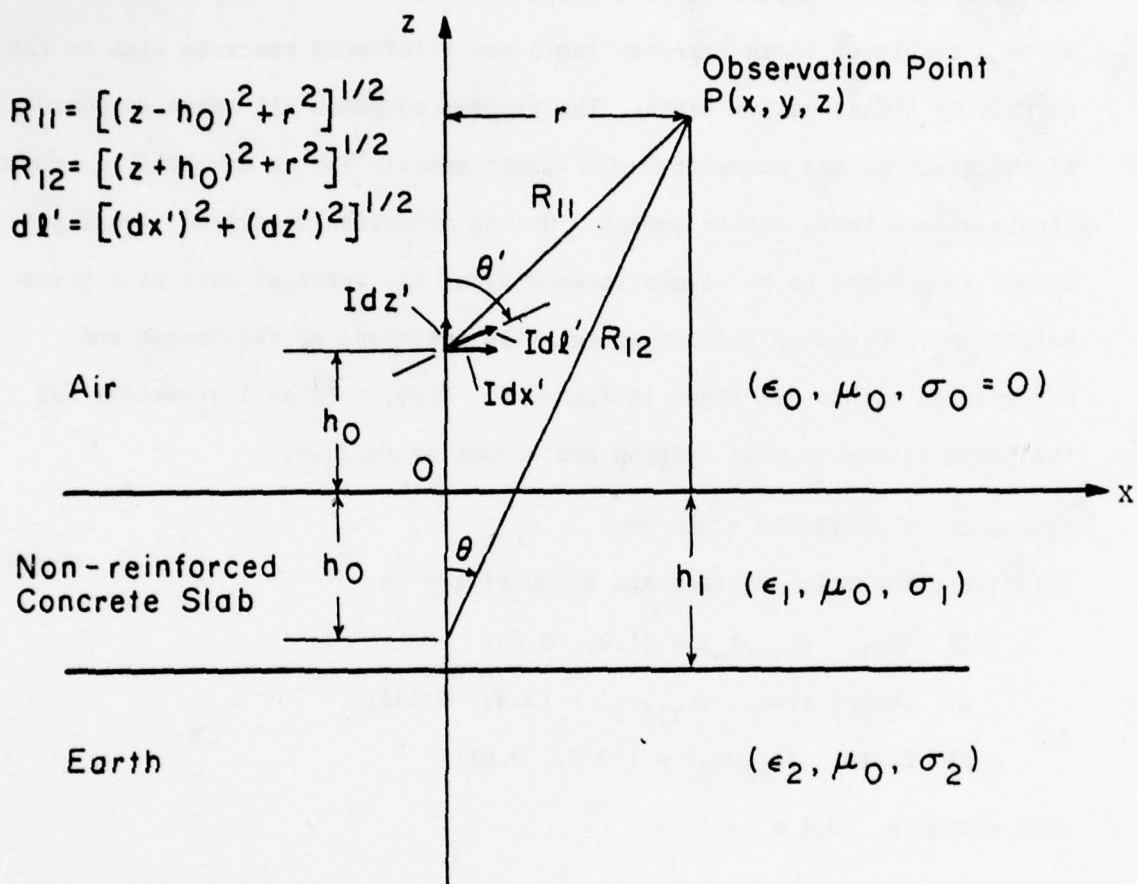
Fig. 5: A tilted dipole above a two layer half-space.

observation point and the result is shown in tables 4 through 9 together with the
sky-wave (plane wave) solution for three different orientations of
sources, a vertical dipole (Case I); a horizontal dipole ibserved in
the plane of the dipole (Case II); and a horizontal dipole observed in the
plane perpendicular to the dipole (Case III). Our results from the exact evalu-
ation of the Sommerfeld integrals are all within a fraction of a percent for
distances about 5 meters or larger (in this case, a free-space wavelength
is 1 meter). Only when the distance drops to within 1 meter do the
two results show any significant difference.

Comparison is also made for a fixed observation distance $R = 40$ meters,
($R = R_{12}$), and a varying observation angle ranging from $5°$ to $80°$ (tables 10
through 12). The agreement is again excellent until the observation angle is
near grazing (i.e. the case when $\theta = 80°$). This is obviously due to the
limitation of the sky-wave solution near the slab surface.

The electromagnetic field components as obtained by a two-term
asymptotic expansion with the inclusion of the contribution from the ground
wave correction (see Section IV.1) are tabulated in table 13 for angles
$\theta = 30°$, $45°$ and $80°$ and $R = 40$ meters. Clearly, these results with
ground wave corrections are now in good agreement with the exact numerical
results given in tables 10 through 12. We note, however, that computation
time for the asymptotic result is much less than the time spent in evaluating
the exact Sommerfeld integrals.

Comparison of the quasi-static and exact results is shown in Table 14
for $R = 0.005$ meter and $\theta = 4.5°$. As a rule of thumb, the time consumed
in computing the quasi-static result is less than one third the time spent
in getting the exact answer.

COMPARISON OF THE EXACT DIPOLE SOLUTIONS WITH THE PLANE WAVE SOLUTIONS
FOR R = 40 M and θ = 5°

TABLE 4

FREQUENCY = 3.00E+08 C/S
REFRACTIVE INDICES OF AIR, CEMENT AND EARTH RESPECTIVELY
NO= 1.0600+J 0.0000   EPSRO= 1.0E+00 SIGMA0= 0.
N1= 1.7324+J .0346   EPSR1= 3.0E+00 SIGMA1= 2.000E-03
N2= 3.1637+J .0947   EPSR2= 1.0E+01 SIGMA2= 1.000E-02

Z= 0.   M   OBSERVATION HEIGHT
H0=3.985E+01 M   DIPOLE HEIGHT
H1=1.000E-01 M   SLAB WIDTH
R= 4.000E+01 M   SOURCE TO OBSERVATION DISTANCE
THETA= 5.0 DEG   ANGLE OF INCIDENCE

	PLANE WAVE SOLUTION	EXACT DIPOLE SOLUTION	RELATIVE DIF.
Case I	PARALLEL POLARIZATION	VERTICAL DIPOLE	
EX=	3.056898E-02+J 3.7030096E-01	3.097773E-02+J 3.703326E-01	1.10164E-03
EZ=	2.400224E-02+J 5.427249E-02	2.394655E-02+J 5.430786E-02	1.11149E-03
HY=	4.743142E-04+J-1.160146E-03	4.754081E-04+J-1.160098E-03	8.73337E-04
Case II	PARALLEL POLARIZATION	HORIZONTAL DIPOLE	
EX=	3.832980E-01+J 4.229588E+00	3.802394E-01+J 4.227314E+00	8.98025E-04
EZ=	-1.814701E-01+J 4.339812E-01	-1.818789E-01+J 4.339581E-01	8.70079E-04
HY=	5.421436E-05+J-1.326053E-02	5.413494E-03+J-1.326665E-02	6.99900E-04
Case III	PERPENDICULAR POLARIZATION	HORIZONTAL DIPOLE	
EX=	3.907456E-01+J 4.251730E+00	3.876019E-01+J 4.249454E+00	9.09567E-04
HY=	5.434058E-03+J-1.328765E-02	5.426073E-03+J-1.329364E-02	6.95111E-04
EZ=	-9.039869E-05+J-9.8363337E-04	-8.650202E-05+J-9.814461E-04	4.53562E-03

40

TABLE 5

COMPARISON OF THE EXACT DIPOLE SOLUTIONS WITH THE PLANE WAVE SOLUTIONS
FOR R = 20 M and θ = 5°

FREQUENCY = 3.00E+08 C/S
REFRACTIVE INDICES OF AIR, CEMENT AND EARTH RESPECTIVELY
N0= 1.0000+J 0.0000   EPSR0= 1.0E+00   SIGMA0= 0.
N1= 1.7324+J .0346   EPSR1= 3.0E+00   SIGMA1= 2.000E-03
N2= 3.1637+J .0947   EPSR2= 1.0E+01   SIGMA2= 1.000E-02

Z= 0.   M   OBSERVATION HEIGHT
H0= 1.992E+01 M   DIPOLE HEIGHT
H1= 1.000E-01 M   SLAB WIDTH
R= 2.000E+01 M   SOURCE TO OBSERVATION DISTANCE
THETA= 5.0 DEG   ANGLE OF INCIDENCE

	PLANE WAVE SOLUTION	EXACT DIPOLE SOLUTION	RELATIVE DIF.
Case I	PARALLEL POLARIZATION	VERTICAL DIPOLE	
EX=	1.163509E-01+J 7.340270E-01	1.180111E-01+J 7.339473E-01	2.23592E-03
EZ=	1.383776E-01+J 1.299066E-01	1.381797E-01+J 1.302282E-01	1.98841E-03
HY=	7.535151E-04+J-2.390850E-03	7.579462E-04+J-2.391171E-03	1.77109E-03
Case II	PARALLEL POLARIZATION	HORIZONTAL DIPOLE	
EX=	1.463992E+00+J 8.366519E+00	1.45;;00E+00+J 8.358589E+00	1.78407E-03
EZ=	-2.970482E-01+J 8.927332E-01	-2.987085E-01+J 8.928127E-01	1.76554E-03
HY=	8.612717E-03+J-2.732754E-02	8.579327E-03+J-2.734948E-02	1.39371E-03
Case III	PERPENDICULAR POLARIZATION	HORIZONTAL DIPOLE	
EX=	1.481989E+00+J 8.409508E+00	1.468764E+00+J 8.401593E+00	1.80705E-03
HY=	8.633389E-03+J-2.738369F-02	8.599879E-03+J-2.740508E-02	1.38418E-03
HZ=	-3.428739E-04+J-1.995624E-03	-3.266890E-04+J-1.938306E-03	9.03639E-03

TABLE 6

COMPARISON OF THE EXACT DIPOLE SOLUTIONS WITH THE PLANE WAVE SOLUTIONS

FOR R = 10 M and θ = 5°

FREQUENCY = 3.00E+08 C/S

REFRACTIVE INDICES OF AIR, CEMENT AND EARTH RESPECTIVELY

N0=	1.0000+J	0.0000	EPSR0= 1.0E+00	SIGMA0= 0.
N1=	1.7324+J	.0346	EPSR1= 3.0E+00	SIGMA1= 2.000E-03
N2=	3.1637+J	.0947	EPSR2= 1.0E+01	SIGMA2= 1.000E-02

Z= 0.   M   OBSERVATION HEIGHT

H0= 9.962E+00 M   DIPOLE HEIGHT

H1= 1.000E-01 M   SLAB WIDTH

R= 1.000E+01 M   SOURCE TO OBSERVATION DISTANCE

THETA= 5.0 DEG   ANGLE OF INCIDENCE

	PLANE WAVE SOLUTION	EXACT DIPOLE SOLUTION	RELATIVE DIF.
Case I	PARALLEL POLARIZATION	VERTICAL DIPOLE	
EX=	2.613969E-01+J 1.463647E+00	2.682098E-01+J 1.462810E+00	4.61551E-03
EZ=	6.155241E-01+J 3.410448E-01	6.150482E-01+J 3.436857E-01	3.80874E-03
HY=	1.336817E-03+J-4.832545E-03	1.354862E-03+J-4.835663E-03	3.64639E-03
Case II	PARALLEL POLARIZATION	HORIZONTAL DIPOLE	
EX=	3.520552E+00+J 1.661682E+01	3.468397E+00+J 1.658793E+01	3.51825E-03
EZ=	-5.592796E-01+J 1.797238E+00	-5.660924E-01+J 1.798075E+00	3.64123E-03
HY=	1.527989E-02+J-5.523624E-02	1.514558E-02+J-5.532048E-02	2.76431E-03
Case III	PERPENDICULAR POLARIZATION	HORIZONTAL DIPOLE	
EX=	3.557541E+00+J 1.670189E+01	3.504112E+00+J 1.667305E+01	3.56371E-03
HY=	1.531724E-02+J-5.534993E-02	1.518255E-02+J-5.543214E-02	2.74547E-03
HZ=	-8.232444E-04+J-3.864878E-03	-7.581100E-04+J-3.838788E-03	1.79317E-02

42

TABLE 7

COMPARISON OF THE EXACT DIPOLE SOLUTIONS WITH THE PLANE WAVE SOLUTIONS
FOR R = 5 M and θ = 5°

FREQUENCY = 3.00E+08 C/S
REFRACTIVE INDICES OF AIR, CEMENT AND EARTH RESPECTIVELY

NO= 1.0000+J 0.0000   EPSR0= 1.0E+00   SIGMA0= 0.
N1= 1.7324+J .0346   EPSR1= 3.0E+00   SIGMA1= 2.000E-03
N2= 3.1637+J .0947   EPSR2= 1.0E+01   SIGMA2= 1.000E-02

Z= 0.   M   OBSERVATION HEIGHT
H0= 4.981E+00 M   DIPOLE HEIGHT
H1= 1.000E-01 M   SLAB WIDTH
R= 5.000E+00 M   SOURCE TO OBSERVATION DISTANCE
THETA= 5.0 DEG   ANGLE OF INCIDENCE

	PLANE WAVE SOLUTION	EXACT DIPOLE SOLUTION	RELATIVE DIF.
Case I	PARALLEL POLARIZATION	VERTICAL DIPOLE	
EX=	4.469625E-01+J 2.943260E+00	4.758635E-01+J 2.937652E+00	9.89271E-03
EZ=	2.556915E+00+J 1.032260E+00	2.559207E+00+J 1.053921E+00	7.87004E-03
HY=	2.618556E-03+J-9.684097E-03	2.693199E-03+J-9.706489E-03	7.73629E-03
Case II	PARALLEL POLARIZATION	HORIZONTAL DIPOLE	
EX=	7.238051E+00+J 3.317812E+01	7.033542E+00+J 3.307163E+01	6.81941E-03
EZ=	-1.213086E+00+J 3.568223E+00	-1.241987E+00+J 3.573827E+00	7.78098E-03
HY=	2.993023E-02+J-1.106897E-01	2.940826E-02+J-1.110340E-01	5.44369E-03
Case III	PERPENDICULAR POLARIZATION	HORIZONTAL DIPOLE	
EX=	7.304887E+00+J 3.334953E+01	7.095719E+00+J 3.324287E+01	6.90723E-03
HY=	3.000363E-02+J-1.109176E-01	2.948051E-02+J-1.112547E-01	5.40718E-03
HZ=	-1.691910E-03+J-7.723011E-03	-1.435503E-03+J-7.626778E-03	3.52895E-02

43

TABLE 8

COMPARISON OF THE EXACT DIPOLE SOLUTIONS WITH THE PLANE WAVE SOLUTIONS
FOR R = 2 M and θ = 5°

FREQUENCY = 3.00E+08 C/S
REFRACTIVE INDICES OF AIR, CEMENT AND EARTH RESPECTIVELY
NO= 1.0000+J   0.0000   EPSRO= 1.0E+00   SIGMA0= 0.
N1= 1.7324+J   .0346   EPSR1= 3.0E+00   SIGMA1= 2.000E-03
N2= 3.1637+J   .0947   EPSR2= 1.0E+01   SIGMA2= 1.000E-02

Z= 0.   M   OBSERVATION HEIGHT
H0= 1.992E+00 M   DIPOLE HEIGHT
H1= 1.000E-01 M   SLAB WIDTH
R= 2.000E+00 M   SOURCE TO OBSERVATION DISTANCE
THETA= 5.0 DEG   ANGLE OF INCIDENCE

	PLANE WAVE SOLUTION	EXACT DIPOLE SOLUTION	RELATIVE DIF.
Case I	PARALLEL POLARIZATION	VERTICAL DIPOLE	
EX=	1.545409E-01+J 7.501099E+00	3.753434E-01+J 7.440945E+00	3.07164E-02
EZ=	1.615506E+01+J 5.831475E+00	1.632323E+01+J 6.192073E+00	2.27907E-02
HY=	7.398143E-03+J-2.403323E-02	7.903052E-03+J-2.432010E-02	2.27088E-02
Case II	PARALLEL POLARIZATION	HORIZONTAL DIPOLE	
EX=	1.520181E+01+J 8.329597E+01	1.406266E+01+J 8.273756E+01	1.51167E-02
EZ=	-4.198126E+00+J 8.520029E+00	-4.418928E+00+J 8.580113E+00	2.37102E-02
HY=	8.456116E-02+J-2.747011E-01	8.166476E-02+J-2.771462E-01	1.31191E-02
Case III	PERPENDICULAR POLARIZATION	HORIZONTAL DIPOLE	
EX=	1.529195E+01+J 8.374011E+01	1.413194E+01+J 8.317381E+01	1.53008E-02
HY=	8.476476E-02+J-2.752657E-01	8.186386E-02+J-2.776816E-01	1.30404E-02
HZ=	-3.569897E-03+J-1.949360E-02	-2.067248E-03+J-1.895070E-02	8.38119E-02

44

COMPARISON OF THE EXACT DIPOLE SOLUTIONS WITH THE PLANE WAVE SOLUTIONS
FOR R = 1 M and θ = 5°

TABLE 9

FREQUENCY = 3.00E+08 C/S
REFRACTIVE INDICES OF AIR, CEMENT AND EARTH RESPECTIVELY
NO= 1.0000+J 0.0000   EPSRO= 1.0E+00   SIGMAO= 0.
N1= 1.7324+J .0346   EPSR1= 3.0E+00   SIGMA1= 2.000E-03
N2= 3.1637+J .0947   EPSR2= 1.0E+01   SIGMA2= 1.000E-02

Z= 0.   M   OBSERVATION HEIGHT
H0= 9.962E-01 M   DIPOLE HEIGHT
H1= 1.000E-01 M   SLAB WIDTH
R= 1.000E+00 M   SOURCE TO OBSERVATION DISTANCE
THETA= 5.0 DEG   ANGLE OF INCIDENCE

	PLANE WAVE SOLUTION	EXACT DIPOLE SOLUTION	RELATIVE DIF.
Case I	PARALLEL POLARIZATION	VERTICAL DIPOLE	
EX=	-3.269468E+00+J 1.510750E+01	-2.054056E+00+J 1.480040E+01	8.38968E-02
EZ=	6.391610E+01+J 2.673160E+01	6.635744E+01+J 2.977550E+01	5.36491E-02
HY=	1.848267E-02+J-4.727991E-02	2.063998E-02+J-4.916431E-02	5.37204E-02
Case II	PARALLEL POLARIZATION	HORIZONTAL DIPOLE	
EX=	1.745629E+01+J 1.668591E+02	1.408939E+01+J 1.653235E+02	2.23030E-02
EZ=	-1.247930E+01+J 1.507274E+01	-1.369472E+01+J 1.537938E+01	6.08701E-02
HY=	2.112579E-01+J-5.404118E-01	2.019166E-01+J-5.521007E-01	2.54531E-02
Case III	PERPENDICULAR POLARIZATION	HORIZONTAL DIPOLE	
EX=	1.735417E+01+J 1.677735E+02	1.395721E+01+J 1.661773E+02	2.25070E-02
HY=	2.117521E-01+J-5.415180E-01	2.024030E-01+J-5.531612E-01	2.53506E-02
HZ=	-4.276396E-03+J-3.977823E-02	1.152342E-03+J-3.781872E-02	1.52540E-01

45

TABLE 10

COMPARISON OF THE EXACT DIPOLE SOLUTIONS WITH THE PLANE WAVE SOLUTIONS
FOR R = 40 M and θ = 30°

FREQUENCY = 3.00E+08 C/S
REFRACTIVE INDICES OF AIR, CEMENT AND EARTH RESPECTIVELY
N0= 1.0000+J 0.0000   EPSR0= 1.0E+00   SIGMA0= 0.
N1= 1.7324+J .0346   EPSR1= 3.0E+00   SIGMA1= 2.000E-03
N2= 3.1637+J .0947   EPSR2= 1.0E+01   SIGMA2= 1.000E-02

Z= 0.   M   OBSERVATION HEIGHT
H0= 3.464E+01 M   DIPOLE HEIGHT
H1= 1.000E-01 M   SLAB WIDTH
R= 4.000E+01 M   SOURCE TO OBSERVATION DISTANCE
THETA= 30.0 DEG   ANGLE OF INCIDENCE

	PLANE WAVE SOLUTION	EXACT DIPOLE SOLUTION	RELATIVE DIF.
	PARALLEL POLARIZATION	VERTICAL DIPOLE	
Case I			
EX=	1.437133E-01+J 1.893798E+00	1.474782E-01+J 1.894765E+00	2.04542E-03
EZ=	-4.784605E-01+J 1.238629E+00	-4.819455E-01+J 1.237909E+00	2.67874E-03
HY=	2.695425E-03+J-6.511408E-03	2.708718E-03+J-6.508282E-03	1.93700E-03
	PARALLEL POLARIZATION	HORIZONTAL DIPOLE	
Case II			
EX=	2.836756E-01+J 3.277238E+00	2.795649E-01+J 3.275409E+00	1.36870E-03
EZ=	-8.962937E-01+J 2.117395E+00	-9.000589E-01+J 2.116427E+00	1.69039E-03
HY=	4.668614E-03+J-1.127809E-02	4.664216E-03+J-1.128116E-02	4.39537E-04
	PERPENDICULAR POLARIZATION	HORIZONTAL DIPOLE	
Case III			
EX=	5.380985E-01+J 3.943960E+00	5.323133E-01+J 3.943285E+00	1.46378E-03
HY=	5.062744E-03+J-1.225890E-02	5.060208E-03+J-1.225636E-02	2.71151E-04.
HZ=	-7.141734E-04+J-5.234488E-03	-6.879130E-04+J-5.226215E-03	5.22310E-03

46

TABLE 11

COMPARISON OF THE EXACT DIPOLE SOLUTIONS WITH THE PLANE WAVE SOLUTIONS
FOR R = 40 M and θ = 45°

FREQUENCY = 3.00E+08 C/S
REFRACTIVE INDICES OF AIR, CEMENT AND EARTH RESPECTIVELY
N0= 1.0000+J 0.0000   EPSR0= 1.0E+00   SIGMA0= 0.
N1= 1.7324+J .0346   EPSR1= 3.0E+00   SIGMA1= 2.000E-03
N2= 3.1637+J .0947   EPSR2= 1.0E+01   SIGMA2= 1.000E-02

Z= 0.   M   OBSERVATION HEIGHT
H0= 2.828E+01 M   DIPOLE HEIGHT
H1= 1.000E-01 M   SLAB WIDTH
R= 4.000E+01 M   SOURCE TO OBSERVATION DISTANCE
THETA=45.0 DEG   ANGLE OF INCIDENCE

	PLANE WAVE SOLUTION	EXACT DIPOLE SOLUTION	RELATIVE DIF.
Case I	**PARALLEL POLARIZATION**	**VERTICAL DIPOLE**	
EX=	1.344091E-01+J 2.307705E+00	1.404201E-01+J 2.309452E+00	2.70551E-03
EZ=	-9.663265E-01+J 2.339685E+00	-9.780035E-01+J 2.336757E+00	4.75238E-03
HY=	3.697138E-03+J-8.753624E-03	3.730370E-03+J-8.744980E-03	3.61170E-03
Case II	**PARALLEL POLARIZATION**	**HORIZONTAL DIPOLE**	
EX=	1.710933E-01+J 2.305275E+00	1.625238E-01+J 2.30260E+00	3.88864E-03
EZ=	-1.003414E+00+J 2.324021E+00	-1.009424E+00+J 2.322275E+00	2.47166E-03
HY=	3.697138E-03+J-8.753624E-03	3.692385E-03+J-8.755548E-03	5.39685E-04
Case III	**PERPENDICULAR POLARIZATION**	**HORIZONTAL DIPOLE**	
EX=	6.785937E-01+J 3.479004E+00	6.697619E-01+J 3.481107E+00	2.56099E-03
HY=	4.397418E-03+J-1.088206E-02	4.406347E-03+J-1.087186E-02	1.15536E-03
HZ=	-1.273699E-03+J-6.529977E-03	-1.231597E-03+J-6.527462E-03	6.34941E-03

47

TABLE 12

COMPARISON OF THE EXACT DIPOLE SOLUTIONS WITH THE PLANE WAVE SOLUTIONS
FOR R = 40 M and θ = 80°

FREQUENCY = 3.00E+08 C/S
REFRACTIVE INDICES OF AIR, CEMENT AND EARTH RESPECTIVELY

NO=	1.0000+J	0.0000	EPSRO= 1.0E+00 SIGMAO= 0.
N1=	1.7324+J	.0346	EPSR1= 3.0E+00 SIGMA1= 2.000E-03
N2=	3.1637+J	.0947	EPSR2= 1.0E+01 SIGMA2= 1.000E-02

Z= 0.   M   OBSERVATION HEIGHT
H0= 6.946E+00 M   DIPOLE HEIGHT
H1= 1.000E-01 M   SLAB WIDTH
R= 4.000E+01 M   SOURCE TO OBSERVATION DISTANCE
THETA= 80.0 DEG ANGLE OF INCIDENCE

	PLANE WAVE SOLUTION	EXACT DIPOLE SOLUTION	RELATIVE DIF.
Case I	PARALLEL POLARIZATION	VERTICAL DIPOLE	
EX=	-1.017360E-01+J 1.228208E+00	-1.270977E-01+J 1.221023E+00	2.14724E-02
EZ=	-1.092006E+00+J 2.027570E+00	-1.162065E+00+J 1.983039E+00	3.61174E-02
HY=	2.944724E-03-J-5.464346E-03	3.116624E-03-J-5.352220E-03	3.31373E-02
Case II	PARALLEL POLARIZATION	HORIZONTAL DIPOLE	
EX=	3.920985E-02+J 2.208427E-01	2.117261E-03+J 2.130390E-01	1.77914E-01
EZ=	-1.954812E-01+J 3.559357E-01	-1.701755E-01+J 3.629195E-01	6.54922E-02
HY=	5.192342E-04+J-9.635117E-04	4.324112E-04+J-9.836515E-04	8.29486E-02
Case III	PERPENDICULAR POLARIZATION	HORIZONTAL DIPOLE	
EX=	4.760656E-01+J 1.082661E+00	4.616274E-01+J 1.100581E+00	1.92824E-02
HY=	9.865458E-04+J-3.776933E-03	1.046706E-03+J-3.784495E-03	1.54418E-02
HZ=	-1.244486E-03+J-2.830190E-03	-1.198245E-03+J-2.878184E-03	2.13767E-02

TABLE 13

STEEPEST DESCENT RESULTS

FOR R = 40 M, and θ = 30°, 45°, 80°

FREQUENCY = 3.00E+08 C/S

REFRACTIVE INDICES OF AIR,CEMENT AND EARTH RESPECTIVELY

N0=	1.0000+J	0.0000	EPSR0= 1.0E+00	SIGMA0= 0.
N1=	1.7324+J	.0346	EPSR1= 3.0E+00	SIGMA1= 2.000E-03
N2=	3.1637+J	.0947	EPSR2= 1.0E+01	SIGMA2= 1.000E-02

Z= 0.   M   OBSERVATION HEIGHT

H1= 1.000E-01 M   SLAB WIDTH

R= 4.000E+01 M   SOURCE TO OBSERVATION DISTANCE

	θ = 30°, h_o = 34.64 m	θ = 45°, h_o = 28.28 m	θ = 80°, h_o = 6.946 m
Parallel Polarization			
Vertical Dipole			
EX =	1.476711E-01+J 1.894917E+00	1.412327E-01+J 2.309387E+00	-1.293017E-01+J 1.219652E+00
EZ =	-4.813033E-01+J 1.238235E+00	-9.769887E-01+J 2.336869E+00	-1.163315E+00+J 1.979569E+00
HY =	2.708173E-03+J-6.508386E-03	3.729027E-03+J-8.745169E-03	3.121152E-03+J-5.342210E-03
Parallel Polarization			
Horizontal Dipole			
EX =	2.790657E-01+J 3.274560E+00	1.619211E-01+J 2.302223E+00	2.012439E-03+J 2.119788E-01
EZ =	-8.998380E-01+J 2.116889E+00	-1.008123E+00+J 2.323156E+00	-1.692147E-01+J 3.641888E-01
HY =	4.662933E-03+J-1.128274E-02	3.689543E-03+J-8.757071E-03	4.332300E-04+J-9.896551E-04
Perpendicular Polarization			
Horizontal Dipole			
EX =	5.322586E-01+J 3.943356E+00	6.701051E-01+J 3.481016E+00	4.621943E-01+J 1.101173E+00
HY =	5.059257E-03+J-1.225730E-02	4.404040E-03+J-1.087320E-02	1.056692E-03+J-3.786900E-03
HZ =	-6.884591E-04+J-5.226918E-03	-1.233093E-03+J-6.527412E-03	-1.198232E-03+J-2.883319E-03

49

Table 14

COMPARISON OF THE EXACT DIPOLE SOLUTIONS WITH THE QUASI-STATIC SOLUTIONS
FOR R = 0.005 M AND θ = 4.5°

FREQUENCY= 3.00E+08 C/S
REFRACTIVE INDICES OF AIR,CEMENT AND EARTH RESPECTIVELY

N0= 1.0000+J	0.0000	EPSR0= 1.0E+00	SIGMA0= 0.
N1= 1.7324+J	.0346	EPSR1= 3.0E+00	SIGMA1= 2.000E-03
N2= 3.1637+J	.0947	EPSR2= 1.0E+01	SIGMA2= 1.000E-02

Z= 0.   M   OBSERVATION HEIGHT
H0= 4.985E-03 M DIPOLE HEIGHT
H1= 1.000E-01 M SLAB WIDTH
R= 5.000E-03 M SOURCE TO OBSERVATION DISTANCE
THETA= 4.5 DEG ANGLE OF INCIDENCE

QUASI-STATIC SOLUTION

Parallel Polarization

EX = -1.339861E+05 + J-4.472028E+06
EZ = -1.135130E+06 + J 1.134747E+08
HY = 3.749333E+02 + J 3.750498E+00

Parallel Polarization

EX = -5.590979E+05 + J-1.868388E+07
EZ = 1.339565E+05 + J-1.343289E+07
HY = 3.962958E+03 + J 2.035858E+01

Perpendicular Polarization

EX = -5.702029E+05 + J-1.901706E+07
HY = 3.970331E+03 + J 2.057906E+01
HZ = 2.499527E+02 + J 1.257811E-02

EXACT DIPOLE SOLUTION

Vertical Dipole

-1.337351E+05 + J-4.498663E+06
-1.134994E+06 + J 1.134375E+08
3.747873E+02 + J 3.749815E+00

Horizontal Dipole

-5.618232E+05 + J-1.867090E+07
1.337351E+05 + J-1.344194E+07
3.966040E+03 + J 2.433938E+01

Horizontal Dipole

-5.722937E+05 + J-1.902040E+07
3.973397E+03 + J 2.455947E+01
2.498108E+02 + J 1.093684E-02

To further demonstrate the range of validity of the approximate methods, we show in figure 6 the magnitude of E_z on the slab surface versus the distance R $(R = R_{12})$ for a fixed observation angle $\theta = 5°$. The solid curve represents the exact field calculation for the two different orientations of the dipole source (vertical and horizontal) observed in the plane of the dipole $(\theta = 0°)$. The long dash line represents the asymptotic results while the long dash-short dash line represents the quasi-static result. Similar comparison can be made for other components of the field.

As pointed out by Lytle, et al.(ref.14) a convenient way to display the electromagnetic field structure near the dipole source involves the use of the power flux or the time-average Poynting vector $\bar{P}$ defined as $\frac{1}{2}Re(\bar{E} \times \bar{H}^*)$. It is well-known that in the far-zone the power flux $\bar{P}_o$ of an isolated dipole in free space can be given as

$$\bar{P}_o = \bar{a}_r P_o \sin^2\theta; \quad P_o = \eta_o (2\lambda R_{11})^{-2}$$

where $\eta_o = 120\pi$ ohm is the free-space characteristic impedance and λ is the free-space wavelength. Thus, the power flux density in this case points radially outward, while decaying with the rate of R_{11}^{-2}. The magnitude of the power flux on the other hand vanishes along the dipole axis at $\theta = 0°$ but is at maximum in the broadside direction, i.e. $\theta = 90°$.

The power flux of a vertical dipole source, normalized to P_o above a two-layer earth surface, is plotted in figure 7. It is seen that the direction of the power flux , as indicated by the direction of the arrow, departs significantly from the radial direction near the slab surface. Magnitude of the normalized power flux (1 cm of the thick arrow corresponds
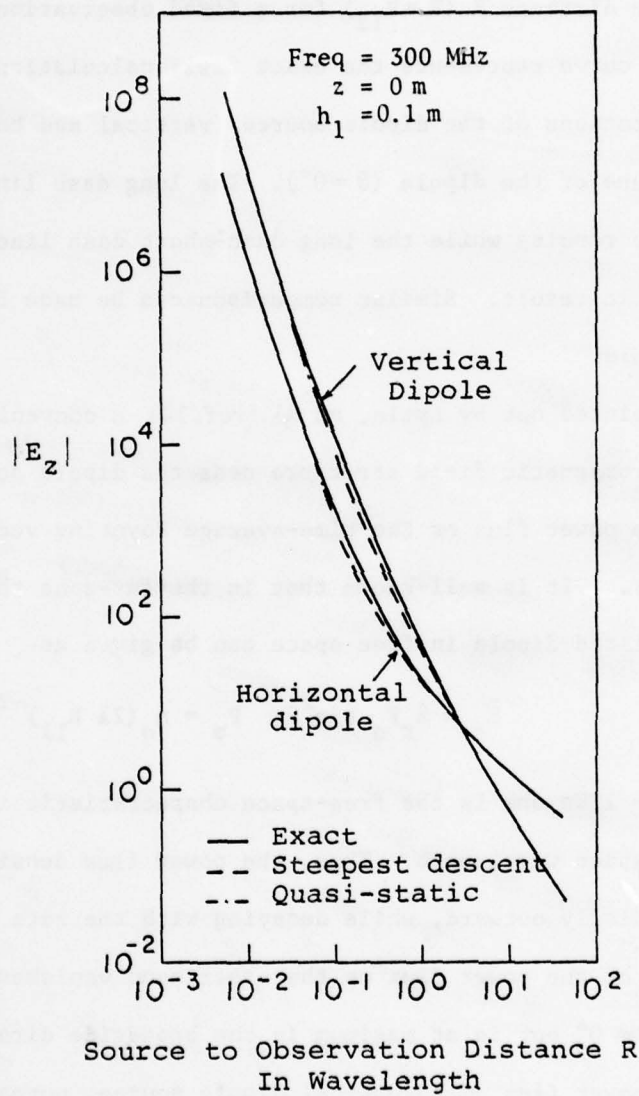
Figure 6. Magnitude of the vertical electrical field E_z on the slab surface as a function of distance R for an angle $\theta = 5°$.
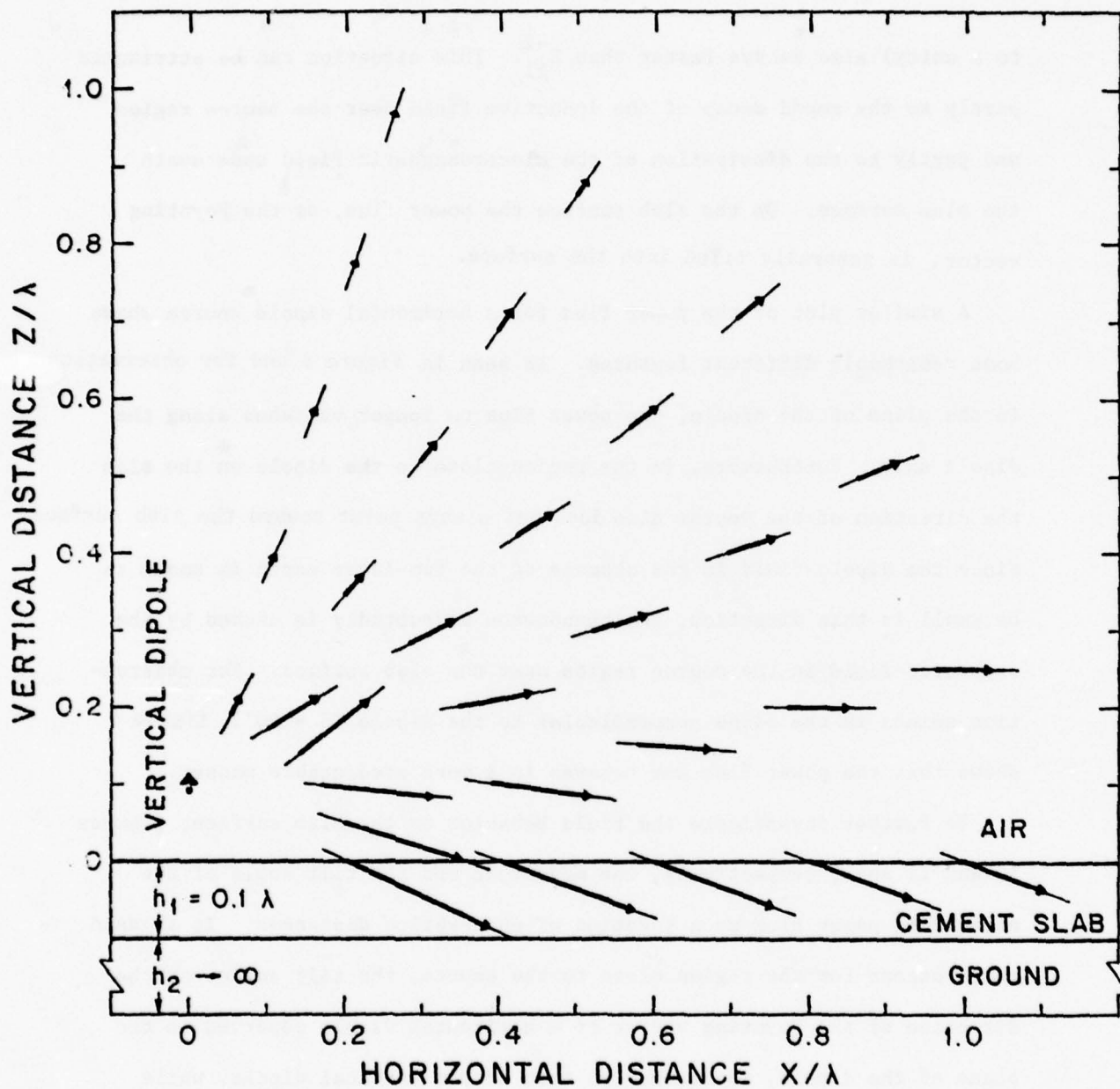
Figure 7. Magnitude and direction of the normalized time average power
density distribution for a vertical dipole source
(1 cm of arrow length ≡ unity): f = 300 MHz, λ = 1 meter,
n_1 = 1.732 + i0.0346 and n_2 = 3.1637 + i0.0947.

to a unity) also decays faster than R_{11}^{-2}. This situation can be attributed

partly to the rapid decay of the inductive field near the source region

and partly to the dissipation of the electromagnetic field underneath

the slab surface. On the slab surface the power flux, or the Poynting

vector, is generally tiled into the surface.

A similar plot of the power flux for a horizontal dipole source shows

some remarkably different features. As seen in figure 8 and for observation

in the plane of the dipole, the power flux no longer vanishes along the

dipole axis. Furthermore, in the region close to the dipole on the slab

the direction of the vector also does not always point toward the slab surface.

Since the dipole field in the absence of the two-layer earth is known to

be small in this direction, the phenomenon undoubtedly is caused by the

scattered field in the source region near the slab surface. For observa-

tion points in the plane perpendicular to the dipole ($\theta = 90°$), figure 9

shows that the power flux now behaves in a more predictable manner.

To further investigate the field behavior on the slab surface, figures

10 and 11 show, respectively, the magnitude and the tilt angle of the

normalized power flux as a function of observation distances. It is seen

that, except for the region close to the source, the tilt angle, or the

direction of the Poynting vector of a horizontal dipole observed in the

plane of the dipole, approaches to that of the vertical dipole, while

the tilt angle observed in the perpendicular plane approaches to a

different limit. As is well known in the theory of ground wave propa-

gation (ref. 2), the tilt angle depends, in addition to the

refractive indices of the different media, mainly upon the type of

polarization of the impinging wave, rather than the exact orientation

54
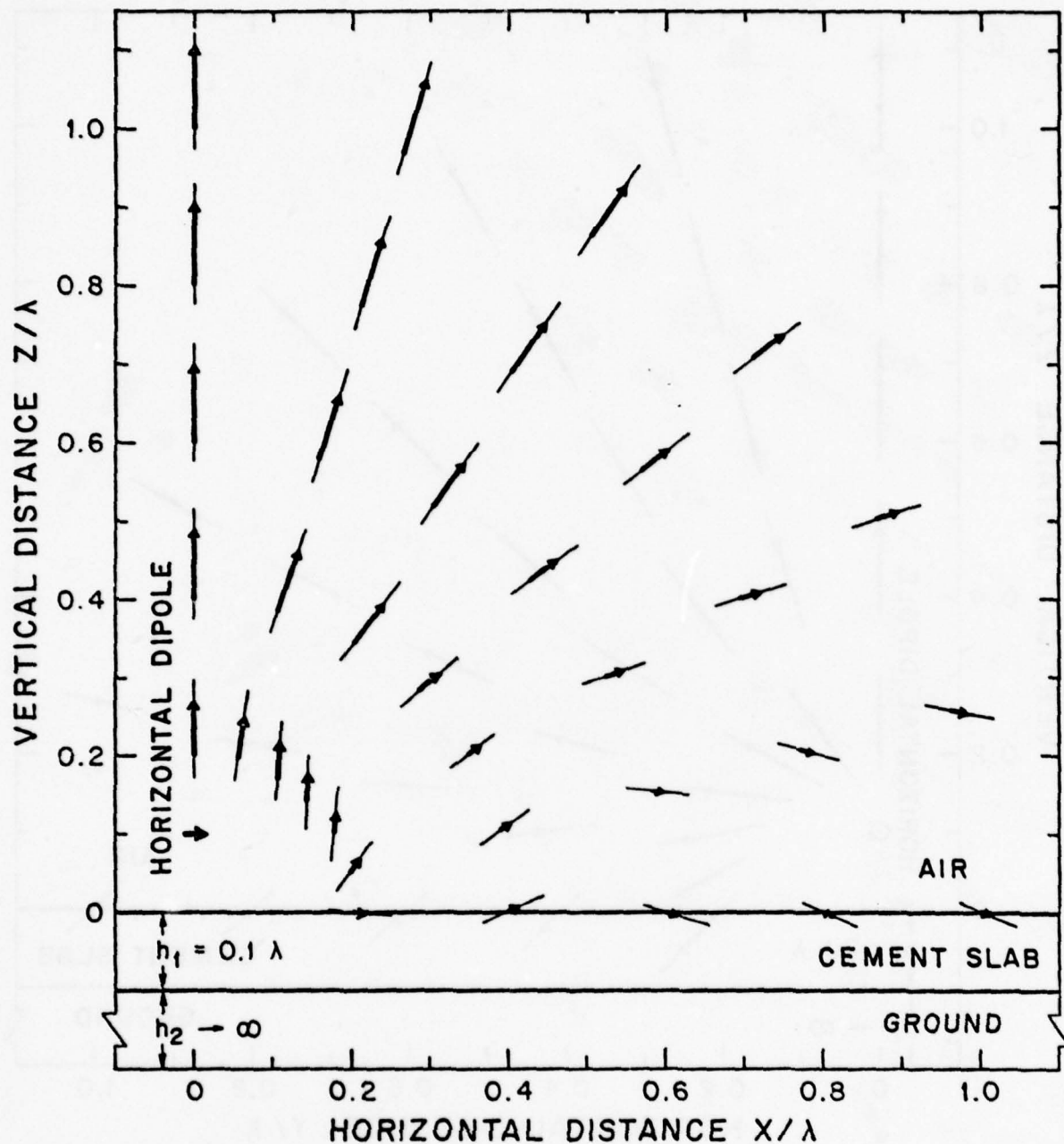
Figure 8. Magnitude and direction of the normalized time-average power
density distribution for a horizontal dipole source in the
plane of incidence; $\phi = 0°$, (1 cm of arrow length $\equiv$ unity),
f = 300 MHz, λ = 1 meter, n_1 = 1.732 + i0.0346 and n_2 = 3.1637
+ i0.0947.

55

VERTICAL DISTANCE Z/λ

HORIZONTAL DIPOLE
⊙

1.0

0.8

0.6

0.4

0.2

0

AIR

h₁ = 0.1 λ

CEMENT SLAB

GROUND

h₂ → ∞

0   0.2   0.4   0.6   0.8   1.0

HORIZONTAL DISTANCE Y/λ
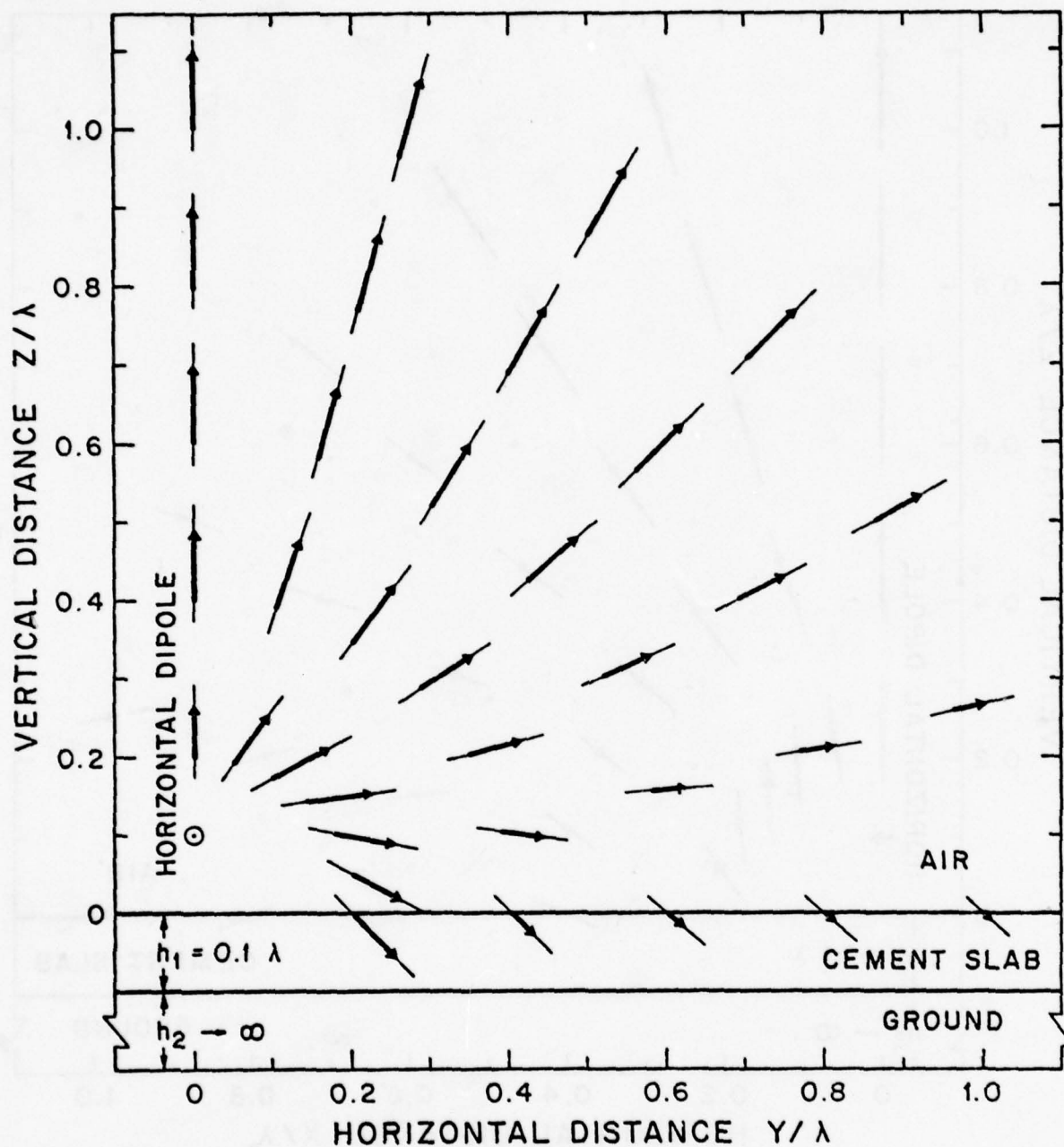
Figure 9. Magnitude and direction of the normalized time-average power
density distribution in the plane perpendicular to the dipole;
$\phi = 90°$, (1 cm of arrow length ≡ unity), f = 300 MHz,
λ = 1 meter, n_1 = 1.732 + i0.0346 and n_2 = 3.1637 + i0.0947.

56
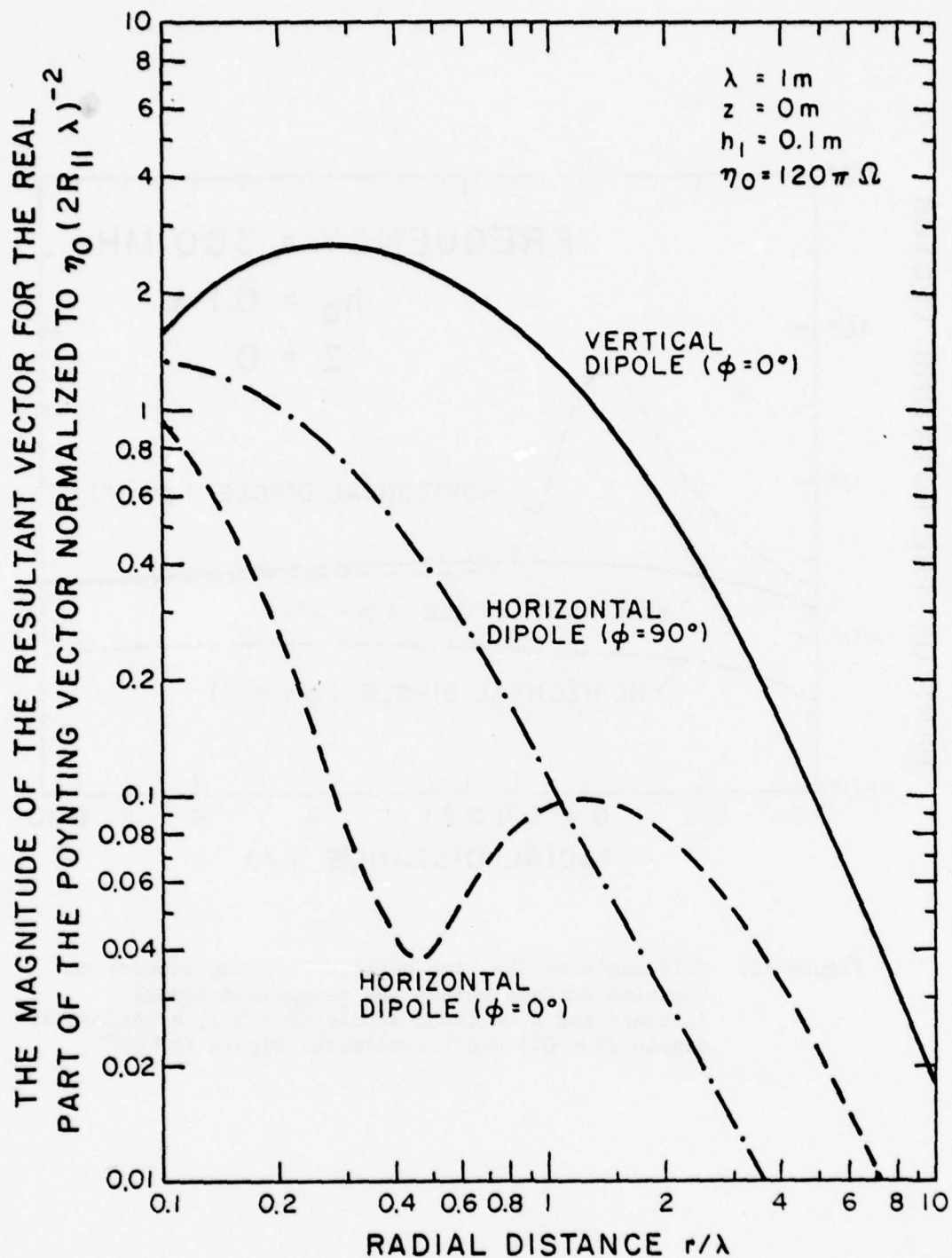
Figure 10. Magnitude of the normalized time-average power density on the slab surface as a function of observation distance for a vertical dipole ($\phi = 0°$), a horizontal dipole ($\phi = 0°$) and a horizontal dipole ($\phi = 90°$).
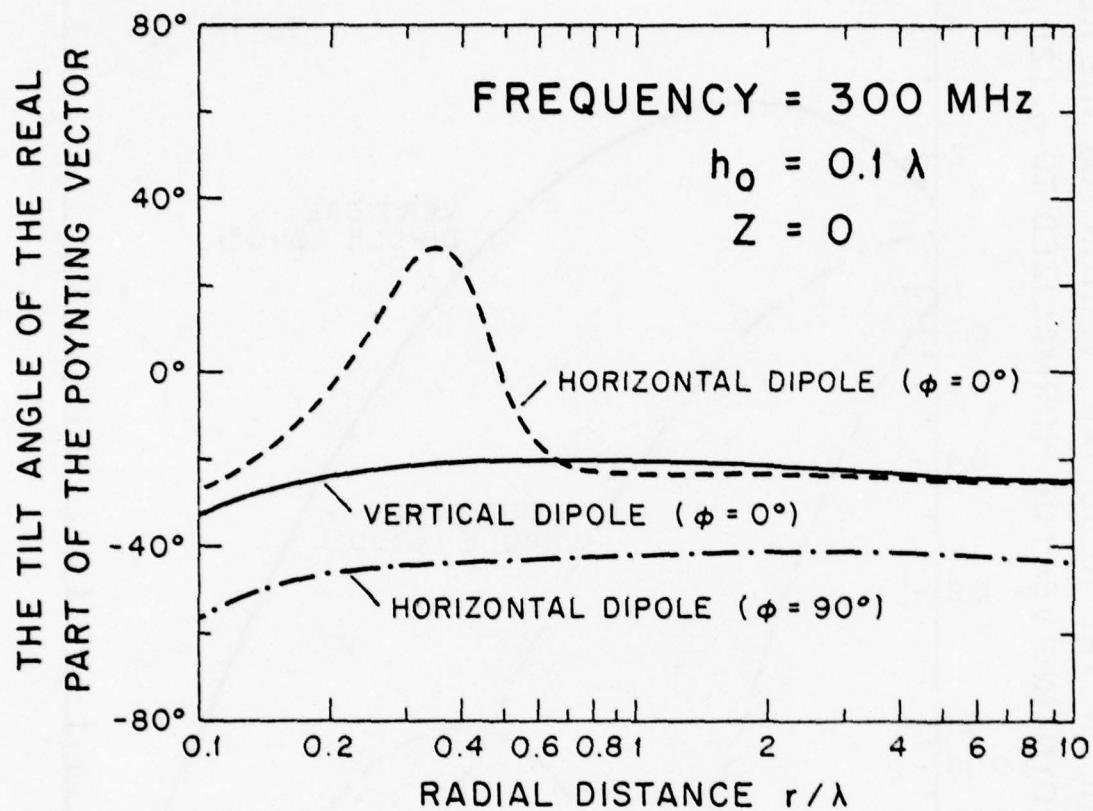
Figure 11. Tilt angle of the time average Poynting vectors on
the slab surface versus the normalized radial
distance for a vertical dipole ($\phi = 0°$), a horizontal
dipole ($\phi = 0°$) and a horizontal dipole ($\phi = 90°$).

58

of the dipole source. Thus, the tilt angle of both the vertical and the horizontal dipoles observed in the plane of the dipole should approach to the wave tilt of a TM-wave, while the other approaches to the wave tilt of a TE-wave.

As shown in figure 10, the change in the magnitude of the power flux along the slab surface for the three dipole arrangements as a function of observation distance also differs significantly. In the case of a horizontal dipole, a minimum and then a maximum are observed as one moves away in the plane of the dipole. The tip occurs at $\frac{r}{\lambda} \simeq 0.45$ or for an observation angle of 77.5°. However, no such tip is observed in the other two arrangements. To examine the occurrence of this tip in detail, included in figure 12 is the magnitude of the power flux versus observation distance for several slab thicknesses, including $h_1 = 0$ which corresponds exactly to the case of a homogenous earth in the absence of the slab. It is shown in this case, the tip occurs at $\frac{r}{\lambda} \simeq 0.65$. As the slab thickness increases the location of the tip moves toward the source until $h_1 = 0.3$ m; thereafter, a second tip emerges. Figures 13 and 14 show the change in the magnitude of the power flux for the other two dipole arrangements. However, no drastic change in the magnitude of the power flux is observed as one moves away on the slab surface in these cases.

59
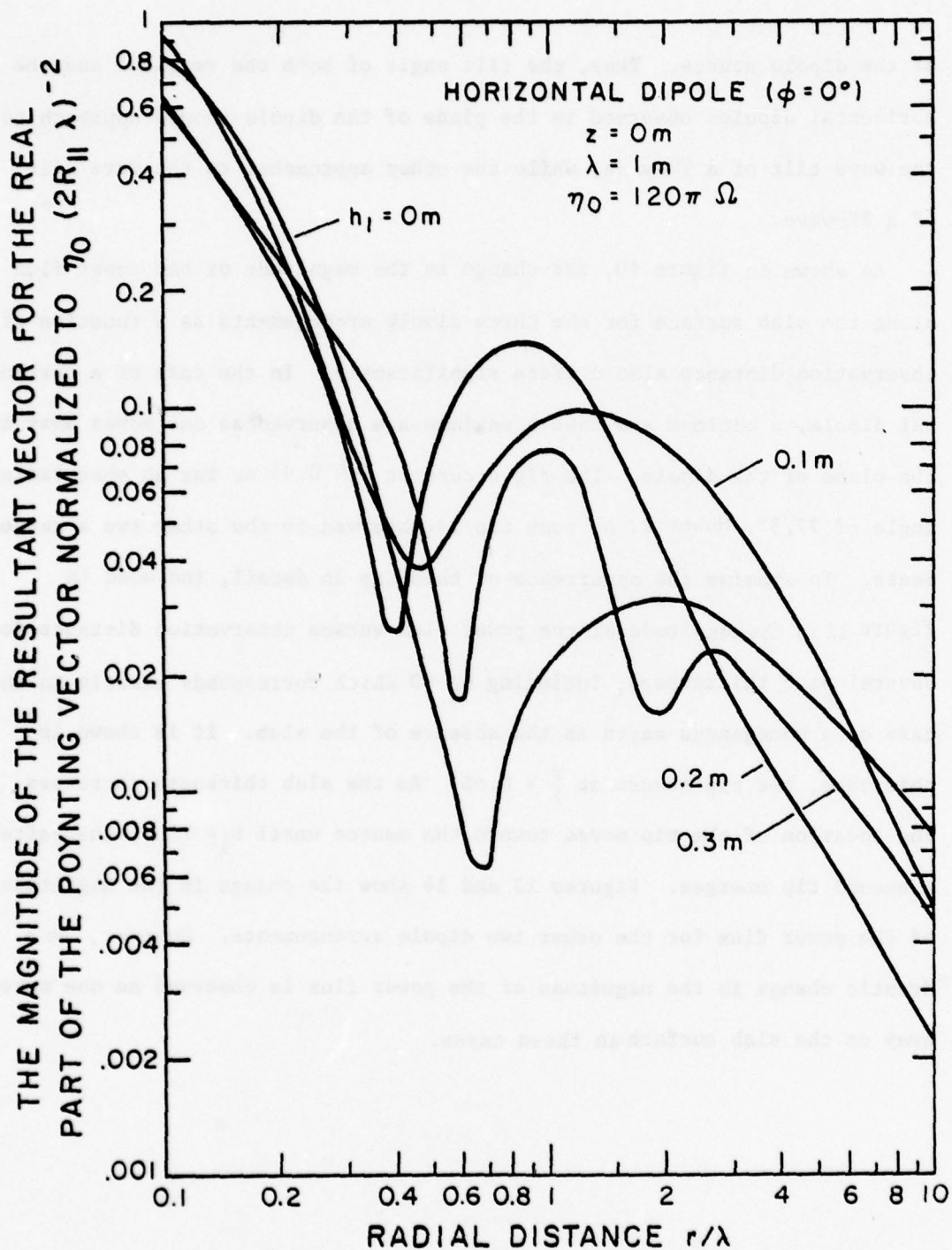
Figure 12. Magnitude of the normalized time average power density
on the slab surface for a horizontal dipole source
observed in the plane of incidence (φ= 0°)
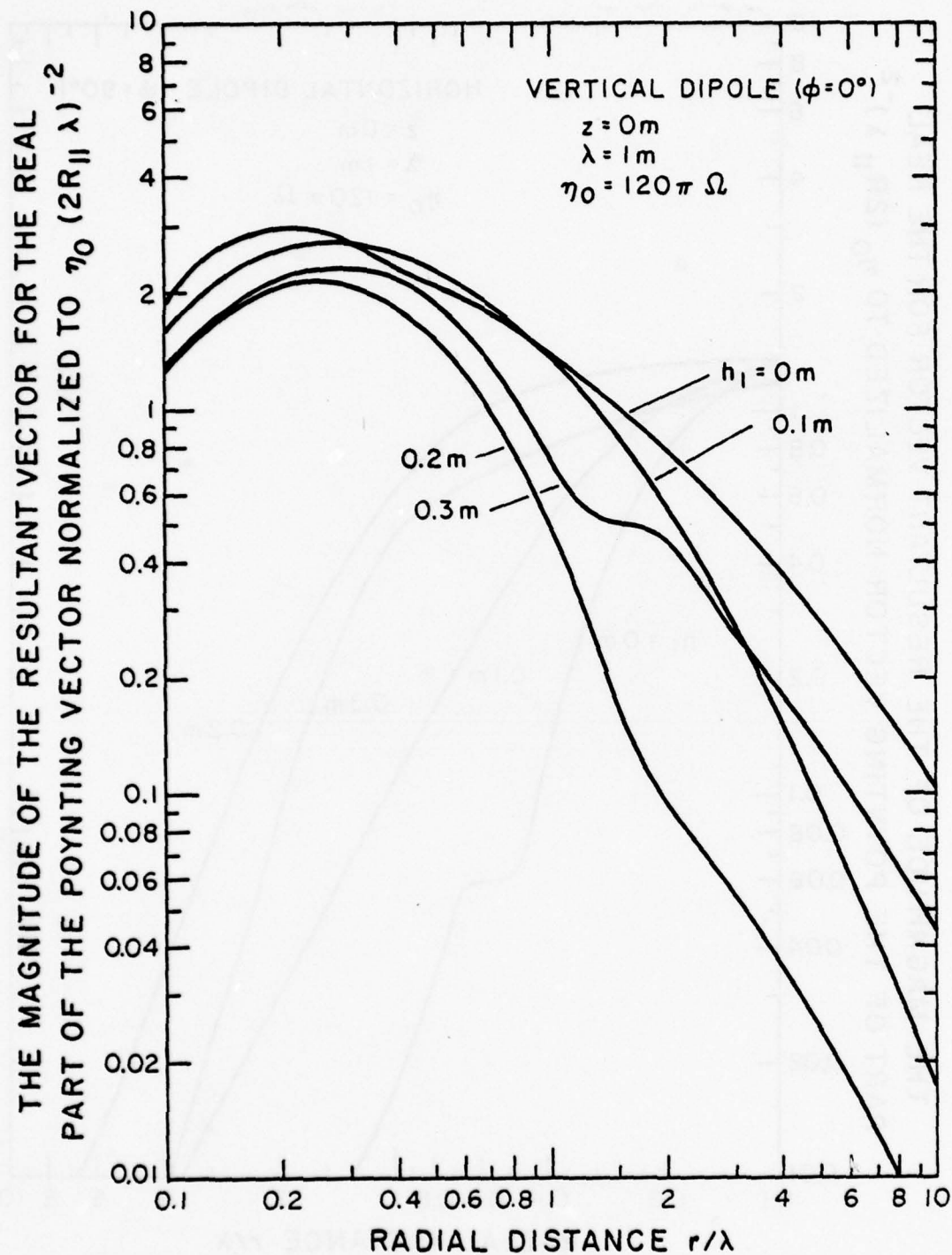
Figure 13. Magnitude of the normalized time-average power density on the slab surface for a vertical dipole source.
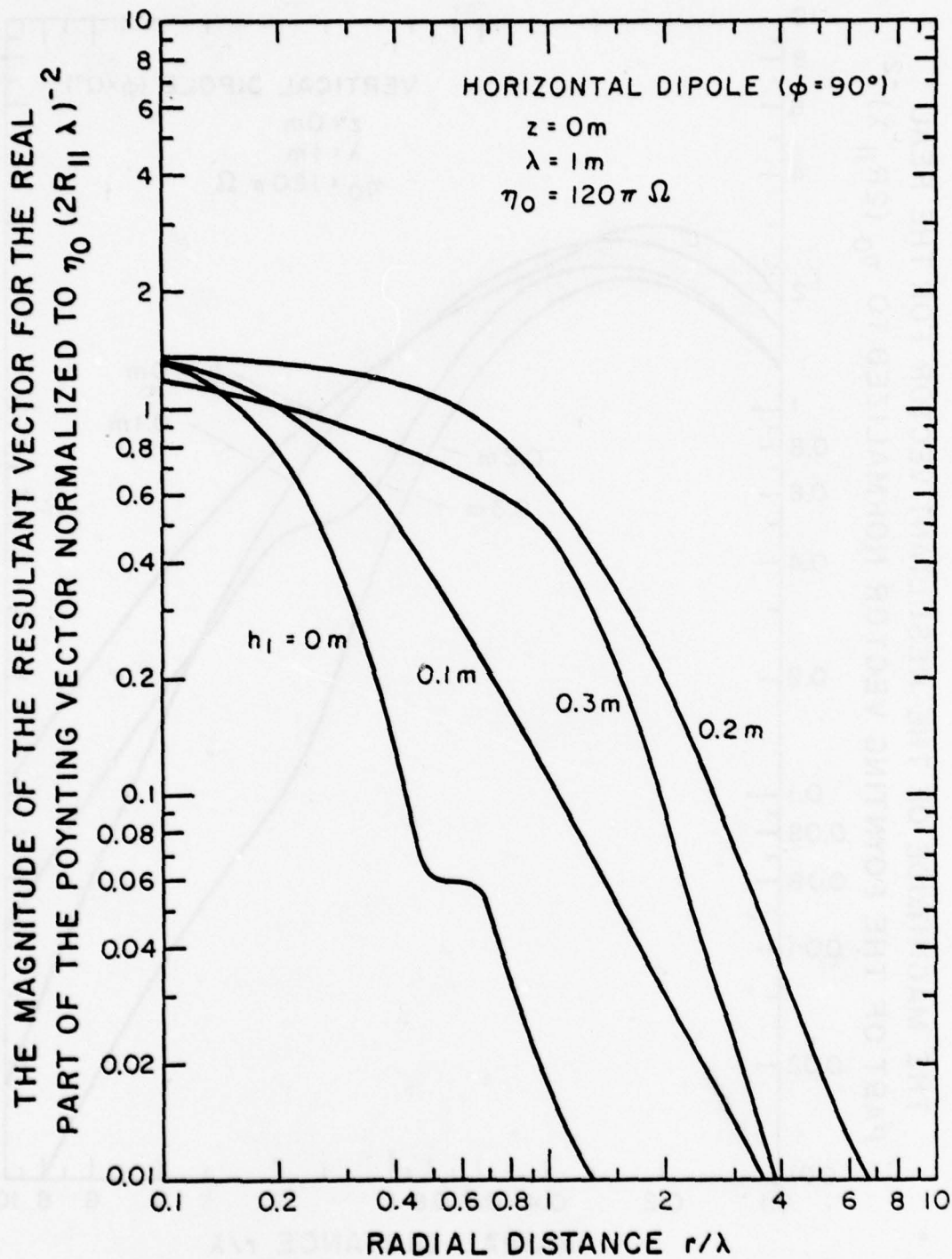
Figure 14. Magnitude of the normalized time-average power density
on the slab surface for a horizontal dipole source
observed in the plane perpendicular to the dipole
($\phi = 90°$)

SECTION VI
CONCLUSION

In this report a numerical program is devised which computes all components of the electromagnetic field simultaneously by integrating an array of functions along the real axis in the complex α-plane. Increased efficiency is obtained with the incorporation of the quasi-static and asymptotic approximations. The inclusion of a root finder in the program also makes it possible to integrate efficiently for the case when a pole is close to the path of integration. It should be noted, however, for the typical parameters we have studied, the poles were sufficiently away from the real axis so that no particular effort is needed. In principle, we can also extend the method to treat the case involving more than one pole.

The computer program is also capable of finding the field for a semi-infinite half-space problem. In this case, the slab width h_1 will be either zero or infinity. However, if quasi-static approximation is used, the the case where h_1 approaches infinity should be chosen. The reason for this restriction is that the approximations we have used assume a finite h_1 so that beyond a certain value of α_o analytical expression for the integral can be obtained.

63

REFERENCES

1. Baum, C.E. (1972), EMP similators for various types of nuclear EMP environ-
      ments. An interm categorization sensor and simulation, Note 151,
      AFWL, Kirtland AFB, New Mexico.

2. Wait, J.R. (1962), Electromagnetic Waves in Stratified Media, Pergamon,
      New York.

3. Wait, J.R. (1966), Fields of a horizontal dipole over a stratified aniso-
      tropic half-space, IEEE AP-14, 790-792.

4. Lytle, R.J., and D.L. Lager (1974), Numerical evaluation of Sommerfeld
      integrals, Report no. UCRL-51688, Lawrence Livermore Lab., U. of
      California, Livermore, Calif. 94550.

5. Lager, D.L., and R.J. Lytle (1975), Fortran subroutines for the numerical
      evaluation of Sommerfeld integrals under anderem, Report no. UCRL-51821,
      Lawrence Livermore Lab., U. of Calif., Livermore, Calif. 94550.

6. Tsang, L., and J.L. Kong (1974), Electromagnetic field due to a horizontal
      electric dipole antenna laid on the surface of a two-layered medium,
      IEEE AP-22, 709-711.

7. Baum, C.E. (1976), Emerging technology for transient and Broad-band
      analysis and synthesis of antennas and scatterers, Proceeding of the
      IEEE, vol. 64, no. 11, 1598-1616.

8. Baños, A. (1966), Dipole Radiation in the Presence of a Conducting Half-
      Space, Pergamon, Oxford.

9. Shevchenko, V.V. (1972), On the behavior of wave number beyond the critical
      value for waves in dielectric waveguides (media with losses), Radio-
      physics and Quantum Electronics, vol. 15, 194-200.

10. Brekhovskikh, K.M. (1960), Waves in Layered Media, Academic Press,
      New York.

11. Felsen, L.B., and N. Marcuvitz (1973), Radiation and Scattering of Waves,
      Prentice-Hall, Englewood Cliffs, N.J.

12. Chang, D.C., and J.R. Wait (1970), Appraisal of near-field solution for a
      Hertzian dipole over a conducting half-space, Can. J. Phys., vol. 48,
      no. 5, 737-743.

13. Chang, D.C., and R.J. Fisher (1974), A unified theory on radiation of a
      vertical electric dipole above a dissipative earth, Radio Science,
      vol. 9, no. 12, 1129-1138.

14. Lytle, R.J., D.L. Lager, and K. Miller (1976), Poynting vector behavior
      in lossy media and near a half space, Radio Science, vol. 11, no. 11,
      875-883.

15. Gradshteyn, I.S., and I.M. Ryshik (1965), Table of Integrals Series Products,
      4th Ed., p. 707, Academic Press, New York.

16. Abramowitz, M., and I.A. Stegun (1964), Handbook of Mathematical Functions,
      Dover, New York.

APPENDIX A

QUASI-STATIC APPROXIMATIONS OF $V_1^{(2)}$ and $V_2^{(2)}$

In this appendix, the analytical expression for $V_\ell^{(2)}$, $\ell = 1,2$ given in (50) is derived.

$$V_\ell^{(2)} = \int_{\alpha_0}^{\infty} [F_\ell(\alpha) - F_{\ell q}(\alpha)] e^{-\gamma_0 b} J_0(\alpha\rho)\alpha d\alpha \qquad (A-1)$$

Now, if we use the choice of α_0 to be large such that $\tanh|\gamma_1 H_1| \simeq 1$, then the expressions for N_0 and K_0 in (8) and (9) will reduce to γ_1 and γ_1/n_1^2, respectively. Therefore $V_1^{(2)}$ and $V_2^{(2)}$ can be written as

$$V_1^{(2)} \simeq \int_{\alpha_0}^{\infty} \left[\frac{1}{\gamma_0 + \gamma_1/n^2} - \frac{2n_1^2}{(n_1^2 + 1)\gamma_0} \right] e^{-\gamma_0 b} J_0(\alpha\rho)\alpha d\alpha \qquad (A-2)$$

and

$$V_2^{(2)} \simeq \int_{\alpha_0}^{\infty} \left[\frac{1}{\gamma_0 + \gamma_1} - \frac{1}{\gamma_0} \right] e^{-\gamma_0 b} J_0(\alpha\rho)\alpha d\alpha \qquad (A-3)$$

By expanding in the inverse power of γ_0, $V_\ell^{(2)}$, $\ell = 1,2$ can be approximated to the following form:

$$V_\ell^{(2)} = C_\ell V \qquad \ell = 1,2 \qquad (A-4)$$

where

$$V = \int_{\alpha_0}^{\infty} e^{-\gamma_0 b} J_0(\alpha\rho)\alpha \gamma_0^{-3} [1 + 0(\gamma_0^{-2}) + \dots] d\alpha \qquad (A-5)$$

The constants C_1 and C_2 are given by

$$C_1 = -2n_1^2/(n_1^2 + 1)^2$$

and

$$C_2 = (n_1^2 - 1)/4$$

Thus if we just keep the leading terms of (A-5) and the assumption that $\alpha_0 \gg 1$ then

$$V \simeq \int_{\alpha_0}^{\infty} e^{-\alpha b} J_0(\alpha\rho)\frac{d\alpha}{\alpha^2}$$

The above integral can be evaluated by taking the derivatives with respect to ρ and then splitting up the integral into two parts; one has the limit of 0 to infinity and the other from 0 to α_0.

$$\frac{\partial V}{\partial \rho} = -\{ \int_{0}^{\infty} e^{-\alpha b} J_1(\alpha\rho)\frac{d\alpha}{\alpha} - \int_{0}^{\alpha_0} e^{-\alpha b} J_1(\alpha\rho)\frac{d\alpha}{\alpha} \}$$

The first integral can be found exactly [Gradshteyn and Ryzhik (ref. 15)],

$$\int_{0}^{\infty} e^{-\alpha x} J_\nu(\beta x) \frac{dx}{x} = \frac{(\sqrt{\alpha^2 + \beta^2} - \alpha)^\nu}{\nu\beta^\nu} \qquad (A\text{-}6)$$
$$\text{Re } \nu > 0, \text{ Re } \alpha > |\text{Im }\beta|$$

therefore

$$\int_{0}^{\infty} e^{-\alpha b} J_1(\alpha\rho) \frac{d\alpha}{\alpha} = (R-b)\rho^{-1} = \rho(R+b)^{-1}$$

However, the second integral has been evaluated approximately by using Taylor expansion of two variables b and ρ around $b, \rho = 0$

$$\int_{0}^{\alpha_0} e^{-\alpha b} J_1(\alpha\rho) \frac{d\alpha}{\alpha} \simeq \frac{\alpha_0}{2}\rho + O(R^2)$$

After substituting the values of the first and second term in (A-6), we can integrate back with respect to ρ which will lead to

$$V = -R + b \ln(R+b) + \frac{\alpha_0}{2}\rho^2 - C(b)$$

where $C(b)$ is a function of b only and is given by

$$-C = b - b \ln 2b + \frac{E_2(\alpha_0 b)}{\alpha_0}$$

Here E_2 is the exponential integral of order 2 and is given by [Abramowitz and Stegun (ref. 16)],

66

$$E_2(\alpha_o b) = e^{-\alpha_o b} + \gamma(\alpha_o b) + \alpha_o b \ln(\alpha_o b) + \alpha_o b \sum_{n=1}^{\infty} \frac{(-1)^n (\alpha_o n)^n}{nn!}$$

where γ is Euler's constant 0.5772.

Since $R << 1$, terms of the order R^2 or greater will be ignored. Also, it should be noted that we have assumed that $\alpha_o b$ and $\alpha_o \rho$ are small compared to the leading terms that are of the order R^{-1}. Thus V can be written in a simpler form as

$$V = -R + t[\gamma + \ln(\alpha_o/2)] + \frac{e^{-\alpha_o b}}{\alpha_o} + b \ln(b + R) \qquad (A-7)$$

The substituion of (A-7) into (A-4) then gives the analytical expression for the correction terms $V_\ell^{(2)}$, $\ell = 1,2$ as indicated in (50).

67

APPENDIX B

QUASI-STATIC APPROXIMATIONS OF $V_3^{(1)}$, $V_3^{(2)}$ and $V_3^{(3)}$

In this appendix, approximate solutions for $V_3^{(j)}$, (j = 1,2 and 3) is obtained as R approaches zero. As in appendix A, we assume that α_o is large compared to H_1 so that $\tanh|\gamma_1 H_1| \simeq 1$ can be used. However, the product of $\alpha_o R$ is still assumed to be small compared to 1 as $R \to 0$. The leading term $V_3^{(1)}$ in (54) is written here as

$$V_3^{(1)} = B_3 \cos \phi \frac{\partial}{\partial \rho} \int_b^\infty db \int_0^\infty e^{-\gamma_o b} J_o(\alpha\rho)\alpha\gamma_o^{-1} d\alpha \qquad (B-1)$$

The integral with respect to α is known as $G_{12} = e^{iR_{12}}/R_{12}$. If we now split up the integration over b into two parts, one runs from 0 to ∞ and the other from 0 to b, the first integral then reduces to the Hankel function form $\frac{\pi i}{2} H_o^{(1)}(\rho)$. However, for the second integral, Taylor expansion of G_{12} will be used since R_{12} is very small. After integrating the first three terms of the expansions, it is easy to show that $V_3^{(1)}$ can be given as

$$V_3^{(1)} \simeq B_3 \cos \phi \{-\frac{\pi i}{2} H_1^{(1)}(\rho) + \frac{b}{\rho R} + \frac{\rho}{2} \sinh^{-1}(b/\rho)\} \qquad (B-2)$$

It should be noted that in obtaining the above result the differentiation with respect to ρ is applied after the integration over b is performed. Expression for $V_3^{(1)}$ can be further simplified if we replace the Hankel function by its small argument expansion to yield

$$V_3^{(1)} = -B_3 \rho \cos \phi \{[R(R+b)]^{-1} - 0.5 \ln(R+b) - \frac{1}{2}(\gamma - \frac{1}{2} - \pi i/2 - \ln 2)\} \qquad (B-3)$$

where $\gamma = 0.5772$ is Euler's constant.

The second term from (54) that needs to be evaluated analytically is $V_3^{(2)}$ and is given by

$$V_3^{(2)} = B_3 \cos \phi \, \frac{\partial}{\partial \rho} \int_0^\infty [\frac{1}{\gamma_1^2} - \frac{1}{\gamma_0^2}] e^{-\gamma_0 b} J_0(\alpha\rho)\alpha d\alpha \qquad (B-4)$$

Again, the integral can be divided into two parts, one runs from 0 to α_0 and the other from α_0 to ∞ and approximation techniques similar to the ones given in appendix A can be applied here. It should be noted that the outcome of the integration should be independent of α_0. Now $V_3^{(2)}$ can be written as

$$V_3^{(2)} = V_{31}^{(2)} + V_{32}^{(2)} \qquad (B-5)$$

where

$$V_{31}^{(2)} = B_3 \cos \phi \, \frac{\partial}{\partial \rho} \int_0^{\alpha_0} [\frac{1}{\gamma_1^2} - \frac{1}{\gamma_0^2}] e^{-\gamma_0 b} J_0(\alpha\rho)\alpha d\alpha \qquad (B-6)$$

and

$$V_{32}^{(2)} = B_3 (n_1^2 - 1) I \cos \phi \qquad (B-7)$$

$$I = \frac{\partial}{\partial \rho} \int_{\alpha_0}^\infty e^{-\gamma_0 b} J_0(\alpha\rho) \frac{\alpha d\alpha}{(\gamma_0\gamma_1)^2} \simeq \frac{\partial}{\partial \rho} \int_{\alpha_0}^\infty e^{-\gamma_0 b} J_0(\alpha\rho)\frac{\alpha d\alpha}{\gamma_0^4}$$

$$(B-8)$$

In writing $V_{32}^{(2)}$ above, we have replaced $(\frac{1}{\gamma_1^2} - \frac{1}{\gamma_0^2})$ by $[(n_1^2 - 1)/(\gamma_0\gamma_1)^2]$.

Then, we have used the assumption that α_0 is large so that γ_1 would be replaced by γ_0. Thus, the differentiation of I with respect to b is known as $-\frac{\partial V}{\partial \rho}$, where V is given by (A-5) and known explicitly in (A-7). Hence, $\frac{\partial I}{\partial \rho}$ can be written as

$$\frac{\partial I}{\partial b} \simeq \frac{\rho}{R} - \frac{b}{\rho} (1 - \frac{b}{R})$$

Integrating the above expression to get the value of I as

$$I = \frac{1}{2}[\rho \sinh^{-1}(b/\rho) + b\rho (R + b)^{-1} - K(\rho)] \qquad (B-9)$$

69

and the integration constant $K(\rho)$ is determined from the condition at $b = 0$

$$K(\rho) = \int_{\alpha_0}^{\infty} J_1(\alpha\rho)\alpha^2 \frac{d\alpha}{\gamma_0^4}$$

$$\simeq \int_{\alpha_0}^{\infty} J_1(\alpha\rho) \frac{d\alpha}{\alpha^2}$$

It is then not difficult to show that $K(\rho)$ satisfies the first order differential equation

$$\frac{\partial K}{\partial \rho} + \frac{K}{\rho} = \int_{\alpha_0}^{\infty} J_0(\alpha\rho)\frac{d\alpha}{\alpha}$$

The integral on the right side of the differential equation can be replaced by a two term expansion, ignoring the series terms which are of the order ρ^2 or greater [Abramowitz (ref.16) page 481, Eq.11.1.20]. Thus the differential equation reduces to the following form

$$\frac{\partial K}{\partial \rho} + \frac{K}{\rho} = - \gamma - \ln(\alpha_0\rho/2)$$

which has a known solution of the form

$$K(\rho) = - \frac{\rho}{2} [\gamma + \ln(\alpha_0/2) - \tfrac{1}{2}] - \frac{\rho}{2} \ln \rho$$

where γ here is Euler's constant. The substitution of the above value of $K(\rho)$ into (B-9) and then the value of I into (B-7) will give $V_{30}^{(2)}$ as

$$V_{32}^{(2)} = \frac{(n_1^2-1)}{2} \rho B_3 \cos \phi \ [\ln(b+R) + b(R+b)^{-1} + (\gamma - \tfrac{1}{2} - \ln 2 + \ln \alpha_0)] \qquad \text{(B-10)}$$

Clearly, the result we have obtained for $V_{32}^{(2)}$ is dependent on α_0, and this term should cancel out with the contribution from $V_{31}^{(2)}$ up to the order of

R^2. Since b and ρ are both small a two variable Taylor expansion around b, $\rho = 0$ gives approximate expression of $V_{31}^{(2)}$ and is given by

$$V_{31}^{(2)} \simeq B_1 \rho \cos \phi \int_0^{\alpha_0} \alpha^3 [\frac{1}{\gamma_1^2} - \frac{1}{\gamma_0^2}] d\alpha \qquad (B-11)$$

The evaluation of the integral can be readily carried out, provided the integration path is understood as being indented into the lower half-plane at $\alpha = 1$.

$$V_{31}^{(2)} = - \tfrac{1}{4} B_3 \cos \rho \ [n_1^2 \ln\left(\frac{\alpha_0^2 - n_1^2}{\alpha_0^2 - 1}\right) + (n_1^2 - 1)\ln(\alpha_0^2 - 1)$$
$$- n_1^2 \ln n_1^2 + \pi i (n_1^2 - 1)\} \qquad (B-12)$$

Thus, with the assumption that $\alpha_0 \gg |n_1|$ we finally have the resultant expression in the form of

$$V_{31}^{(2)} = \frac{(n_1^2 - 1)}{2} B_3 \rho \cos \phi \ [- \ln \alpha_0 + \frac{n_1^2}{(n_1^2 - 1)} \ln n_1 - \frac{\pi i}{2}] \qquad (B-13)$$

Substitution of the expressions for $V_{31}^{(2)}$ in (B-13) and $V_{32}^{(2)}$ in (B-10) into (B-5) now yields the result

$$V_3^{(2)} = \frac{(n_1^2 - 1)}{2} B_3 \rho \cos \phi \ \{\ln(b+R) + b(R + b)^{-1}$$
$$+ (\gamma - \tfrac{1}{2} - \pi i/2 - \ln 2) + \frac{n_1^2}{(n_1^2 - 1)} \ln n_1\} \qquad (B-14)$$

which is then independent of the parameter α_0 that we somewhat arbitrarily have chosen.

The last integral that needs to be evaluated is $V_3^{(3)}$ in (54). Since α_0 is large such that $\tanh|\gamma_1 H_1| \simeq 1$, then N_0 and K_0 will be replaced by γ_1 and γ_1/n_1^2, respectively. Thus, $V_3^{(3)}$ can be written here as

$$V_3^{(3)} = B_3 \cos\phi \frac{\partial}{\partial\rho} \int_{\alpha_0}^{\infty} \left[\frac{2(n_1^2 - 1)}{n_1^2(\gamma_0 + \gamma_1)(\gamma_0 + \gamma_1/n_1^2)} - \frac{(n_1^2 - 1)}{(n_1^2 + 1)\gamma_1^2} \right] e^{-\gamma_0 b} J_0(\alpha\rho)\alpha d\alpha$$

(B-15)

If we now approximate $\gamma_1 \simeq \gamma_0 + \frac{1}{2}\frac{(n_1^2 - 1)}{\gamma_0}$, the leading term of $V_3^{(3)}$ in

(B-17) can be shown to be associated with the integral I given in (B-8) which

is evaluated in (B-9). Consequently, we have

$$V_3^{(3)} = - C_3 \rho \cos\phi \left[\ell n(b+R) + b(R+b)^{-1} + (\gamma - \tfrac{1}{2} - \ell n\, 2 - \ell n\, \alpha_0) \right]$$

(B-16)

where
$$C_3 = (3n_1^2 + 1)[(n_1^2 - 1)/(n_1^2 + 1)]^2/8$$

72

APPENDIX C
PROGRAMMING PROCEDURE

A computer program was developed to find the electromagnetic field response of a tilted dipole above a finitely conducting two layered earth according to the numerical scheme described in Section III, with provision for the asymptotic and quasi-static calculation as explained in section IV. A flow chart of the program is shown in figure C-1. The program mainly consists of three subroutines called QSTATC, RESULT and ASMPT, each of which is capable of calculating field components for different ranges of observations in space.

The subroutine RESULT is used to integrate along the real axis of the complex α-plane for a given integrand. It follows the same steps given in section III, where the integration has been split up into two different regions as given in (34). As mentioned before, a provision is made when the location of the pole is close to the path of integration. By drawing a circle of influence with a radius $\alpha_s = |\alpha_p - 1|$ and centered at α_p, we can integrate separately the interval within this circle in order to insure good numerical accuracy. Thus, α_s determines how the integration path should be split up, for example if $\alpha_s \geq 1$ then the integration will proceed exactly according to (34). But if $\alpha_s < 1$ then the path of integration will be subdivided. Obviously our path of integration is taken beneath the branch cut for α between 0 and 1 and the pole could have stronger influence if it is close to or beyond the branch point at $\alpha = 1$. Usually the situation where the pole is close to the branch point at $\alpha = 1$, occurs when we have a two region conducting half-space (such as air and earth). For a typical application of a concrete slab above a homogenous earth and for the frequency range (100 to 1000 MHz), the poles are actually not very close to the path of integration as shown in table 3.

73
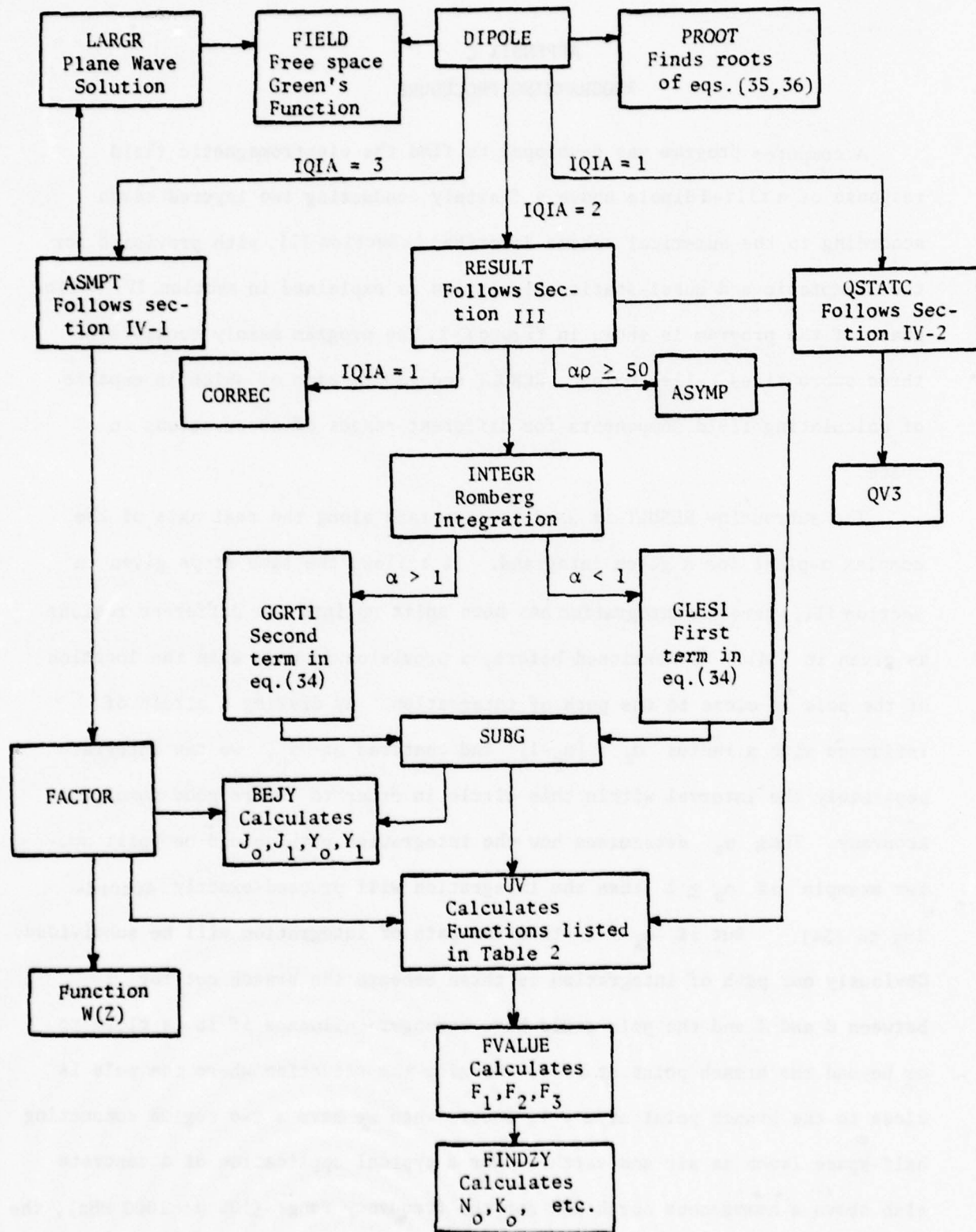
Figure C-1. A flow chart of the computer program

However, we have left these subdivision criteria in the program so that the program can be a general purpose one. Our program without further modification cannot handle the cases where the poles are directly on the real axis which corresponds to lossless slab above a perfectly conducting sheet. But in most of the cases which involve losses in both media, the poles usually move upward away from the real axis. A root finder called PROOT was developed which uses the poles of a lossless slab above a perfectly conducting sheet as a basis to march toward the roots for a lossy slab and earth. A combination of bisectional and Newton's methods is used to search the complex roots of (35) and (36). Figure C-2 is a flow chart of the root finder, where the subroutine ROOT will first search the real roots of the lossless slab above a perfectly conducting sheet; then these roots (if any) will be used in ZROOT to search for the complex roots of a lossy slab above a finitely conducting earth.

Except for the region nearby the pole, the two integrals in (34) are further broken up into segments where numerical integration based upon a modified Romberg scheme is performed. Segment interval is determined either from the nature cycle of the Bessel functions, i.e. $\Delta\alpha \simeq 2\pi/\rho$, or from the decay rate of the exponential function, i.e. $\Delta\alpha \simeq 3/(Z+H_0)$. Obviously, the number of integrations and the computation time increase when ρ and $(Z + H_0)$ are either very small or very large. In such cases, the program is then switched to the quasi-static and asymptotic routines even though the normal integration method can be performed.

We now discuss the type of convergence criteria adopted for the truncation of the infinite integral in (34). Judging from the expression for the integrand as given in (30), it is obvious that one can simply integrate until the argument of the exponential function $\gamma_0(Z+H_0)$ is large

```
                    ┌─────────────┐
                    │    PROOT    │◄──────────────┐
                    └──────┬──────┘               │
              ┌────────────┘                      │
              ▼                                    ▼
      ┌───────────────┐              ┌─────────────────────┐
      │     ZROOT     │              │        ROOT         │
      │    Complex    │              │        Real         │
      │   functions   │              │     functions       │
      │     root      │              │   root finder       │
      │    finder     │              │    bisection        │
      └───────┬───────┘              │   method only       │
              │                      └──────┬──────────┬───┘
              ▼                             ▼          ▼
      ┌───────────────┐          ┌──────────┐  ┌──────────┐
      │     CROOT     │          │ Function │  │ Function │
      │  Searches for │          │  FY(Z)   │  │  FX(Z)   │
      │  complex root │          │given in eq.│ │given in eq.│
      │ by using both │          │   (39)   │  │   (40)   │
      │   Newton's and│          └──────────┘  └──────────┘
      │   bisection   │
      │    method     │
      └───┬───────┬───┘
          │       │
          ▼       ▼
  ┌──────────┐ ┌──────────┐
  │ Function │ │ Function │
  │  CY(Z)   │ │  CX(Z)   │
  │given in eq.│ │given in eq.│
  │   (35)   │ │   (36)   │
  └──────────┘ └──────────┘
```
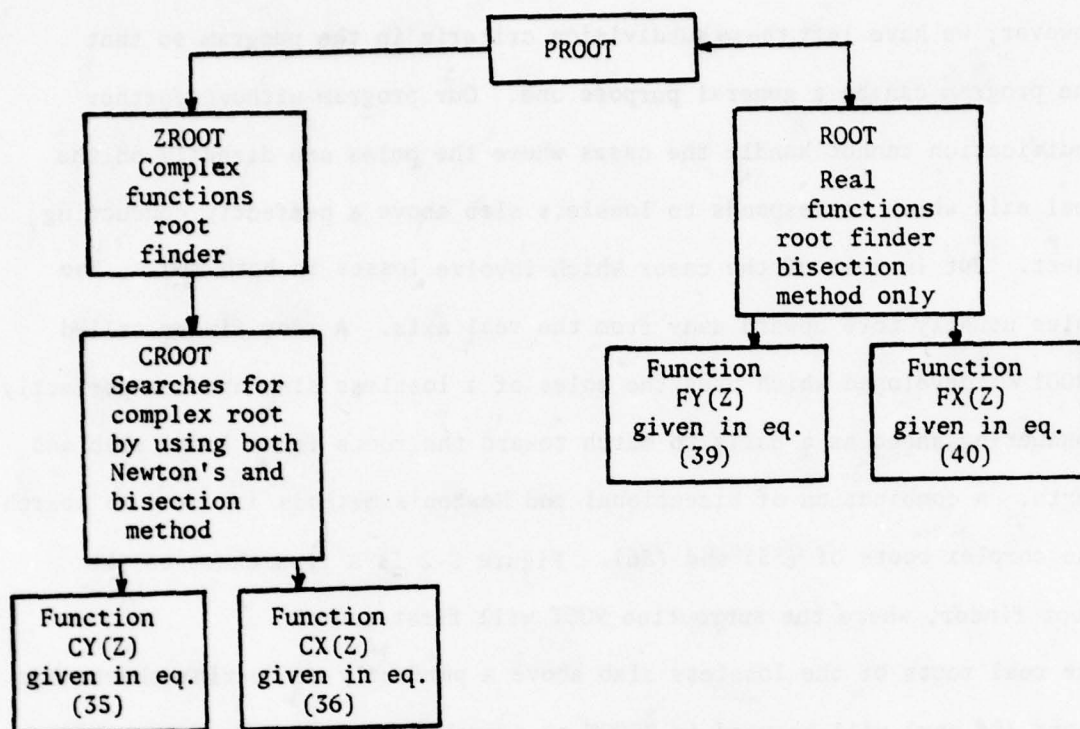
Figure C-2. A flow chart of the root finder

enough, say 12, so that the remainder of the integration will be of the order 10^{-7} or smaller. However, this criterion becomes less effective for observation near the surface when $(Z + H_o)$ is small. In that case, we switch the truncation criterion to one that depends on the argument of the Bessel function $\alpha\rho$, where $\rho = k_o r$ and r is the horizontal distance from the source to the observation point. When $\alpha\rho$ reaches a certain large number, say 50 or more, we can replace the Bessel function by its asymptotic form [Abramowitz (ref.16)]. Then the remainder of the integral can be evaluated analytically by an asymptotic series. Since each term of the series decreases by the factor $(\alpha\rho)^{-1}$ from its previous term, we used a two term expression and estimate the error bound. The truncation is then determined by a specified accuracy of five digits. These remainder terms can be deduced from (30) and typically given as follows:

$$T_m(\alpha_t) = \int_{\alpha_t}^{\infty} F(\alpha)[\cos \chi - P(\alpha) \sin \chi]d\alpha \qquad m = 0,1 \qquad (C-1)$$

where $\chi = (\alpha\rho - \frac{m\pi}{2} - \frac{\pi}{4})$, $P(\alpha) = \frac{4m^2-1}{8\alpha\rho}$ and α_t is the limit where the Bessel function can be replaced by its asymptotic form. $F(\alpha)$ is given by

$$F(\alpha) = (2/\pi\alpha\rho)^{\frac{1}{2}} \alpha G(\alpha)/\gamma_o$$

and $G(\alpha)$ is a typical function listed in table 2. Now, if we twice perform the integration by parts in C-1, $T_m(\alpha_t)$ will reduce to approximately

$$T_m(\alpha_t) = - \frac{\sin \chi_o}{\rho} F(\alpha_t) - \frac{\cos \chi_o}{\rho^2} \left. \frac{dF}{d\alpha} \right|_{\alpha = \alpha_t}$$
$$- \frac{(4m^2-1)}{8\alpha_o} \frac{\cos\chi_o}{\rho^2} F(\alpha_t) + O(\rho^{-3}) \qquad (C-2)$$

where $\qquad \chi_o = (\alpha_t\rho - \frac{m\pi}{2} - \frac{\pi}{4})$

The result given in (C-2) will be added to the truncated integral if the truncation was made on the Bessel function argument. The subroutine that

77

handles the evaluation of $T_m(\alpha_t)$ is called ASYMP. In the case of the quasi-static method, we have added a third criterion for the truncation of the integration, and that depends on α_o according to the method discussed in section IV-2.

As we mentioned before, numerical integration of individual segment along the real axis is performed by a modified quadrature Romberg scheme. The subroutine that performs the integration is called INTEGR, which is known to be a fast convergent one unless there is a discontinuity in the function within the integrated limits. INTEGR has been developed to integrate an array of functions. Thus, all six integrations of the EM field components in the space region can be performed at once. The usual criterion the integration is by checking if either the absolute or relative error of the integration has reached the needed tolerance. More specifically in figure C-1, the integration routine calls two functions, GLES1 and GGRT1, which represent the functions of the first and second integral in (34), respectively. SUBG gives the value of T(x) for any x as required in (34). SUBG calls two other subroutines; One, BEJY calculates the Bessel function J_o and J_1; the other, UV computes the values of the functions $(\mathcal{E}_w^\ell, \mathcal{H}_w^\ell)$, $\ell = 0,1$ and w = x,y,z, listed in table 2. Two other subroutines, EVALUE and FINDZY, are used in UV for the purpose of calculating the functions $F_\ell(\alpha)$, $\ell = 1,2,3$, and N_o, K_o, etc., as given respectively by (29) and (8) for a single slab.

As we have noted earlier the usual method of integration becomes a time consuming one for large R. For such a case, we switch the program to a subroutine called ASMPT, based upon the asymptotic solution derived in section IV.1. For computing efficiently, this part of the program is further split up into a sky-wave region and a ground-wave region. This means we use

78

a two term sky-wave solution where the observation is made away from the ground (subroutine LARGR) and a two-term ground wave solution as described in section IV.1 (subroutine FACTOR).

The subroutine QSTATC serves the purpose of finding the fields for a very small value of R, where $R = k_o R_{12}$ is the normalized distance from the dipole image to the observation point, $R_{12} = [(z + h_o)^2 + r^2]^{\frac{1}{2}}$. This subroutine follows exactly the procedure described under section IV-2 except Maxwell equations have to be used first to find the electromagnetic field components. The finite integration from 0 to α_o for ΔV_ℓ ($\ell = 1,2,3$) in (51) and (55) was performed by calling the subroutine RESULT. However, analytical expression has been used to replace the integration from α_o to infinity, i.e. $V_\ell^{(2)}$ ($\ell = 1,2$) in (53) and $V_3^{(3)}$ in (58). This analytical result has been built in subroutine CORREC which is called from RESULT automatically when the integration has reached the upper limit α_o. The leading terms, i.e., $V_\ell^{(1)}$ ($\ell = 1,2$) in (52) and $V_3^{(1)}$ in (56), are calculated in QSTATC by calling two other subroutines, FIELD and QV3, the first calculates the free space Greens functions given in (24) and the second calculates the leading term of the cross coupling field V_3 given by (56).

Finally, we emphasize that the subroutines QSTATC and ASMPT are built to speed up the program. They are auxiliary routines to the main program, which provide adequate approximate answers as an alternative to the exact but time consuming results available from the subroutine RESULT.

APPENDIX D

LIST OF THE COMPUTER PROGRAM

```
      SUBROUTINE DIPOLE(FREQN,EPSR,SIGMA,H1,HO,R,TH,PH,THP,NOROOT,AO,
     1                  ACCINT,TOTFLD,IFLAG)

C     SUBROUTINE DIPOLE WAS DESIGNED TO FIND THE EM FIELD DUE TO AN
C     ARBITRARY-ORIENTATED DIPOLE SOURCE ABOVE A TWO LAYER CONDUCTING
C     EARTH . THE INPUTS TO THE PROGRAM ARE:
C     FREQN=FREQUENCY OF OPERATION.
C     (EPSR) AND (SIGMA) EACH OF WHICH SHOULD HAVE THE DIMENSION OF 3
C     REPRESENTING THE DIELECTRIC CONSTANT AND CONDUCTIVITY (MHO/M)
C     IN THE THREE MEDIA:AIR,SLAB REGION AND GROUND RESPECTIVELY.
C     H1=SLAB WIDTH.
C     HO=HEIGHT OF THE DIPOLE FROM THE SLAB SURFACE.
C     R=THE DISTANCE OF THE DIPOLE IMAGE ABOVE A PERFECTLY CONDUCTING
C        GROUND TO THE OBSERVATION POINT. R=SQRT((Z+HO)**2+(SR)**2) :
C        WHERE SR=SMALL R ,IS THE PROJECTION OF R INTO THE X-Y PLANE.
C     TH=THETA IS THE IMAGE ANGLE (IN DEGREES) WHICH THE OBSERVATON
C        POINT MAKES WITH THE Z-AXIS (REFER TO FIG-5 OF THE REPORT).
C     PH=PHI IS THE OBSERVATION ANGLE (IN DEGREES) MEASURED IN THE X-Y
C        PLANE.
C     THP=THETA-PRIME IS THE ANGLE (IN DEGREES) THAT THE DIPOLE MAKES
C         WITH THE VERTICAL AXIS. IF THP=0 THE DIPOLE IS VERTICAL AND
C         IF THP=90 THEN THE DIPOLE IS HORIZONTAL.
C     NOROOT=IS A LOGICAL STATEMENT WHEN IT IS TRUE NO SEARCH WILL BE
C            MADE FOR THE POLES (PHYSICALLY ,SURFACE WAVE MODES) IN THE
C            SLAB REGION ALSO NO CALCULATON OF THE SOMMERFELD POLE WILL
C            BE MADE IN THE HALF-SPACE CASE.IF (NOROOT) IS FALSE THEN
C            A SEARCH FOR POLES WILL BE MADE.
C     AO=IS THE POLE CLOSEST TO THE REAL-AXIS IN THE COMPLEX ALPHA-PLANE
C        . IT SHOULD BE SPECIFIED ARBITRARILY IF THE ROOT FINDER IS NOT
C        USED.
C     ACCINT=IS THE ERROR TOLERANCE OF THE NUMERICAL INTEGRATION.
C     TOTFLD=ARE THE CALCULATED VALUES OF ALL THE EM FIELD COMPONENTS.
C            IT SHOULD BE DIMENSIONED AS TOTFLD(3,2). THE FIRST COLUMN
C            ARE THE E-FIELD COMPONENTS (EX,EY AND EZ), AND THE SECOND
C            COLUMN ARE THE H-FIELDS (HX,HY AND HZ).
C     IFLAG=IS A LOGICAL STATEMENT WHICH IF IT IS TRUE QUASI-STATIC AND
C           ASYMPTOTIC APPROX. WILL BE USED. IF (IFLAG) IS FALSE THEN
C           USUAL NUMERICAL INTEGRATION METHOD WILL BE PERFORMED ON
C           THE SO CALLED SOMMERFELD INTEGRALS.

      COMMON /MAIN1/N(3),H,EPSR(3),RKO,KO,ZHM,TOL
      COMMON /MAIN2/B,PHI,THETAP,CT1,ST1,CP1,SP1,CP2,SP2
      COMMON /MAIN3/SS(3),EE(3),HH,OM
      COMMON /TYPE/IQIA
      LOGICAL NOROOT,IFLAG
      COMPLEX N,AO,J,FA,A
      COMPLEX DI,DS,SOMFLD,TOTFLD,WAVE,PZS,PXS,PZI,PXI
      REAL KO,MUO
      DIMENSION A(5),SIGMA(3)
      DIMENSION DI(3,2),DS(3,2),SOMFLD(3,2),PZS(3,2),PXS(3,2)
     1,PZI(3,2),PXI(3,2),WAVE(3,2),TOTFLD(3,2)
      TOL=ACCINT
      J=(0.,1.)
      PI=3.141592653
      C=2.99793E+08
      EPSO=8.854E-12    S     MUO=4.*PI*1.0E-07
      EGZI=SQRT(MUO/EPSO)
      CONV=PI/180.
      OMEGA=2.*PI*FREQN
      KO=OMEGA/C
      H=H1*KO
      FB=KO*KO/4./PI    S     FA=J*EGZI*FB
```

81

```
      DO 12 L=1,3
  12 N(L)=CSQRT(EPSR(L)+(0.,1.)*SIGMA(L)/OMEGA/EPSO)
  51 THETA=TH*CONV
     Z=R*COS(THETA)-HO   S    RO=R*SIN(THETA)
     ZH=Z+HO       S    ZHM=Z-HM
     B=ZH*KO       S    RKO=RO*KO
     PRINT 88,FREQN,(N(L),EPSR(L),SIGMA(L),L=1,3)
  88 FORMAT (1H1*FREQUENCY=*E9.2,1X*C/S*/,1X*REFRACTIVE INDICES OF AIR,
    1CEMENT AND EARTH RESPECTIVELY*/1X*NO=*F9.4,*+*J*F9.4,10X*EPSRO=*E8.
    21,3X*SIGMA0=*E10.3/1X*N1=*F9.4,*+*J*F9.4,10X*EPSR1=*E8.1,3X*SIGMA1=
    3*E10.3/,1X*N2=*F9.4,*+*J*F9.4,10X*EPSR2=*E8.1,3X*SIGMA2=*E10.3/)
     PRINT 14,Z,HO,HM,R,TH
  14 FORMAT   (1X,*Z=*E10.3,2X*M*,3X*OBSERVATION HEIGHT*/1X*HO=*E10.3,1X
    1*M*,3X*DIPOLE HEIGHT*/1X*HM=*E10.3,1X*M*,3X*SLAB WIDTH*/1X*R=*E10.
    23,2X*M*,3X*SOURCE TO OBSERVATION DISTANCE*/1X*THETA=*F5.1,1X*DEG*,
    33X*ANGLE OF INCIDENCE*/)

C    NO SEARCH FOR POLES WILL BE AVAILABLE WHEN NOROOT IS TRUE.THUS THE
C    POLE LOCATION AO SHOULD BE SPECIFIED .IF THESE POLES ARE FAR AWAY
C    FROM THE REAL AXIS,ASSIGN ANY ARBITRARY POLE IN THE FIRST QUADRANT
C    OF THE COMPLEX ALPHA-PLANE. THIS POLE SHOULD NOT BE CLOSE TO THE
C    PATH OF INTEGRATION.

     IF (NOROOT) GO TO 22

C    CHECK IF WE HAVE A TWO-LAYER EARTH MODEL.IF SO CALL RROOT !

     IF (H.GT.1.0E-05.OR.H.LT.1.0E-05) GO TO 26

C    IF NOT, WE HAVE A SINGLE LAYER EARTH .HENCE WE NEED TO FIND THE
C    SOMMERFELD POLE!

     IF (H.LE.1.0E-05) AO=N(3)/CSQRT(N(3)*N(3)+1.)
     IF (H.GE.1.0E-05) AO=N(2)/CSQRT(N(2)*N(2)+1.)
     GO TO 22

C    SUBROUTINE RROOT WAS DESIGNED TO FIND THE SURFACE WAVE MODES THAT
C    EXIST IN A DIELECTRIC SLAB ABOVE A DISSIPATIVE EARTH.

  26 DO 23 I=1,3
     EE(I)=EPSR(I)
  23 SS(I)=SIGMA(I)
     OM=OMEGA     S    HH=H
     CALL RROOT(A,AO)

C    AO WILL BE THE POLE CLOSEST TO THE PATH OF INTEGRATION.
C    (A) WILL BE THE POLES THAT ARE FOUND . PLACES WHERE RROOT FAILS A
C    MESSAGE WILL BE PRINTED AND THE ARBITRARY POLE (.95,.15) WILL BE
C    ASSIGNED. UP TO 5 POLES WILL BE SEARCHED WITH THE EXISTING DIMENSION
C    OF A(5). IF MORE EXIST ,THE DIMENSION OF (A) IN DIPOLE AND (ZERO)
C    IN RROOT SHOULD BE INCREASED.

  22 PHI=PH*CONV    S    THETAP=THP*CONV
     CT1=COS(THETAP)    S    ST1=SIN(THETAP)
     CP1=COS(PHI)     S    SP1=SIN(PHI)
     CP2=COS(2.*PHI)    S    SP2=SIN(2.*PHI)
     IF (IFLAG.LE.0) GO TO 165

C    THE FOLLOWING THREE ROUTINES WILL BE USED FOR THE EVALUATION OF
C    THE SOMMERFELD INTEGRALS
C    (1) QUASI-STATIC APPROX. .
     (2) NORMAL INTEGRATION ALONG THE REAL AXIS IN THE COMPLEX ALPHA-
```

```
C        PLANE .
C     (3) ASYMPTOTIC TECHNIQUES (USING STEEPEST DESCENT METHOD ).

      RN=R*K0
      IF (RN.GT.5.0E-02.OR.RN.LT.3.0E+01) GO TO 165
      IF (RN.GE.3.0E+01) GO TO 77

C     QUASI-STATIC APPROX. WILL BE PERFORMED .

      IQIA=1
      CALL QSTATC(A0,WAVE,3,2,IQIA)
      GO TO 33

C     ASYMPTOTIC APPROX. WILL BE PERFORMED .

   77 IQIA=3
      CALL ASMPT(A0,THETA,WAVE,3,2)
      GO TO 33

C     IN HERE, JUST REGULAR INTEGRATION METHOD WILL BE USED TO FIND THE
.C     SOMMERFELD INTEGRALS .

  165 CALL FIELD(DS,K0,ZHM,RO,PZS,PXS,3,2)
      CALL FIELD(DI,K0,ZM,RO,PZI,PXI,3,2)
      IQIA=2
      CALL RESULT(A0,SOMFLD,3,2,IQIA)
      DO 6 JJ=1,2
      DO 6 II=1,3
    6 WAVE(II,JJ)=DS(II,JJ)-DI(II,JJ)+SOMFLD(II,JJ)
   33 DO 2 JJ=1,2
      DO 4 II=1,3
      IF (JJ.EQ.2) GO TO 56
      TOTFLD(II,JJ)=FA*WAVE(II,JJ)
      GO TO 4
   56 TOTFLD(II,JJ)=FB*WAVE(II,JJ)
    4 CONTINUE
    2 CONTINUE
      RETURN
      END
```

```fortran
      SUBROUTINE FIELD(D,K,ZH0,RO,X,Y,I,M)

C     THIS SUBROUTINE EVALUATES ALL THE ELECTROMAGNETIC FIELD COMPONENTS
C     DUE TO AN ELECTRIC VECTOR POTENTIAL OF THE FORM G11=EXP(J*R11)/R11
C     OR G12=EXP(J*R12)/R12 .WHERE R11=SQRT((Z-H0)**2+RHO**2) AND
C     R12=SQRT((Z+H0)**2+RHO**2).Z,H0 AND RHO ARE NORMALIZED TO THE FREE
C     SPACE WAVELENGTH K0'. THE INPUTS ARE :
C     (1) K IS FREE SPACE WAVELENGTH.
C     (2) RO IS A RADIAL DISTANCE.
C     (3) ZH0 REPRESENTS THE NON-NORMALIZED DISTANCE (Z-H0)' OR (Z+H0).
C     THE OUTPUTS ARE :
C     (1) D REPRESENTS THE FIELD DUE TO G11 OR G12.
C     (2) X AND Y REPRESENT THE FIELD DUE TO A VERTICAL AND A HORIZONTAL
C         DIPOLE RESPECTIVELY.

      COMMON /MAIN2/BB,P,T,CT,ST
      COMPLEX G11,J,F,D,X,Y
      REAL K
      DIMENSION X(3,2),Y(3,2),D(3,2)
      J=(0.,1.)
      R=SQRT(RO*RO+ZH0*ZH0)
      A=1./(K*R)
      G11= CEXP(J*K*R)*A
      B=A*A
      XR=RO*COS(P)/R      S      YR=RO*SIN(P)/R
      ZR=ZH0/R
      F=1.+3.*J*A-3.*B


      X(1,1)=-F*XR*ZR*G11*CT S    Y(1,1)=-(F*XR*XR-1.-J*A+B)*G11*ST
      X(2,1)=-F*YR*G11*ZR*CT   S    Y(2,1)=-F*YR*G11*XR*ST
      X(3,1)=-(F*ZR*ZR-1.-J*A+B)*G11*CT     S    Y(3,1)=-F*XR*ZR*G11*ST
      X(1,2)=(J-A)*YR*G11*CT   S    Y(1,2)=(0.,0.)
      X(2,2)=(A-J)*G11*XR*CT   S    Y(2,2)=(J-A)*G11*ZR*ST
      X(3,2)=(0.,0.)    S    Y(3,2)=(A-J)*YR*G11*ST

      DO 22 JJ=1,2
      DO 22 II=1,3
   22 D(II,JJ)=X(II,JJ)+Y(II,JJ)

      RETURN
      END
```

```
      SUBROUTINE LARGR(THETA,FLD,II,MM)

C    THIS SUBROUTINE EVALUATES THE EM FIELD COMPONENTS IN THE AIR REGION
C    ASSUMING A PLANE WAVE INCIDENCE ON THE AIR AND SLAB INTERFACE (SKY-
C    WAVE ASYMPTOTIC APPROXIMATION OF THE SOMMERFELD INTEGRALS).THE INPUT
C    IS THETA=ARCTAN(RO/(Z+H0)).THE OUTPUT IS FLD. II AND MM ARE VARIABLE
C    DIMENSIONS.

      COMMON /MAIN1/N(3),H,E(3),RK,K0,ZHM
      COMMON /MAIN2/B,P,TP,CT,ST,CP
      COMMON /ZYY/YZ(3)
      COMMON /FUV/AL,GG0,GG1,GG2
      REAL K0
      COMPLEX GG0,GG1,GG2,PZS,PXS,PZI,PXI,YZ,REFL1,REFL2
     1,DI,DS,FLD,N,J
      DIMENSION DI(3,2),DS(3,2),FLD(II,MM) ,PZS(3,2),PXS(3,2)
     1,PZI(3,2),PXI(3,2)
      J=(0.,1.)
      AL=SIN(THETA)     S  GG0=-J*COS(THETA)
      GG1=CSQRT(AL*AL-N(2)*N(2))
      GG2=CSQRT(AL*AL-N(3)*N(3))
      ZH=B/K0          S   RO=RK/K0

      CALL FINDZY

C    PARALLEL POLARIZATION REFLECTION COEFFICIENT.

      REFL1=(GG0-YZ(1))/(GG0+YZ(1))

C    PERPENDICULAR POLARIZATION REFLECTION COEFFICIENT.

      REFL2=(GG0-YZ(2))/(GG0+YZ(2))

C    EM FIELD DUE TO G11=EXP(I*R11)/R11

      CALL FIELD(DS,K0,ZHM,RO,PZS,PXS,II,MM)

C    EM FIELD DUE TO G12=EXP(I*R12)/R12

      CALL FIELD(DI,K0,ZH,RO,PZI,PXI,II,MM)

      DO 5 M=1,MM
      DO 5 I=1,II
    5 FLD(I,M)=PZS(I,M)+REFL1*PZI(I,M)+PXS(I,M)+
     1(-REFL1*CP+REFL2*(1.-CP))*PXI(I,M)
      RETURN
      END
```

85

```
      SUBROUTINE RESULT(ALPHA0,VALUE,KK,LL,IQ)

C     THIS SUBROUTINE CALCULATES THE SOMMERFELD INTEGRALS GIVEN IN EQ.
C     (30) OF THE REPORT,HOWEVER WHEN IQ=1,THEN IT CALCULATES THE
C     INTEGRALS OF (51) AND (55).
C     INPUT Ξ(ALPHA0) IS POLE LOCATION IN COMPLEX ALPHA PLANE.
C     OUTPUT Ξ(VALUE),KK AND LL ARE VARIABLE DIMENSIONS.

      COMMON /MAIN1/N(3),H,EPSR(3),RK,FK,ZM,TOLRNS
      COMMON /MAIN2/B,PHI,THETAP
      COMPLEX N,ALPHA0,VALUE
      COMPLEX SUM,SAVE
      DIMENSION SUM(3,2),SAVE(3,2),VALUE(KK,LL)
      EXTERNAL GLES1,GGRT1
      LOGICAL TEST
      PI=3.141592653
      NI=2048
      EE=1.0E-06

C     CRITERIA FOR THE SUBDIVISION OF THE INTEGRATION.

      CR=6.0/(RK*EE)    S    CZ=3.0/(B*EE)    S    CH=1.0/(H*EE)
      FACT1 =AMIN1(CR,CZ,CH)
C     CRITERION FOR UPPER LIMIT TRUNCATION IN THE QUASI-STATIC CASE
C     SEE SECTION 4.2 OF THE REPORT.

      EN=CABS(N(2))    S    EN1=10.*EN
      HC=SQRT(50.0*CH*CH*EN*EN)    S    CCH=AMAX1(HC,EN1)
      DO 1 LI=1,LL
      DO 1 KI=1,KK
    1 SAVE(KI,LI)=(0.,0.)
      ACC=TOLRNS

C     HERE,WE DETERMINE THE CIRCLE OF INFLUENCE DUE TO THE POLE MOTION
C     AS DISCUSSED IN SECTION 3.

      AR=REAL(ALPHA0)    S    AI=AIMAG(ALPHA0)
      RR=SQRT((AR-1.)**2+AI**2)
      IF (AR.GT.1.) GO TO 33
      DIF=1.-4.*RR    S    ADD=1.+4.*RR
      GO TO 36
   33 DIF=AR-4.*RR    S    ADD=AR+4.*RR
   36 IF (DIF) 15,15,16

C     THE POLE HAS NO INFLUENCE ON THE PATH OF INTEGRATION ,THUS THE
C     PATH WILL BE SUBDIVIDED AS GIVEN BY EQ. (34) OF THE REPORT

   15 T1=0.    S    T2=1.
      IJ=1    S    GO TO 27
   16 IF (DIF.LE.1.) GO TO 105

C     THE POLE HAS AN INFLUENCE BEYOND THE BRANCH POINT AT ALPHA=1.

      EPS1=SQRT(DIF*DIF-1.)    S    EPS2=SQRT(ADD*ADD-1.)
      T1=0.    S    T2=1.
      IJ=3    S    II=1
      EPS=EPS1
      RZ=AMIN1(CR,CZ)
      IF (EPS1.GE.RZ) EPS=RZ
      GO TO 27

C     HERE, THE POLE HAS AN INFLUENCE IN THE REGION FOR ALPHA BETWEEN
C     0 AND 1.

  105 EPS1=SQRT(1.-DIF*DIF)    S    EPS=SQRT(ADD*ADD-1.)
      T1=0.    S    T2=EPS1
      IJ=2    S    II=0
      EPS2=AMIN1(EPS,CR,CZ)
```

86

```
C     FIRST INTEGRATION FOR ALPHA BETWEEN 0 AND 1 AS GIVEN IN THE FIRST
C     TERM OF (34). GLES1=REPRESENTS THE FUNCTIONS TO BE INTEGRATED IN
C     THIS REGION.

   27 CALL INTEGR(T1,T2,ACC,NI,GLES1,SUM,KK,LL,X,XREL,NUSED,TEST)
      DO 3 LI=1,LL
      DO 3 KI=1,KK
    3 SAVE(KI,LI)=SAVE(KI,LI)+(A.,1.)*SUM(KI,LI)
      IF (TEST) PRINT 200,X,XREL,T1,T2,((SUM(KI,LI),SAVE(KI,LI)
     1,KI=1,KK),LI=1,LL),NUSED
      IF (IJ.EQ.1) GO TO 35
      IF (II.EQ.1) GO TO 30
      T1=T2        S        T2=1.0
      II=1      S        ACC=TOLRNS        S        GO TO 27
   30 NI=1024    S    IF (IJ.EQ.3) GO TO 90
      T1=0.      S    T2=EPS2    S    II=2
      ACC=TOLRNS/3.0
      GO TO 40
   90 T1=0.      S    T2=EPS1    S    II=1
      GO TO 40
   45 T1=T2      S    T2=EPS2
      ACC=TOLRNS        S    II=2
      GO TO 40
   35 T1=0.      S    T2=T2+FACT1

C     SECOND INTEGRATION IS FOR THE REGION BEYOND THE BRANCH POINT AT
C     ALPHA=1. GGRT1=REPRESENTS THE FUNCTIONS TO BE INTEGRATED.

   40 CALL INTEGR(T1,T2,ACC,NI,GGRT1,SUM,KK,LL,X,XREL,NUSED,TEST)
      DO 5 LI=1,LL
      DO 5 KI=1,KK
    5 SAVE(KI,LI)=SAVE(KI,LI)+SUM(KI,LI)
      IF (TEST) PRINT 200,X,XREL,T1,T2,((SUM(KI,LI),SAVE(KI,LI)
     1,KI=1,KK),LI=1,LL),NUSED
      IF (IJ.EQ.3.AND.II.EQ.1) GO TO 45
      ACC=TOLRNS/3.0
      A=SQRT(1.+T2*T2)
      FACT2=A*RK

C     CHECK IF THE ARGUMENT OF THE BESSEL FUNCTION HAD REACHED THE VALUE
C     OF 50. IF SO ,USE ASYMPTOTIC APPROX. FOR THE REGION BEYOND THIS
C     POINT AS DESCRIBED IN APPENDIX-C EQ. C-2 OF THE REPORT.

      IF (FACT2.GE.50.0.AND.T2.GE.EPS) GO TO 39

C     CHECK IF WE HAVE A QUASI-STATIC CASE,IF SO, PERFORM THE INTEGRATION
C     GIVEN IN EQ. (51) AND (55) AND ,THEN,ADD THE CORRECTION TERMS
C     WHICH REPRESENTS ANALYTICAL APPROX. OF THE INTEGR. FROM ALPHAT
C     TO INFINITY AS DESCRIBED IN APPENDICES A AND B.

      IF (IQ.EQ.1.AND.T2.GE.CCH) GO TO 115
  202 TT=B*T2

C     CHECK IF THE EXPONENTIAL FUNCTION EXP(-GAMMA0*B) HAS REACHED
C     THE VALUE OF  EXP(-12)  .IF SO, STOP THE INTEGRATION.

      IF (TT.GT.12.) GO TO 100
      T1=T2      S        T2=T2+FACT1
      GO TO 40
  115 CALL CORREC(A,SUM,KK,LL)
      GO TO 110
   39 CALL ASYMP(A,SUM,KK,LL)
  110 DO 7 LI=1,LL
      DO 7 KI=1,KK
    7 SAVE(KI,LI)=SAVE(KI,LI)+SUM(KI,LI)
  100 DO 9 LI=1,LL
      DO 9 KI=1,KK
    9 VALUE(KI,LI)=SAVE(KI,LI)
  200 FORMAT (/5X,*ABS.,REL. ERRS.=*2(2XE13.6),3X*LL=*E13.5,3X*UL=*E13.5
     1/1X*SUM MATRIX*/1X,6(2E13.5,5X,2E13.5/),2X*NUMB. OF ITER.=*I6/)
      RETURN
      END
```

87

```
          SUBROUTINE INTEGR (A,B,EPS,NSTEP,F,VALUE,L,M,X,XRELTV,K,G)

C     THIS SUBROUTINE PERFORMS AN (L,M) ARRAY OF COMPLEX FUCTIONS
C     INTEGRITION USING MODIFIED ROMBERG TECHNIQUE.
C         A≡LOWER LIMIT , B≡UPPER LIMIT  OF THE INTEGRATION
C         EPS≡REQUIRED TOLERANCE.
C         NSTEP≡ MAX. NUMBER OF ITERATION TO BE USED FOR PERFORMIG THE
C             INTEGRATION.
C         F≡ A SUBROUTINE HAS AN (L,M) ARRAY OF FUNCTIONS (INTEGRANDS).
C         VALUE≡ OUTPUT OF THE INTEGRATION ,(L,M) ARRAYS OF VALUES.
C         X≡ RETURNED ABSOLUTE ERROR .     XRELTV≡ RETURNED RELATIVE ERROR.
C         K≡NUMBER OF ITERATION USED IN PERFORMING THE INTEGRATION.
C         G≡LOGICAL STATEMENT IF IT IS FALSE ,THEN ,THE INTEGRATION WAS
C             PERFORMED WITHIN THE REQUIRED TOLERANCE (EPS) AND THE ITERATION
C             SIZE (NESTEP). OTERWISE IF IT IS TRUE ,THEN X ,XRELTV AND K
C             WILL BE RETURNED.

      COMPLEX     FCNA,FCNB,FCNXI,T,SUM,QX1,QX2,VALUE,Q
      DIMENSION SUM(3,2),FCNA(3,2),FCNB(3,2),T(3,2),FCNXI(3,2),
     1QX1(3,2),QX2(3,2),VALUE(L,M),Q(16,3,2)
      LOGICAL G
      H=B-A
      CALL F(A,FCNA,L,M)     S  CALL F(B,FCNB,L,M)
      DO 67 MJ=1,M
      DO 67 LJ=1,L
   67 T(LJ,MJ)=(FCNA(LJ,MJ)+FCNB(LJ,MJ))*H/2.
      NX=1
      N=1
    1 K=2**N
      H=H/2.
      DO 22 MJ=1,M
      DO 22 LJ=1,L
   22 SUM(LJ,MJ)=(0.,0.)
      DO 2 I=1,NX
      XI=2.*FLOAT(I)-1.
      XA=A+XI*H
      CALL F(XA,FCNXI,L,M)
      DO 24 MJ=1,M
      DO 24 LJ=1,L
   24 SUM(LJ,MJ)=SUM(LJ,MJ)+FCNXI(LJ,MJ)
    2 CONTINUE
      DO 26 MJ=1,M
      DO 26 LJ=1,L
      T(LJ,MJ)=T(LJ,MJ)/2.+H*SUM(LJ,MJ)
   26 Q(N,LJ,MJ)=(T(LJ,MJ)+H*SUM(LJ,MJ))*2./3.
      IF (N-2) 10,3,3
    3 F=4.
      DO 4 J=2,N
      I=N+1-J
      F=F*4.
      DO 27 MJ=1,M
      DO 27 LJ=1,L
   27 Q(I,LJ,MJ)=Q(I+1,LJ,MJ)+(Q(I+1,LJ,MJ)-Q(I,LJ,MJ))/(F-1.)
    4 CONTINUE
      IF (N-3) 9,5,5
    5 X=0.        S   XRELTV=0.
      DO 29 MJ=1,M
      DO 29 LJ=1,L
      XREAL=ABS(REAL(Q(1,LJ,MJ)-QX2(LJ,MJ)))+ABS(REAL(QX2(LJ,MJ)
     1-QX1(LJ,MJ)))
      XIMAG=ABS(AIMAG(Q(1,LJ,MJ)-QX2(LJ,MJ)))+ABS(AIMAG(QX2(LJ,MJ)
     1-QX1(LJ,MJ)))
      CR=CABS(Q(1,LJ,MJ))
      IF (CR.EQ.0.0) GO TO 33
      XR=AMAX1(XREAL,XIMAG)/CR    S      GO TO 107
```

88

```fortran
   33 XR=0.0
  107 XRELTV=AMAX1(XR,XRELTV)
   29 X=AMAX1(X,XREAL,XIMAG)
      COMPA=X-3.*EPS
      COMPR=XRELTV-3.*EPS
      IF (COMPA.LE.0.0.OR.COMPR.LE.0.0) 11,8
    8 IF (NSTEP-K) 11,11,9
    9 DO 37 MJ=1,M
      DO 37 LJ=1,L
   37 QX1(LJ,MJ)=QX2(LJ,MJ)
   10 DO 39 MJ=1,M
      DO 39 LJ=1,L
   39 QX2(LJ,MJ)=Q(1,LJ,MJ)
   12 NX=NX*2
      N=N+1
      GO TO 1
   11 DO 41 MJ=1,M
      DO 41 LJ=1,L
   41 VALUE(LJ,MJ)=Q(1,LJ,MJ)
      G=NSTEP.LT.K
      RETURN
      END




      SUBROUTINE GLES1(T,GL,I,J)

C  HERE, WE EVALUATE THE FIRST INTEGRAND OF EQ. (34) OF THE REPORT.
C  THE REGION IS FOR ALPHA BETWEEN 0 AND 1.
C  T IS THE INPUT .OUTPUT=GG IS AN ARRAY OF (I,J) FUCTIONS.

      COMPLEX G,GL
      DIMENSION GL(I,J),G(3,2)
      X=SQRT(1.-T*T)
      CALL SUBG(X,G,I,J)
      DO 10 N=1,J
      DO 10 M=1,I
   10 GL(M,N)=G(M,N)
      RETURN
      END




      SUBROUTINE GGRT1(T,GG,I,J)

C  THIS SUBROUTINE EVALUATES THE SECOND INTEGRAND OF EQ. (34) OF THE
C  REPORT. THIS REGION IS FOR ALPHA GREATER THAN 1.
C  T IS THE INPUT .OUTPUT=GG IS AN ARRAY OF (I,J) FUCTIONS.

      COMPLEX G,GG
      DIMENSION GG(I,J),G(3,2)
      X=SQRT(1.+T*T)
      CALL SUBG(X,G,I,J)
      DO 10 N=1,J
      DO 10 M=1,I
   10 GG(M,N)=G(M,N)
      RETURN
      END
```

```
      SUBROUTINE SUBG(ALPHA,G,II,JJ)

C    HERE, WE CALCULATES THE FUNCTIONS GIVEN IN EQ. (30) OF THE REPORT.
C    INPUT=ALPHA      ,  OUTPUT=G IS AN ARRAY OF (II,JJ) FUCTIONS.

      COMMON /MAIN1/N(3),H,EPS(3),RK0
      COMMON /MAIN2/B
      DIMENSION BESSJ(2),BESSY(2),Y(3,2),Z(3,2),G(II,JJ)
      COMPLEX N,CX,GAMA0,Y,Z,J0,J1,G
      X=ALPHA
      IF (X-1.0) 10,20,30
   10 GAMA0=(0.,-1.)*SQRT(1.-X*X)     S      GO TO 40
   20 GAMA0=(0.,0.)     S      GO TO 40
   30 GAMA0=SQRT(X*X-1.)
   40 RA=X*RK0
      CX=CEXP(-GAMA0*B)

C    A CALL WILL BE MADE TO SUBROUTINE (UV) TO EVALUATE THE FUNCTIONS
C    LISTED IN TABLE-2 OF THE REPORT.

      CALL UV(X,GAMA0,Y,Z,II,JJ)

C    THE OTHER CALL WILL BE MADE TO BEJY TO EVALUATE  THE BESSEL
C    FUCTIONS  J0 AND J1 .

      CALL BEJY(RA,BESSJ,BESSY,2,0)
      J0=BESSJ(1)     S     J1=BESSJ(2)
      DO 22 JM=1,JJ
      DO 22 IM=1,II
   22 G(IM,JM)=CX*(Y(IM,JM)*J0+Z(IM,JM)*J1)
      RETURN
      END




      SUBROUTINE UV(ALPHA,G0,U,V,IJ,IK)

C    SUBROUTINE UV CALCULATES THE FUNCTIONS LISTED IN TABLE-2.INPUTS ARE:
C      (1) ALPHA,WHICH IS REAL SINCE THE INTEGRATION IS ALONG THE REAL-
C          AXIS IN THE COMPLEX ALPHA-PLANE.
C      (2) G0=SQRT((ALPHA)**2-1) ,HERE G0 IS COMPLEX AND THE CHOICE OF
C          THE BRANCH CUT IS G0=-J*SQRT(1-(ALPHA)**2) FOR ALPHA<1.
C    THE OUTPUTS ARE :
C      (1) U AND V REPRESENT THE VALUES OF THE LEFT AND THE RIGHT COLUMNS
C          OF TABLE-2 RESPECTIVELY. IJ AND IK ARE VARIABLE DIMENSIONS.

      COMMON /MAIN1/N(3),H,EPSR(3),RK0
      COMMON /MAIN2/B,P,T,CT,ST,CP,SP,CP2,SP2
      COMMON /FINDF/F(3)
      COMMON /FUV/A,GAMA0,G1,G2
      COMPLEX N,G0,G1,G2,GAMA0
      COMPLEX F,FG,U,V
      DIMENSION U(3,2),V(3,2)
      A=ALPHA
      GAMA0=G0
      G1=CSQRT(A*A-N(2)*N(2))
      G2=CSQRT(A*A-N(3)*N(3))
      RK=RK0
      A2=A*A
```

90

```
C     FIND THE VALUES OF (G0*F1),(G0*F2) AND (G0*F3),WHERE F1,F2 AND F3
C     ARE GIVEN IN EQ. (29) OF THE REPORT.

      CALL FVALUE

      FG=F(2)-G0*F(3)

      U(1,1)=(F(2)-FG*A2*CP*CP)*ST
      V(1,1)=(FG*CP2*ST/RK+G0*F(1)*CP*CT)*A
      U(2,1)=-A2*FG*SP2*ST/2.
      V(2,1)=A*(FG*SP2*ST/RK+G0*F(1)*SP*CT)
      U(3,1)=A2*F(1)*CT
      V(3,1)=A*(G0*FG-F(3))*CP*ST
      U(1,2)=-A2*F(3)*SP2*ST/2.
      V(1,2)=A*(F(3)*SP2*ST/RK-F(1)*SP*CT)
      U(2,2)=(-G0*F(2)+A2*F(3)*CP*CP)*ST
      V(2,2)=A*(-F(3)*CP2*ST/RK+F(1)*CP*CT)
      U(3,2)=(0.,0.)
      V(3,2)=A*F(2)*SP*ST

      RETURN
      END




      SUBROUTINE FVALUE

C     THIS SUBROUTINE EVALUATES DIFFERENT TYPES OF FUNCTIONS DEPENDING
C     ON THE VALUE OF (I) IN THE COMMON BLOCK (TYPE). (I) DETERMINE THE
C     FOLLOWING CASES
C        (1) IF I=1, THEN ,IT CALCULATES THE QUASI-STATIC FUNCTIONS LISTED
C            IN EQ. (51) AND (55) OF THE REPORT.
C        (2) FOR I=2, FVALUE CALCULATES (G0*F1),(G0*F2) AND (G0*F3) WHERE
C            F1,F2, AND F3 ARE GIVEN IN (29) OF THE REPORT AND
C            G0=SQRT((ALPHA)**2-1.) .
C        (3) WHEN I=3, (FVALUE) CALCULATES F1,F2 AND F3 AND THEY WILL BE
C            USED IN THE ASYMPTOTIC FORM FOR THE EM FIELD COMPONENTS.
C     THE OUTPUT OF THIS SUBROUTINE IS THE COMMON BLOCK /FINOF/ .
C     THE INPUTS ARE THRU THE FOLLOWING COMMON BLOCKS
C     /MAIN1/ N(3) AND EPSR(3) ARE THE REFRACTIVE INDICES AND RELATIVE
C     DIELECTRIC CONSTANTS OF THE THREE MEDIA.
C     /FUV/ (A) =(ALPHA) , (G0)=(GAMMA0) , (G1)=(GAMMA1) ,(G2)=(GAMMA2),
C           H IS THE NORMALIZED SLAB WIDTH.
C     /ZYY/ ZY(1) =(K0) , ZY(2)=(N0) , ZY(3)=1/w1  AS GIVEN IN EQ. (8),
C           (9) AND (11) OF THE REPORT.

      COMMON /MAIN1/N(3),H,EPSR(3)
      COMMON /FINOF/F(3)
      COMMON /FUV/A,G0,G1,G2
      COMMON /ZYY/ZY(3)
      COMMON /TYPE/I
      COMPLEX F,ZY,LAMDA1,LAMDA2
      COMPLEX N,G0,G1,G2,E1,E2
      CALL FINDZY
      E1=N(2)*N(2)       S      E2=N(3)*N(3)
      LAMDA2=1./E2-1./E1
      LAMDA1=LAMDA2*ZY(3)-1.+1./E1

      F(1)=2.*G0/(G0+ZY(1))
      F(2)=2.*G0/(G0+ZY(2))
      F(3)=LAMDA1*(F(2)-F(1))/(ZY(2)-ZY(1))
```

91

```
      IF (I-2) 10,20,30

10 F(1)=F(1)-2.*E1/(E1+1.)
   F(2)=F(2)-1.
   F(3)=F(3)-(E1-1.)*G0/((E1+1.)*G1**2)

   RETURN

30 F(1)= 2./(G0*ZY(1))
   F(2)= 2./(G0*ZY(2))
   F(3)=LAMDA1*(F(2)-F(1))/(ZY(2)-ZY(1))

20 RETURN
   END




   SUBROUTINE FINDZY

C  THIS SUBROUTINE CALCULATES THE VALUES OF K0,N0, AND 1/W1 AS GIVEN IN
C  (8),(9) AND (11) OF THE REPORT . THE OUTPUT IS THRU THE COMMON
C  BLOCK /ZYY/

   COMMON /MAIN1/N(3),H,EPS(3)
   COMMON /FUV/A,G0,G1,G2
   COMMON /ZYY/ZY(3)
   COMPLEX N,G0,G1,G2,Z2,Y2,Z,ZY,T,E1,E2,CT,DENY,DENZ
   E1=N(2)*N(2)      S    E2=N(3)*N(3)
   Z=(0.,1.)*G1      S    T=Z*H
   Y2=G2             S    Z2=Y2/E2
   ZI=AIMAG(2.*T)
   IF (ABS(ZI).GE.60.0) GO TO 10
   CT=CSIN(T)/CCOS(T)
   DENY=Z+Y2*CT           S    DENZ=Z/E1+Z2*CT
   ZY(3)=Z*Z/(E1+DENZ*DENY*0.5*(1.+CCOS(2.*T)))
20 ZY(1)=(Z/E1)*(Z2-Z*CT/E1)/DENZ
   ZY(2)=Z*(Y2-Z*CT)/DENY
   RETURN
10 ZY(3)=(0.,0.)      S    CT=(0.,1.)
   DENY=Z+Y2*CT    S    DENZ=Z/E1+Z2*CT
   GO TO 20
   END
```

92

```fortran
      SUBROUTINE BEJY(X,BJ,BY,M,N)
      DIMENSION BJ(2),BY(2)

C     BEJY CALCULATES THE BESSEL FUNCTIONS J0,J1,Y0 AND Y1.INPUTS ARE:
C      (1) X WHICH IS THE ARGUMENT OF THE BESSEL FUNCTIONS.
C      (2) M AND N DETERMINES WHICH TYPE OF BESSEL FUNCTIONS IS NEEDED.
C         EXAMPLE WHEN (M,N)=(1,0) J0 WILL BE CALCULATED.
C     THE OUTPUTS ARE BJ AND BY REPRESENTING BESSEL AND NEUMANN FUNCTION
C     RESPECTIVELY.

      T=X/3.
      Y=T*T
      Z=3./X
      IF(X.GE.3.) GO TO 10
      BJ(1)=1.-Y*(2.2499997-Y*(1.2656208-Y*(.3163866-Y*(.0444479-
     1Y*(.0039444-Y*.0002100)))))
      GO TO 11
   10 W=SQRT(X)
      AF=.79788456-Z*(.00000077+Z*(.00552740+Z*(.00009512-Z*(.00137237
     1-Z*(.00072805-Z*.00014476)))))
      THETA=X-.78539816-Z*(.04166397+Z*(.00003954-Z*(.00262573
     1-Z*(.00054125+Z*(.00029333-Z*.00013558)))))
      BJ(1)=AF*COS(THETA)/W
   11 IF(N.GT.0) GO TO 20
      IF(M.EQ.2) GO TO 40
      RETURN
   20 IF(X.GE.3.) GO TO 30
      BY(1)=2./3.14159265*ALOG(X/2.)*BJ(1)+.36746691+Y*(.60559366-
     1Y*(.74350384-Y*(.25300117-Y*(.04261214-Y*(.00427916-Y*.00024846)))
     2))
      GO TO 31
   30 BY(1)=AF*SIN(THETA)/W
   31 IF(M.EQ.2) GO TO 40
      RETURN
   40 IF(X.GE.3.) GO TO 50
      BJ(2)=0.5-Y*(.56249985-Y*(.21093573-Y*(.03954289-Y*(.00443319
     1-Y*(.00031761-Y*.00001109)))))
      BJ(2)=BJ(2)*X
      GO TO 51
   50 AF=.79788456+Z*(.00000156+Z*(.01659667+Z*(.00017105-Z*(.00249511
     1-Z*(.00113653-Z*.00020033)))))
      THETA=X-2.35619449+Z*(.12499612+Z*(.00005650-Z*(.00637879
     1-Z*(.00074348+Z*(.00079824-Z*.00029166)))))
      BJ(2)=AF*COS(THETA)/W
   51 IF(N.EQ.2) GO TO 60
      RETURN
   60 IF(X.GE.3.) GO TO 70
      BY(2)=2./3.14159265*X*ALOG(X/2.)*BJ(2)-.6366198+Y*(.2212091+Y*(
     12.1682709-Y*(1.3164827-Y*(.3123951-Y*(.0400976-Y*.0027873)))))
      BY(2)=BY(2)/X
      GO TO 71
   70 BY(2)=AF*SIN(THETA)/W
   71 RETURN
      END
```

```fortran
      SUBROUTINE ASYMP(X,Z,II,JJ)

C     THIS SUBROUTINE CALCULATES THE TRUNCATED INTEGRALS FROM ALPHAT
C     TO INFINITY AS SHOWN IN C-2 OF THE REPORT.INPUT (X) REPRESENTS
C     THE LOWER LIMIT OF THE INTEGRAL. (Z) IS THE OUTPUT WHICH IS THE
C     CALCULATED ANALYTICAL APPROX. ,II AND JJ ARE JUST VARIABLE DIMENS.

      COMMON /MAIN1/N(3),H,EPS(3),RK
      COMMON /MAIN2/B
      COMPLEX F,GG,FF,YY,ZZ,YX,ZX,N,GAMA0,Z,G1,G2,DYZ,DFY,DFZ,PF,RF
      DIMENSION YY(3,2),ZZ(3,2),YX(3,2),ZX(3,2),G1(3,2),G2(3,2),Z(II,JJ)
     1,PF(3,3,2),RF(3,3,2),DFY(3,2),DFZ(3,2)
      FF(XX,GG,RR)=XX*SQRT(2./(3.141592653*RR))*CEXP(-GG*B)/GG
      PI=3.141592653
      GAMA0=SQRT(X*X-1.)
      RA=X*RK       S   PP=RA-PI/4.
      CALL UV(X,GAMA0,YY,ZZ,II,JJ)
      SI=SIN(PP)    S   CI=COS(PP)
      F=FF(X,GAMA0,RA)
      DO 10 J=1,JJ
      DO 10 I=1,II
      PF(1,I,J)=F*YY(I,J)   S   RF(1,I,J)=F*ZZ(I,J)
   10 G1(I,J)=(-PF(1,I,J)*(SI-CI/(8.*RA))+RF(1,I,J)*(CI-3.*SI/(8.*RA)))
     1/RK
      D=1.0E-04
      DO 39 M=2,3
      XD=X+(M-1)*D   S   RD=XD*RK
      GAMA0=SQRT(XD*XD-1.)
      CALL UV(XD,GAMA0,YX,ZX,II,JJ)
      DYZ=FF(XD,GAMA0,RD)
      DO 37 J=1,JJ
      DO 37 I=1,II
      PF(M,I,J)=DYZ*YX(I,J)
   37 RF(M,I,J)=DYZ*ZX(I,J)
   39 CONTINUE
      R2=RK*RK
      DO 20 J=1,JJ
      DO 20 I=1,II
      DFY(I,J)=(-3.*PF(1,I,J)+4.*PF(2,I,J)-PF(3,I,J))/(2.*D)
      DFZ(I,J)=(-3.*RF(1,I,J)+4.*RF(2,I,J)-RF(3,I,J))/(2.*D)
      G2(I,J)=(-CI*DFY(I,J)-SI*DFZ(I,J))/R2
   20 Z(I,J)=G1(I,J)+G2(I,J)
      RETURN
      END
```

94

```fortran
      SUBROUTINE QSTATC(A0,TOTL,II,JJ,IQ)

C     QUASI-STATIC APPROX. WILL BE EVALUATED IN THIS SUBROUTINE.
C     (A0) REPRESENTS THE POLE LOCATION IN THE COMPLEX ALPHA-PLANE.
C     (TOTL) IS THE OUTPUT OF THIS SUBROUTINE WHICH IS THE CALCULATED
C     ARRAY OF FIELD COMPONENTS. II AND JJ ARE VARIABLE DIMENSIONS.
C     (IQ) IS A FLAG AND IT SHOULD BE 1 IF QUASI-STATIC APPROX. IS NEEDED.

      COMMON /MAIN1/N(3),H,E(3),RK,KO,ZHM
      COMMON /MAIN2/B,PHI,T,CT,ST
      REAL KO
      COMPLEX N,DS,DI,PZS,PZI,PXS,PXI,Q,TOTL,SOM,C,A0,E1
      DIMENSION DS(3,2),DI(3,2),PZS(3,2),PZI(3,2),PXS(3,2),PXI(3,2)
     1,TOTL(II,JJ),SOM(3,2),Q(3,2)
      E1=N(2)**N(2)
      ZH=B/KO          S    RO=RK/KO
      CALL FIELD(DS,KO,ZHM,RO,PZS,PXS,II,JJ)
      CALL FIELD(DI,KO,ZH,RO,PZI,PXI,II,JJ)
      CALL QV3(Q,II,JJ)
      CALL RESULT(A0,SOM,II,JJ,IQ)
      C=2.*E1/(E1+1.)
      DO 10 J=1,JJ
      DO 10 I=1,II
   10 TOTL(I,J)=DS(I,J)-DI(I,J)+C*PZI(I,J)+PXI(I,J)+Q(I,J)+ST*SOM(I,J)
      RETURN
      END



      SUBROUTINE QV3(HE,I,J)
      COMMON /MAIN1/N(3),H,EPSR(3),RK
      COMMON /MAIN2/B,P,T,CT,ST,CP,SP,CP2,SP2
      DIMENSION HE(3,2),T1(3,2),T2(3,2)
      COMPLEX N,C,HE,T1,T2,K,E,E1,J
      PI=3.141592653    S    J=(0.,1.)
      E1=N(2)**N(2)
      K=(E1/(E1-1.))*(-.61593151-.5*J*PI*CLOG(N(2)))
      C=(N(2)*N(2)-1.)/(N(2)*N(2)+1.)
      E=(E1-1.)*C/2.
      R=SQRT(B*B+RK*RK)
      AA=ALOG(R+B)
      R3=1./R**3        S    R5=1./R**5      S    RB1=1./(R+B)
      RB2=RB1*RB1       S    RR=RB1/R        S    RB=(2.*R+B)*R3*RR2
      T1(1,1)= C*(R3-3.*R5*(RK*CP)**2+.5*((B*CP/R)**2+SP**2)/R)
      T1(2,1)=-C*RK*RK*SP2*(1.5*R5+.25*R3)
      T1(3,1)=-C*RK*CP*(RR+3.*R*R5+.5*(R*R3-AA))
      T1(1,2)=C*RK*RK*SP2*(.5*RB+.25*RR)
      T1(2,2)=C*(RR-RB+(RK*CP)**2-.5*(AA+RR*(RK*CP)**2))
      T1(3,2)=(0.,0.)
      T2(1,1)=E*RB1*(B*CP*CP/R+SP*SP)
      T2(2,1)=-E*SP2*(RK*RB1)**2/R
      T2(3,1)=E*RK*CP*(-2.*RR+AA+B*RB1+K)
      T2(1,2)=0.5*E*SP2*(RK*RR1)**2
      T2(2,2)=-E*(AA+RR1+(R*CP*CP+B*SP*SP)+K)
      T2(3,2)=(0.,0.)
      DO 20 JJ=1,J
      DO 20 II=1,I
   20 HE(II,JJ)=T1(II,JJ)+T2(II,JJ)
      RETURN
      END
```

95

```
      SUBROUTINE CORREC(X,F,II,JJ)

C     THIS SUBROUTINE IS USED WHENEVER A QUASI-STATIC CALCULATION IS
C     NEEDED. AFTER THE INTEGRATION HAD REACHED CERTAIN LIMIT (ALPHA0)
C     AS DESCRIBED IN SUBROUTINE (RESULT) THIS SUBROUTINE WILL BE EXCUTED
C     TO GET THE REMAINDER OF THE INTEGRATION IN AN APPROX. FORM.
C     THESE APPROX. HAVE BEEN SHOWN IN SECTION 4.2 , EQS. (50) AND (54)
C     OF THE REPORT.

      COMMON /MAIN1/N(3),H,EPSR(3),RK
      COMMON /MAIN2/B,P,T,CT,ST,CP,SP,CP2,SP2
      DIMENSION F(3,2),T1(3,2),T2(3,2),T3(3,2)
      COMPLEX N,E1,F,J,K1,K2,T1,T2,T3,K3
      E1=N(2)*N(2)        S    J=(0.,1.)    S    PI=3.141592653
      K2=(E1-1.)/4.       S    K1=-2.*E1/(E1+1.)**2
      K3=-(3.*E1+1.)*((E1-1.)/(E1+1.))**2/8.
      R=SQRT(B*B+RK*RK)
      BR=1./(R+B)         S    RR=BR/R
      C=-0.1159315+ALOG(X)
      AL=ALOG(R+B)        S    E=EXP(-X+B)
      T1(1,1)=K1*RK*CP*CT*RR
      T2(1,1)=K2*((-1.+(1.-B/R)*CP*CP)*BR*B*(AL+C)-R*E/X)*ST
      T3(1,1)=2.*K3*(B*CP*CP/R*SP*SP)*BR*ST
      T1(2,1)=K1*SP*CT*RK*RR
      T2(2,1)=0.5*K2*SP2*(R-B)*RR*ST
      T3(2,1)=-K3*SP2*ST*(RK*BR)**2/R
      T1(3,1)=K1*(1./R-(X+1./X)*E+B*(AL+C)-R)*CT
      T2(3,1)=K2*RK*CP*ST*RR
      T3(3,1)=K3*CP*ST*RK*(-2.+RR*AL+B*BR*C)
      T1(1,2)=-K1*RK*SP*CT*BR
      T2(1,2)=(0.,0.)
      T3(1,2)=.5*K3*SP2*ST*(RK*BR)**2
      T1(2,2)=K1*RK*CP*CT*BR
      T2(2,2)=K2*(AL+C-E)*ST
      T3(2,2)=-K3*ST*(AL+C+(R*CP*CP+B*SP*SP)*BR)
      T1(3,2)=(0.,0.)
      T2(3,2)=K2*RK*SP*ST*BR
      T3(3,2)=(0.,0.)
      DO 10 JN=1,2
      DO 10 IN=1,3
   10 F(IN,JN)=T1(IN,JN)+T2(IN,JN)+T3(IN,JN)
      RETURN
      END
```

96

```
      SUBROUTINE ASMPT(POLE,T,EH,II,JJ)

C     THIS SUBROUTINE PERFORMS THE ASYMPTOTIC EVALUATION OF THE EM FIELD
C     COMPONENTS USING STEEPEST DESCENT METHOD. SKY WAVE APPROX. IS
C     PERFORMED BY SUBROUTINE (LARGR) AND GROUND WAVE SOLUTION IS
C     CALCULATED USING SUBROUTINE (FACTOR). THE INPUTS ARE :
C     (1) POLE WHICH IS THE POLE LOCATION IN THE ALPHA PLANE.
C     (2) T IS THETA WHICH IS THE ANGLE GIVEN BY ARCTAN(RO/(Z+H0)).
C     EH IS THE RETURNED ASYMPTOTIC FIELD.II AND JJ ARE VARIABLE DIMENS.

      COMMON /MAIN1/N(3),H,E(3),RR,K0,ZHM
      COMMON /MAIN2/B,PHI,TP
      COMPLEX POLE,EH,SMR,S1,S2,DS,DI,PZS,PXS,PZI,PXI,N,G,GP,IJ,P
      REAL K0
      DIMENSION EH(II,JJ),SMR(3,2)
     1,DS(3,2),DI(3,2),PZS(3,2),PZI(3,2),PXI(3,2),PXS(3,2)
      IJ=(0.,1.)
      GP=-IJ*CSQRT(POLE*POLE-1.)
   20 X=SIN(T)      S      C=COS(T)
      R=SQRT(RR*RR+B*B)
      RO=RR/K0      S      ZH=B/K0
      P=(1.+IJ)*CSQRT((1.-GP*C-X*POLE)*R/2.)
      CP=CABS(P)
      IF (CP.GE.7.5) GO TO 25

      CALL FACTOR(T,X,C,POLE,R,SMR,II,JJ)


      CALL FIELD(DS,K0,ZHM,RO,PZS,PXS,II,JJ)
      CALL FIELD(DI,K0,ZH,RO,PZI,PXI,II,JJ)

      DO 10 J=1,JJ
      DO 10 I=1,II
   10 EH(I,J)=DS(I,J)-DI(I,J)*SMR(I,J)
      GO TO 30
   25 CALL LARGR(T,EH,II,JJ)
   30 RETURN
      END



      SUBROUTINE FACTOR(TT,A,G0,AP,R,HE,KK,LL)

C     THIS SUBROUTINE CALCULATES THE ASYMPTOTIC FORM OF THE EM FIELD
C     IN THE AIR REGION TAKING INTO CONSIDERATION THE GROUND WAVE
C     SOLUTION.TWO TERM APPROX. HAS BEEN USED OUT OF THE ASYMPTOTIC
C     SERIES,FORWARD,CENTRAL AND BACKWARD DIFFERENCE METHOD HAS BEEN
C     USED TO REPLACE THE DERIVATIVES IN THE SECOND TERM.

      COMMON /MAIN1/N(3),H,E(3),RO
      DIMENSION BESJ(2),BESY(2),U(3,2),V(3,2),S0(4,3,2),S1(4,3,2)
     1         ,TR1(3,2),TR2(3,2),DS(3,2),DDS(3,2),SS(3,2),HE(KK,LL)
      COMPLEX WB1,WB2,GG,U,V,S0,S1,CF,TR1,TR2,DS,DDS,SS,HE
      COMPLEX N,AP,J,B,G12,GP,FR,HI0,HI1,F,F0,F1,W,P,W1
      J=(0.,1.)      S      PI=3.141592653
      RAP=REAL(AP*AP)
      IF (RAP.LT.1.0) GO TO 17
      GP=-J*CSQRT(AP*AP-1.)      S      GO TO 34
   17 GP=CSQRT(1.-AP*AP)
   34 B=(1.+J)*CSQRT((1.-GP*G0-AP*A)/2.)
      FB=1.0
      AB=AIMAG(B)
      IF (AB.LT.0.0) FB=-1.0
      P=FB*B*SQRT(R)
```

97

```
        G12=CEXP(J*R)
        W1=W(P)*FB
C-------------------------------------------------
C        W(P)≣EXP(-P*P)*ERFC(-J*P)
C-------------------------------------------------
        WB1=W1/B    S    WB2=B*(J*W1*FB/(P*SQRT(PI)))
        CF=PI*(1.-J)*B*B*G12
        D=5.0E-04
        AD1=TT*D         S        AD2=TT-D
        DO 39 M=1,4
        IF (AD1.GE.1.570796.OR.AD2.LE.0.0)    GO TO 42
        IF (M.GE.4) GO TO 201
        AD=SIN(TT+FLOAT(M-2)*D)
        ID=0
        GO TO 88
     42 IF (AD1.GE.1.0) GO TO 72
        ID=1    S    AD=SIN(TT-FLOAT(M-1)*D)    S    GO TO 88
     72 ID=2    S    AD=SIN(TT-FLOAT(M-1)*D)
     88 GA=SQRT(1.-AD*AD)    S    GG=-J*GA
     40 X=AD*RO
        F=AD*CEXP(-J*X)/SQRT((1.+GA*G0*AD*A)*2.)
        CALL BEJY(X,BESJ,BESY,2,2)
        H10=BESJ(1)+J*BESY(1)    S    H11=BESJ(2)+J*BESY(2)
        FO=H10*F    S    F1=H11*F
        CALL UV(AD,GG,U,V,KK,LL)
        DO 22 L=1,LL
        DO 22 K=1,KK
        S0(M,K,L)=FO*U(K,L)
     22 S1(M,K,L)=F1*V(K,L)
     39 CONTINUE
    201 CONTINUE
        IF (ID.GE.1) GO TO 85
C       CENTRAL DIFFERENCE
        DO 83 L=1,LL
        DO 83 K=1,KK
        DS(K,L)=(S0(3,K,L)-S0(1,K,L)+S1(3,K,L)-S1(1,K,L))/(2.*D)
        DDS(K,L)=(S0(3,K,L)-2.*S0(2,K,L)+S0(1,K,L)+S1(3,K,L)-2.*S1(2,K,L)
       1+S1(1,K,L))/D**2
     83 SS(K,L)=-J*G0*(S0(2,K,L)+S1(2,K,L))
        GO TO 106
     85 IF (ID.EQ.2) D=-D
C       FORWARD OR BACKWARD DIFFERENCE
        DO 93 L=1,LL
        DO 93 K=1,KK
        DS(K,L)=(-3.*S0(1,K,L)+4.*S0(2,K,L)-S0(3,K,L)-3.*S1(1,K,L)
       1+4.*S1(2,K,L)-S1(3,K,L))/(2.*D)
        DDS(K,L)=(2.*S0(1,K,L)-5.*S0(2,K,L)+4.*S0(3,K,L)-S0(4,K,L)
       1+2.*S1(1,K,L)-5.*S1(2,K,L)+4.*S1(3,K,L)-S1(4,K,L))/D**2
     93 SS(K,L)=-J*G0*(S0(1,K,L)+S1(1,K,L))
    106 DO 57 L=1,LL
        DO 57 K=1,KK
        TR1(K,L)=CF*WB1*SS(K,L)
        TR2(K,L)=CF*WB2*(-2.*J*A*DS(K,L)+J*G0*DDS(K,L)+(J/B**2+.75)*
       1SS(K,L))
     57 HE(K,L)=TR1(K,L)+TR2(K,L)
       .RETURN
        END
```

98

```
      COMPLEX FUNCTION W(Z)
C-------------------------------------------------
C     W(Z)≡EXP(-Z*Z)*ERFC(-I*Z)
C-------------------------------------------------
      COMPLEX I,Z,Z1,Z2,ZS,S3,S4,P1,P3,K,K1,FR
      I=(0.,1.)
      X=REAL(Z)     S   Y=AIMAG(Z)
      IF (X.GT.3.9.OR.Y.GT.3.0) 10,100
   10 P1=I*Z    S      ZS=Z*Z
      IF (X.GT.6.0.OR.Y.GT.6.0) GO TO 5
      W=P1*(.4613135/(ZS-.1901635)+.09999216/(ZS-1.7844927)
     1+.002883894/(ZS-5.5253437))
      RETURN
    5 W=P1*(.5124242/(ZS-.2752551)+.05176536/(ZS-2.724745))
      RETURN
  100 P=2./SQRT(3.141592653)
      Z1=-I*Z
      S3=Z1   S   S4=S3   S    Z2=Z1**2
      DO 120 J=1,200
      N=J-1
      A1=FLOAT(2*N+1)      S   A2=FLOAT(2*N**2+5*N+3)
      P3=S3*Z2*A1/A2
      S3=P3   S   P5=CABS(P3)
      IF ((N/2*2).NE.N) GO TO 122
      S4=S4-P3   S      GO TO 124
  122 S4=S4+P3
  124 IF (P5.LE.1.0E-09) GO TO 226
  120 CONTINUE
  226 K=(1.,1.)    S   K1=(1.,-1.)
      FR=K*S4*P/2.
      W=CEXP(-Z*Z)*(1.-K1*FR)
      RETURN
      END
```

99

```fortran
      SUBROUTINE RROOT(ZERO,AP)

C     THIS SUBROUTINE SEARCHES FOR THE SURFACE MODES THAT EXISTS WITHIN
C     A LOSSY DIELECTRIC SLAB ABOVE A FINTELY CONDUCTING GROUND (REFER TO
C     SECTION-3 OF THE REPORT).AT FIRST,THE REAL ROOTS OF A LOSSLESS
C     DIELECTRIC SLAB ABOVE A PERFECTLY CONDUCTING SHEET,WILL BE SEARCHED.
C     THESE ROOTS ARE OF TWO TYPES OF POLARIZATION,TM (EVEN) AND TE (ODD)
C     AS GIVEN BY EQS (39) AND (40) OF THE REPORT.THE ROOTS ARE THEN,
C     PLUGGED IN EQS (37) AND (38) RESPECTIVELY TO SEARCH FOR THE COMPLEX
C     OF A LOSSY SLAB ABOVE A FINITELY CONDUCTING EARTH. UP TO 5 ROOTS ARE
C     SEARCHED AND,THEN SEND BACK TO THE MAIN PROGRAM VIA THE VARIABLE
C     (ZERO) . IF MORE ROOTS EXISTS ,THE DIMENSION OF (ZERO) SHOULD BE
C     INCREASED. THE ROOT CLOSEST TO THE REAL AXIS IN THE COMPLEX ALPHA-
C     PLANE WILL BE SENT THRU THE VARIABLE (AP). IF THE PROGRAM FAILS TO
C     FIND ANY ROOT WITHIN A GIVEN INTERVAL AN ARBITRARY POLE LOCATION
C     (.95,.15) WILL BE ASSIGNED FOR ALPHA. THE INPUTS ARE THRU THE
C     COMMON BLOCK /MAIN3/. SIG(3) AND EPSR(3) REPRESENTS THE
C     CONDUCTIVITIES AND RELATIVE DIELECTRIC CONSTANTS IN THE THREE MEDIA
C     STARTING WITH REGIONS (1) AIR, (2) SLAB AND (3) EARTH.
C     H=SLAB WIDTH . OMEGA= ANGULAR FREQ. IN RADIANS.
C     OUTPUTS ARE:
C     ZERO= ZEROES FOUND.
C     AP= THE ROOT CLOSEST TO THE REAL AXIS IN THE COMPLEX ALPHA-PLANE.

      COMMON /MAIN3/SIG(3),EPSR(3),H,OMEGA
      DIMENSION ZERO(5)
      COMPLEX ZERO,ZZ,AP
      LOGICAL G
      EXTERNAL FX,FY
      PI=3.141592653
      F2=H*SQRT(EPSR(2)-1.)
      IN=INT(2.*F2/PI)+1
      II=IN
      X=FLOAT(IN)/2.     S     Y=FLOAT(IN/2)
      IF (X.EQ.Y) GO TO 55
   62 T1=FLOAT(IN-1)*PI/2.+1.0E-08
      TT2=FLOAT(IN)*PI/2.-1.0E-05
      T2=AMIN1(F2,TT2)
      PRINT 65
   65 FORMAT (1X,*ROOT OF TM TYPE MODES*/)
      CALL ROOT(T1,T2,FY,X1,100,1.0E-05,100.,G)
      IF (G) GO TO 105
      RALPHA=SQRT(EPSR(2)-X1*X1/H/H)
      PRINT 75,X1,RALPHA
      IM=2
      CALL ZROOT(IM,X1,ZZ,G)
      IF (G) GO TO 4
      ZERO(IN)=ZZ        S       GO TO 101
    4 PRINT 79,ZZ
      ZERO(IN)=(.95,.15)
  105 PRINT 72,IN
  101 IN=IN-1
      IF (IN.LE.0) GO TO 15
   55 T1=FLOAT(IN-1)*PI/2.+1.0E-05
      TT2=FLOAT(IN)*PI/2.-1.0E-05
      T2=AMIN1(F2,TT2)
      PRINT 69
   69 FORMAT (1X,*ROOT OF TE TYPE MODES*/)
      CALL ROOT(T1,T2,FX,X1,100,1.0E-05,100.,G)
      IF (G) GO TO 107
      RALPHA=SQRT(EPSR(2)-X1*X1/H/H)
      PRINT 75,X1,RALPHA
      IM=1
      CALL ZROOT(IM,X1,ZZ,G)
      IF (G) GO TO 6
      ZERO(IN)=ZZ        S       GO TO 109
    6 PRINT 79,ZZ
```

100

```
       ZERO(IN)=(.95,.15)
107 PRINT 72,IN
109 IN=IN-1      S      GO TO 62
 75 FORMAT (1X,*GAMA1 H1=*E13.5,3X*ALPHA REAL=*E13.5//)
 72 FORMAT (1X,*REGION*I3,5X*NO REAL ROOTS HAVE BEEN FOUND*/)
 79 FORMAT (1X*NO ROOTS ARE BEING FOUND OR IT DIDNT CONVERGE*,1X
   1*Z=*2(2XE13.5)/)
 15 IF (II.LE.1) GO TO 9
    AA=AIMAG(ZERO(1))
    DO 12 I=2,II
    AI=AIMAG(ZERO(I))
    IF (AA.LE.AI) GO TO 12
    IK=I      S      AA=AI
 12 CONTINUE
    AP=ZERO(IK)      S      GO TO 16
  9 AP=ZERO(1)
 16 RETURN
    END
```

101

```fortran
      SUBROUTINE ROOT(A,B,F,X,JMAX,E,E1,G)

C     THIS SUBROUTINE USES THE BISECTION METHOD TO SOLVE FOR ONE ODD
C     ROOT OF F(X) = 0 ON THE INTERVAL (A,B).  THE FUNCTION PASSED
C     THROUGH F MUST BE DECLARED EXTERNAL IN ALL CALLING PROGRAMS.  E IS
C     INTERVAL OF UNCERTAINTY DESIRED FOR THE ROOT, AND MUST BE SMALLER
C     THAN THE STARTING INTERVAL. W = B-A.  THE NUMBER OF BISECTIONS IS
C     DETERMINED BY NMAX = LN(W/E)/LN(2).  AFTER BISECTING, THE FUNCTION
C     VALUE IS COMPARED TO E1.  IF ABS(F(X0)) > E1 THEN THE SUBROUTINE
C     PRINTS: DISCONTINUITY AT X = X0.  A RANDOM SEARCH OCCURING JMAX
C     TIMES IS USED TO LOOK FOR A CHANGE OF SIGN IF SIGN(F(A)) =
C     SIGN(F(B)).
C     DISCONTINUITY AT X =      .  A RANDOM SEARCH OCCURING JMAX TIMES IS
C     USED TO LOOK FOR A CHANGE OF SIGN IF SIGN(F(A)) = SIGN(F(B)).
C     A PLOT OPTION IS AVAILABLE THROUGH ENTRY POINT PLOT
C     THAT WILL PLOT THE FUNCTION F ON THE INTERVAL (A,B) AT JMAX
C     EQUALLY SPACED POINTS.  WHEN USING THE PLOT ENTRY, JMAX MUST BE
C     ≤ 100, AND THE FOLLOWING SUBROUTINES ARE NEEDED: KPXNYN, KPRINT,
C     AND KSC120.

      LOGICAL G
      REAL LN2
      DIMENSION Y(3)

C     QUESTION: DOES F(A) = 0.

      Y1=F(A)
      IF(Y1.NE.0.) GOTO 10
      X=A
      GOTO 80

C     QUESTION: DOES F(B) = 0.

   10 Y2=F(B)
      IF(Y2.NE.0.) GOTO 20
      X=B
      GOTO 80

C     QUESTION: ARE THE SIGNS OF F(A) AND F(B) DIFFERENT.

   20 I1=SIGN(1.,Y1)
      I2=SIGN(1.,Y2)
      W=B-A
      IF(I1.NE.I2) GOTO 60

C     SEARCH FOR A CHANGE IN SIGN.

      DO 30 J=1,JMAX
      X=A+RANF(0.)*W
      I3=SIGN(1.,F(X))
      IF(I3.NE.I1) GOTO 50
      JM=J
   30 CONTINUE
      PRINT 40
   40 FORMAT(1X*NO CHANGE OF SIGN FOUND*/)
      G=JM.EQ.JMAX
      RETURN
   50 B=X

C     DETERMINE NUMBER OF BISECTIONS

   60 LN2=0.6931+7181
      NMAX=ALOG(W/E)/LN2+1.
      Y(2+I1)=A
```

```
      Y(2-I1)=B
C     BEGIN BISECTION

      DO 70 N=1,NMAX
      X=(Y(1)+Y(3))/2.
      Y3=F(X)
      IF(Y3.EQ.0.) GOTO 80
      I3=SIGN(1.,Y3)
   70 Y(2-I3)=X
   80 IF(ABS(F(X)).LE.E1) GOTO 85

C     CONVERGENCE TO A DISCONTINUITY

      PRINT 82,X
   82 FORMAT(1X*DISCONTINUITY AT X = *E12.4/)
      G=ABS(F(X)).GT.E1
      RETURN

C     CONVERGENCE TO A ROOT

   85 PRINT 90,X
   90 FORMAT(1X*ONE ODD ROOT AT X = *E12.4/)
      G=ABS(F(X)).GT.E1
      RETURN

      END




      FUNCTION FX(Z)

C  EQ. (40) ,SECTION 3 OF THE REPORT. TE (ODD) TYPE ROOTS WILL BE
C  SEARCHED.

      COMMON /MAIN3/S(3),E(3),H
      FX=Z*TAN(Z)*SQRT((E(2)-1.)*H*H-Z*Z)
      RETURN
      END




      FUNCTION FY(Z)

C  EQ. (39) ,SECTION 3 OF THE REPORT. TM (EVEN) TYPE ROOTS WILL BE
C  SEARCHED.

      COMMON /MAIN3/S(3),E(3),H
      E1=E(2)
      FY=(Z/E1)*TAN(Z)-SQRT((E1-1.)*H*H-Z*Z)
      RETURN
      END
```

103

```
      SUBROUTINE ZROOT(IT,X,Z,GGG)

C     THIS SUBROUTINE WILL SEARCH FOR THE COMPLEX ROOT OF A LOSSY SLAB
C     ABOVE A FINITELY CONDUCTING EARTH, BY USING THE REAL ROOT FOUND FROM
C     THE SUBROUTINE (ROOT) AND SENT THRU THE VARIABLE (X) TO THIS PROGRAM
C     FROM THE SUBROUTINE (PROOT) . A COMPLEX ROOT WILL BE SEARCHED FOR
C     THE   SITUATION OF A LOSSY SLAB ABOVE GROUND . THE VARIABLE (IT)
C     DETERMINE IF THE ROOT IS IN THE TM OR TE CATAGORIES. (Z) IS THE
C     RETURNED COMPLEX ROOT .(GGG) IS A LOGICAL STATEMENT .IF IT IS TRUE
C     NO COMPLEX ROOT IS FOUND OR PROBABELY FAILED TO CONVERGE TO A ROOT.
C     OTHERWISE, (GGG) IS FALSE AND ,THUS, A COMPLEX ROOT IS FOUND.
      COMMON /ZZZZ/N(3),H,EPSR(3)
      COMMON /MAIN3/S(3),E(3),HH,OMEGA
      COMPLEX N,CX,CENTR,ZERO,Z,CY,ALPHA
      EXTERNAL CX,CY
      DIMENSION SIGMA(3)
      LOGICAL GG,GGG
      PI=3.141592653
      EPSO=8.854E-12
      FREQN=OMEGA/2./PI
      H=HH
      DO 99 JJ=1,3

      SIGMA(JJ)=S(JJ)
   99 EPSR(JJ)=E(JJ)
      DO 12 J=1,3
   12 N(J)=CSQRT(EPSR(J)+(0.,1.)*SIGMA(J)/OMEGA/EPSO)
      CENTR=X
      IF (IT.EQ.2) GO TO 115
      CALL CROOT(CX,CENTR,ZERO,TT,GG)
      IF (GG) GO TO 66
      GO TO 90
  115 CALL CROOT(CY,CENTR,ZERO,TT,GG)
      IF (GG) GO TO 66
   90 PRINT 88,FREQN,(N(J),J=1,3)
   88 FORMAT (1X,*FREQ.=*E11.3/20X*N0=*F7.3,*+J*F9.4/,
     120X*N1=*F7.3,*+J*F9.4/,20X*N2=*F7.3,*+J*F9.4//)
      ALPHA=CSQRT(-ZERO*ZERO/H/H*N(2)*N(2))
      PRINT 18,ALPHA
   18 FORMAT (1X,*ALPHA=*E13.5,*+J*E13.5/)
  109 Z=ALPHA
      GGG=TT.GT.1.0E-5
      RETURN
   66     Z=CSQRT(-ZERO*ZERO/H/H*N(2)*N(2))
      PRINT 67,Z,TT
   67 FORMAT (1X,*IT FAILED TO CONVERGE*,4X*ZERO=*E13.5,*+J*E13.5,
     14X*TEST=*E13.5/)
      GGG=TT.GT.1.0E-5
      RETURN
      END
```

```
      SUBROUTINE CROOT(CF,Z0,ROOT,TEST,G)

C    IN THIS SUBROUTINE A NEWTONS METHOD PLUS A HALVING TECHNIQUE WILL
C    BE USED TO SEARCH FOR COMPLEX ROOTS.

      COMMON /PRIME/DCF
      COMPLEX CF,DCF
      COMPLEX ROOT,F,DF,Z0,Z1,Z01
      LOGICAL G
      J=0
      I=0
      F=CF(Z0)        S        DF=DCF
      TEST0=CABS(F)
      IF (TEST0.GT.1.0E-05) GO TO 25
      TEST1=TEST0     S     GO TO 100
   25 Z1=Z0-F/DF
   30 F=CF(Z1)        S     DF=DCF
      TEST1=CABS(F)     S    Z01=Z1-Z0        S        Z0=Z1
      IF (TEST1.LE.1.0E-05) GO TO 100
      IF (J.GE.50)  GO TO 100
      J=J+1
      IF (TEST1.LE.TEST0) GO TO 25
      CAB=CABS(Z01)
      IF (CAB.LE.1.0E-05) GO TO 100
      Z1=Z0-Z01/2.        S        I=I+1
      IF (I.GE.10) GO TO 100
      GO TO 30
  100 ROOT=Z0
      TEST=TEST1
      G=TEST.GT.1.0E-05
      RETURN
      END




      COMPLEX FUNCTION CX(Z)

C   EQ. (38) ,SECTION 3 OF THE REPORT.

      COMMON /PRIME/DCX
      COMMON /ZZZZ/N(3),H,EPSR(3)
      COMPLEX DCX
      COMPLEX N,Z,E1,E2,GN2,U,HN
      COMPLEX G0,G2,DG0,DG2,CS,CC,GZ
      H2=H*H     S     E1=N(2)*N(2)     S     E2=N(3)*N(3)
      U=-Z*Z+E1*H2
      HN=E2*H2
      G0=CSQRT(U-H2)
      G2=CSQRT(U-HN)
      CS=CSIN(Z)        S        CC=CCOS(Z)
      DG0=-Z/G0     S        DG2=-Z/G2
      GZ=G0*G2/Z-Z
      CX=GZ*CS/CC-G0+G2
      DCX=GZ/CC/CC+(DG0*G2/Z+DG2*G0/Z-G0*G2/Z/Z-1.)*CS/CC-DG0+DG2
      RETURN
      END
```

105

```fortran
      COMPLEX FUNCTION CY(Z)
C    EQ. (37) .SECTION 3 OF THE REPORT.

      COMMON /PRIME/DCY
      COMMON /ZZZZ/N(3),H,EPSR(3)
      COMPLEX DCY
      COMPLEX N,Z,E1,E2,GN2,U,ZZ,HN
      COMPLEX G0,G2,DG0,DG2,CS,CC,GZ
      H2=H*H     S    E1=N(2)*N(2)    S    E2=N(3)*N(3)
      U=-Z*Z+E1*H2
      HN=E2*H2
      G0=CSQRT(U-H2)
      G2=CSQRT(U-HN)
   67 ZZ=Z/E1         S      GN2=G2/E2
      CS=CSIN(Z)      S      CC=CCOS(Z)
      DG0=-Z/G0       S      DG2=-Z/G2
      GZ=G0*GN2/ZZ-ZZ
      CY=GZ*CS/CC+G0+GN2
      DCY=(-G0*GN2/ZZ/Z+(DG0*GN2+G0*DG2/E2)/ZZ-1./E1)*CS/CC
     1+GZ/CC/CC+DG0+DG2/E2
      RETURN
      END
```